**2025**

# DIPLÔME UNIVERSITAIRE DE GEMMOLOGIE

**Nantes University**
**U.F.R Sciences et Techniques**

# Minerals of the Kornerupine Group

**by**

**GUO, Jin**

**Publicly defended**
**4th November 2025**
**At the Department of Earth and Universe Sciences**
**Before the following jury**

| | | |
|---|---|---|
| **PRESIDENT** | CHAUVIRÉ B. | *Associate professor, Nantes University* |
| **VICE-PRESIDENT** | KARAMPELAS S. | *Assistant professor, University of Thessalonique and scientific consultant of LFG* |
| **EXAMINERS** | DELAUNAY A. | *Head of Laboratoire Français de Gemmologie* |
| | GAILLOU E. | *Head and curator of Musée de Minéralogie des Mines de Paris* |
| | LATOUCHE C. | *Professor, Nantes Université* |
| | NOTARI F. | *Founder of GGTL Laboratories Switzerland and Head of Scientific Research at AIGS (Bangkok)* |
| **INVITED** | FRITSCH E. | *Professor Emeritus, Nantes University* |
| | LASNIER B. | *Founder of DUG* |

# Table of Contents

# Abbreviations

BED: backscattered electron detector
EDXRF: energy-dispersive X-ray fluorescence spectrometry
FTIR: Fourier-transform infrared
FWHM: full width at half maximum
LWUV: long-wave ultraviolet
ND: not detectable
RI: refractive index (n)
SEM: scanning electron Microscope
SED: secondary electron detector
SWUV: short-wave ultraviolet
UV-Vis-NIR : ultraviolet-visible-near infrared

# Introduction

The research project presented here was carried out as part of the preparation for the Diplôme d'Université de Gemmologie (DUG) of Nantes Université.

In September 2024, I travelled to Hong Kong together with Claudio Milisenda to represent the DSEF German Gem Lab during the Hong Kong Jewellery & Gem Fair and offer on site gemstone testing service. While I passed by a booth of a company specialised in tsavorites, my eyes fell upon a few emerald-green stones which looked different. They were actually kornerupines, the "auxiliary products" found together with tsavorites in Tanzania. The bright green colour of these kornerupines is lovely and I acquired two of them (respectively 0.45ct. and 2.39ct., Fig. 1). In November 2024, I participated in the DUG course in Nantes and chose kornerupine as the subject of my research project.

**Fig. 1** Two kornerupines from Tanzania (Top left: 0.45ct., 5.06 x 4.13 mm)

It has been a trip full of discoveries and I feel truly lucky to have received so much support in many aspects.

For the research stones collection, my heartfelt thank goes to Emmanuel Fritsch (Nantes Université, Nantes), Tom Stephan (DgemG - German Gemmological Association, Idar-Oberstein), Michael Wild (Werner Wild e.K., Idar-Oberstein), M.T.M Haris (Emteem Gem Lab, Sri Lanka) and Fabian Schmitz (Rhein-Main-Gem-Consulting, Mainz) for having generously provided me with samples including those with uncommon colours.

I am infinitely greatful to my teachers Emmanuel Fritsch, Boris Chauviré, Stefanos Karampelas and Eloïse Gaillou for their teaching, guidance, encouragement and unconditional support,

to the members of the jury for their valuable feedbacks and suggestions which helped me to further develop this research project,

to Claudio Milisenda for his constant support and advice, for his comments to help me progress and for allowing me to carry out analysis with instruments of the DSEF German Gem Lab,

to Tom Stephan for his friendly help, the careful rereading, the motivating and inspiring discussions and for being available whenever I have questions,

to John Saul for kindly sharing with me his experience with discovery of kornerupines in East Africa,

and to my DUG promotion for the great time spent together and for all the enriching exchange.

# Context of the project

## *History*

### Discovery

Kornerupine was first found at Fiskernæs, West Greenland, as material with a radiating columnar habit in translucent to transparent pieces of pale green to grey green colour. The mineral was reported upon in 1884 (but published in 1886) by J. Lorenzen who named it kornerupine in memory of Andreas Nicolaus Kornerup, a young Danish explorer, geologist and artist who made multiple research trips to Greenland.

In 1886, Sauer proposed the name prismatine for a prismatic mineral from a cut near the Waldheim railroad station, Saxony, Germany. This mineral resembled sillimanite and andalusite in appearance and staurolite in composition. At that time Sauer was presumably unaware of Lorenzen's (1886) name kornerupine for a mineral from Fiskernæs, Greenland, of the composition $MgAl_2SiO_6$ and resembling kyanite and sillimanite. Ussing (1889) compared Sauer's prismatine with Lorenzen's kornerupine and concluded that they were the same mineral on the basis of symmetry, cleavage and optical orientation; differences in optic angle, colour and specific gravity were presumed to be within the ranges found in isomorphic minerals.

A.N. Kornerup
Photo: Budtz Müller

### Kornerupine group

Lacroix carried out research on the role of boron in kornerupines from Madagascar and suggested to integrate boron in the chemical formula of the mineral: $[SiO_4]_7Mg_8[(Al, Fe, B)O]_{12}$ instead of the formula suggested for the material from Greenland $SiO_8$ $Al_2O_3$ MgO. (Lacroix et al., 1921)

Advances in the technology of ion- and electron-microprobe analysis and of crystal structure refinement made accurate measurement of boron in silicate minerals feasible. Analysis of boron using the ion microprobe and crystal structure refinement indicate that the boron content of one tetrahedral site in kornerupine ranges from 0 to 1. Kornerupine and prismatine, from their respective type localities of Fiskernæs, Greenland and Waldheim, Germany, are different minerals, members of an isomorphic series differing in boron content. For this reason, Sauer's name prismatine for kornerupines with B > 0.5 atoms per formula unit (apfu.) of 22(O,OH,F) was re-introduced, and the name kornerupine *sensu stricto* is restricted to kornerupines with B < 0.5 apfu. Kornerupine *sensu lato* is an appropriate group name for kornerupine of unknown boron content. Both minerals form under granulite-facies conditions with sapphirine and phlogopite, but kornerupine *sensu stricto* is associated with anorthite and hornblende or gedrite, whereas prismatine is found with oligoclase (An9-13), sillimanite, garnet, and/or tourmaline. Occurrences at other localities suggest that increasing boron content extends the stability range of prismatine relative to that of kornerupine *sensu stricto*. (Grew et al., 1996)

In 1999, Wopenka et al. described a differentiation method between kornerupine *sensu stricto* and prismatine with Raman spectroscopy. According to this research work, two of the Raman vibrational modes of kornerupines *sensu lato* (at ~803 $\Delta cm^{-1}$ and at ~884 $\Delta cm^{-1}$) are sensitive to the presence of boron and their relative intensities can be used to distinguish kornerupine *sensu stricto* and prismatine. Based on the intensities of those boron-sensitive bands, Raman spectroscopy could potentially provide a semi-quantitative measure of the boron content of kornerupine.

See Fig. 2 for comparison of the fundamental Raman bands of boronfree, boron-poor, and boron-rich kornerupine-group minerals with 0° crystal orientation with respect to the polarisation orientation of the exciting laser beam. Bands **C** (~803 Δcm–1) and **D** (~884 Δcm–1) are sensitive to the presence and the concentration of boron in the mineral. Boron content of samples varied between 0.02 B apfu and 0.84 B apfu. Samples showing both boron-sensitive Raman bands at ~803 Δcm–1 and ~884 Δcm–1 could be identified as "boron-rich," i.e., prismatine (B > 0.5 apfu) by Raman spectroscopy. In "boron-poor" kornerupines (0.5 > B > 0.1 apfu), i.e., kornerupine *sensu stricto*, only the stronger of the two boron-sensitive bands (the one at ~884 Δcm–1) is detected in the Raman spectrum. For samples with B < 0.1 apfu, neither one of the two boron-sensitive Raman bands is detected. (Wopenka et al., 1999)

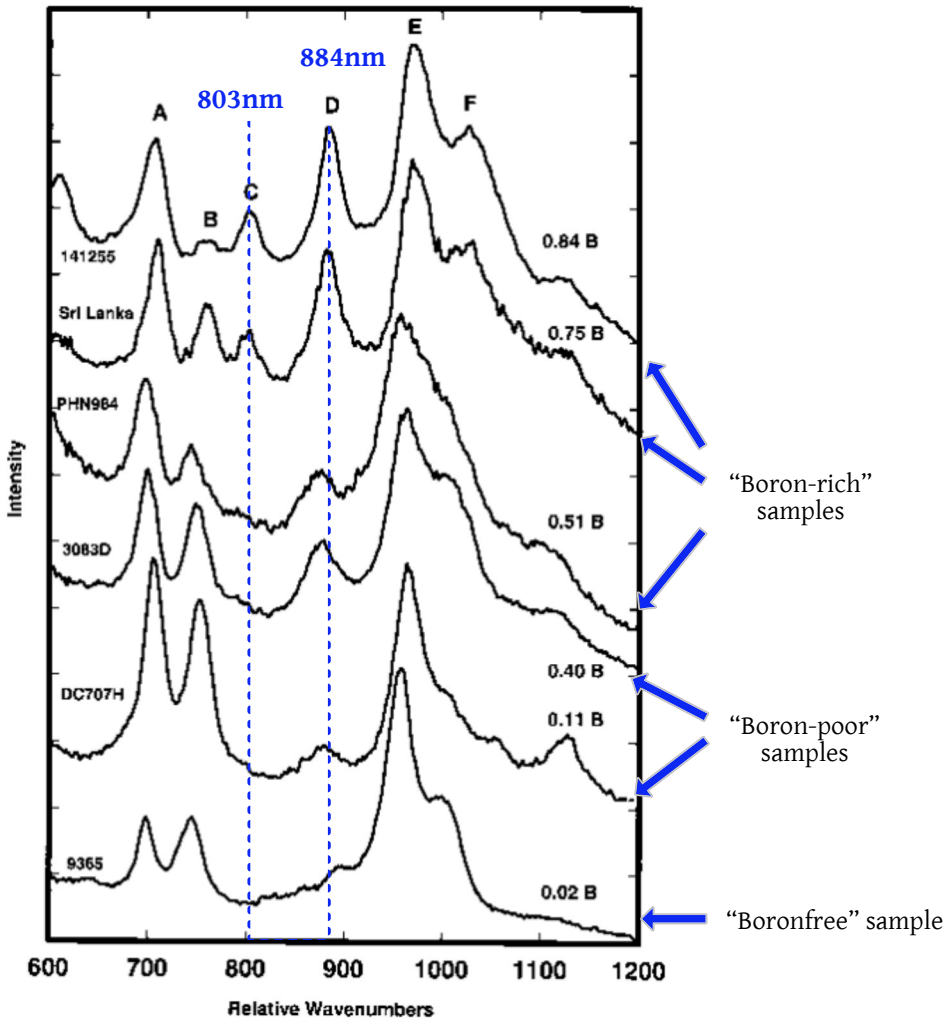


**Fig. 2** Comparison of the fundamental Raman bands of boronfree, boron-poor and boron-rich kornerupine-group minerals (Wopenka et al., 1999)

## Localities

Kornerupine *sensu stricto* and prismatine, the B-poor and B-rich members of the kornerupine group (Grew et al., 1996; Braga et al., 2003), have been reported from some 70 localities worldwide.

The material from Greenland is scarce and has no gem significance. In 1912, an olive green variety of kornerupine, found as transparent crystals, was discovered at Betroka, Madagascar (Lacroix, 1938), and later, in 1922, another deposit of similar coloured material was found at Itrongay on the same island. About 1936, some deep brownish-green cut stones from the illam of Ceylon were identified as kornerupine and a number of such stones have since been found in parcels of Ceylon gravel. In 1952, although a similar but unidentified stone had been known for some time, a green-coloured stone of fine quality was identified as kornerupine, and there is little doubt that the stone came from the Mogok Stone Tract of Burma. It has been credibly reported that a star-kornerupine has been found at this locality. Other sources of kornerupine, but not necessarily of gem quality, are Waldheim in Saxony, where the mineral was first known as prismatine; some opaque material has been found at Port Shepstone in Natal, South Africa, and material of two types, one a dark green and the other a yellow or greenish-yellow, comes form Lac Ste Marie, Gatineau, Quebec, Canada.(Webster, 1977). Kornerupine cat's-eyes have been found in Sri Lanka (Milisenda, 2005).

Specimens of gem quality with bright green colours from the Kwale District, Kenya were described in 1974 (Schmetzer et al., 1974). They are found together with quartz, silimanite, kyanite, tourmaline, muscovite and biotite in prismatic crystals up to 10cm length. John Saul kindly shared his experience with the discovery of kornerupines in East Africa: "Gem kornerpines with an attractive yellowish tint and strong dichroism were found near the town of Daluni in north east Tanzania in the early 1970s. A few rolled gem pebbles found in the Umba River were either kornerupines or sillimanites or both. Crystal-sections, 1 to 3 cm in length, with 'woody' surface alteration were found, perhaps near the south east Kenya-north east Tanzania border c.1972. The specimens looked like crushed logs with bright green broken ends. When cut, they looked like tsavorites. This was very nice material. My impression was that everything came from a one-day find in hardrock. There is a chance I was not told the truth concerning the locality, in which case, the locality would be 'eastern East Africa'."

Bluish-green and blue kornerupines from Kenya (district of Namanga) and Tanzania (southern part of the Usambara Mountains or Daluni in the Umba Region) were described by Schmetzer et al. in 1979. These stones are distinctly different in their optical features from the green kornerupine crystals from the Kwale District, Kenya (Schmetzer et al., 1974). They have been detected in lots of other minerals such as green touralines or green garnets and partly offered as single stones under other names (e.g. silllimanite). (Schmetzer et al., 1979)

According to Claudio Milisenda, the geology of the East African bright green and bluish-green to blue kornerupines is possibly related to the East African Mozambique belt, in whose terranes in Kenia and Tanzania numerous V-bearing minerals occur.

# *Gemmological properties*

## Generalities

Kornerupine *sensu lato*, approximately $(Mg,Fe^{2+},Al,\square)_{10}(Si,Al,B)_5O_{21}(OH,F)_2$ (IMA Formula), also $(\square,Mg,Fe^{2+})Al_4(Mg_3Al_2)[O_4|(OH,O)|Si_2O_7|(Si(Al,B)Si)_{\Sigma 3}O_{10}]$ (Strunz & Nickel, 2001), is a magnesium iron aluminium boron-silicate mineral group occurring in Mg-Al-rich rocks, magnesian metapelites and, very rarely, pegmatites in upper amphibolite- and granulitefacies terrains; it includes kornerupine *sensu stricto* ($0 \leq B < 0.5$ apfu) and prismatine ($1 > B > 0.5$ apfu) (Grew et al., 1999).

Transparent crystals can be cut as gemstones. They are usually green to blue-green, or brownish-green to greenish-brown, or yellow-brown to brownish-yellow in colour and display strong pleochroism. Blue specimens are rare (Henn et al., 2019). The crystallization is orthorhombic. The hardness is 6½ on Mohs scale and the density varies from 3.20 to 3.45. The refractive indices' ranges are as below, with a negative biaxial birefringence between 0.013 and 0.015 (Henn and Milisenda, 2004):

$n_x$ = 1,660 – 1,671

$n_y$ = 1,673 – 1,683

$n_z$ = 1,675 – 1,684

## Colouring agents

Schmetzer et al. analysed speciments of gem quality with light green colours from Kenya and attributed the green colour to vanadium (1974). Analysis of the bluish-green and blue kornerupines *sensu lato* from Kenya led to the following description of the colour variation of vanadium- and chromium-containing East African kornerupines: V > Cr => green, V ≈ Cr => blue-green, Cr > V => blue (Schmetzer, 1982). Iron-bearing kornerupines *sensu lato* in the colour range brown-yellow-green are known to occur in Sri Lanka, Madagascar and Burma (Schmetzer et al., 1974; Henn, 1985).

## Luminescence

Robert Webster described that kornerupines *sensu lato* show a yellow glow under both long and short wavelengths of ultra-violet light. Those found in East Africa show "an even stronger yellow glow".

GIA Gem Database recorded the fluorescence of a kornerupine *sensu lato* (1.64 ct.) from Kwale District (Kenya) which belongs to Edward J. Gübelin Collection: weak yellowish green with even distribution under LWUV and yellowish green with even distribution under SWUV (GIA Gem Database, 2011).

## Pleochroism

Pleochroism of kornerupines *sensu lato* has been described in various publications. Bank et al. reported in 1974 and 1975 the strong pleochroism of transparent gem-quality kornerupines from south of Handeni in Tanzania. A comparative table (Table 1) published by Schmetzer et al. in 1977 (in German) and 1979 (in English) summarised the pleochroism of kornerupines from different localities.

**Table 1** Pleochroism of kornerupines from different localities (Schmetzer et al., 1977&1979)

| | Ceylon and Madagascar | Kwale District, Kenya | Kenya and Tanzania, various localities, somewhat different due to contents of trace elements | | |
|---|---|---|---|---|---|
| X | yellowish-brown | intensely green | emerald-green | emerald-green | |
| Y | brown | slightly green | bluish-grey | reddish-purple | Y and Z show only small differences |
| Z | greenish | greenish-yellow | reddish-purple | bluish-grey | |

## Inclusions

Zircons, negative crystals, needle-like crystals, oriented hollow tubes, apatite, fluid inclusions, two-phase inclusions, etc. have been described as inclusions in kornerupine in the literature. (Henn, 1985; Henn et al., 2004; C. C. Milisenda, 2005; C. C. Milisenda et al., 2009)

## Synthetics

Boron-free kornerupines were synthesised for the first time in 1969 by Schreyer & Seifert (Schreyer et al., 1969). Synthesis experiments suggest that boron incorporation occurs summarily for $Al^{3+}$ (K. Schmetzer, 1979). Synthesised boron-bearing kornerupine was described by G. Werding and W. Schreyer in 1978.

# Materials and Methods

## *Materials*

### Description

Twelve kornerupines *sensu lato*, with colours ranging from yellowish-green to emerald-green, green-blue to blue-violet and yellow-brown to brown-green, were analysed. Not all the origins of the samples are known. (Fig. 3-4, Table 2). The twelve kornerupines were grouped into **the Green-Blue-Violet series** and **the Brown-Yellow-Green series** according to their colours. One andalusite was measured for the purpose of comparative analysis of luminescence. Further description of the andalusite sample will be detailed in the session on luminescence.


**Fig. 3** Twelve kornerupines *sensu lato* :

- **Left**: the Green-Blue-Violet series (KUD5: 7.64 x 5.54 mm)
- **Bottom**: the Brown-Yellow-Green series (KUD3: 10.14 x 9.10 mm)

**Fig. 4** Andalusite sample AUE4100 (8.08 x 6.64 mm)

**Table 2** Description of twelve kornerupines *sensu lato* and one andalusite AUE4100

| Sample N° | Colour | Weight | Dimensions (mm) | Cut | Form | Optical Effect | Origin |
|---|---|---|---|---|---|---|---|
| KTJ1 | Green | 0,45 ct. | 5,06 x 4,13 x 2,97 | Mixed Star/Step cut | Oval | - | Tanzania |
| KTJ2 | Green | 2,39 ct. | 9,52 x 7,40 x 4,61 | Mixed Star/Step cut | Oval | - | Tanzania |
| KUD5 | Green | 1,39 ct. | 7,64 x 5,54 x 3,44 | Step cut | Octagon | - | Unknown |
| KUD7 | Green | 1,53 ct. | 9,02 x 5,37 x 3,46 | Cabochon | Oval | Cat's-eye | Unknown |
| KUF | Green-blue | 3,52 ct. | 9,71 x 8,31 x 5,61 | Mixed Star/Step cut | Cushion | - | Unknown |
| KTM | Blue-violet | 2,08 ct. | 8,98 x 7,03 x 5,23 | Faceted | Oval | - | Tanzania |
| KUD6 | Yellow-brown | 3,13 ct. | 8,66 x 7,96 x 5,57 | Mixed Star/Step cut | Oval | - | Unknown |
| KUD3 | Yellowish-green | 3,88 ct. | 10,14 x 9,10 x 5,53 | Star cut | Cushion | - | Unknown |
| KSE4637 | Greenish-yellow | 1,83 ct. | 7,66 x 7,47 x 5,28 | Star cut | Rounded triangle | - | Sri Lanka |
| KUH | Brownish-green | 1,06 ct. | 6,51 x 5,38 x 3,43 | Step cut | Octagon | - | Unknown |
| KME3887 | Brownish-green | 1,90 ct. | 8,25 x 6,98 x 3,98 | Faceted | Fancy | - | Madagascar |
| KUD8 | Brown-green | 1,54 ct. | 7,30 – 7,39 x 3,26 | Cabochon | Round | Cat's-eye | Unknown |
| AUE4100 | Yellowish-brown | 1,49 ct. | 8,08 x 6,64 x 3,67 | Star cut | Oval | - | Unknown |

Among the research samples are:

- Two speciments with rare colours:
  - Sample **KTM**
    - 2.08 ct.
    - Colour: blue-violet
    - Origin: Tanzania
    - Collection Werner Wild, Idar-Oberstein
  - Sample **KUF**
    - 3.52 ct.
    - Colour: green-blue
    - Collection Fabian Schmitz, Mainz
- Two samples which show very sharp chatoyancy or cat's-eye effect:
  - KUD7 (green) and KUD8 (brown-green)
    - 1.53ct and 1.54 ct.
    - Collection DGemG, Idar-Oberstein

KTM: 8.98x7.03mm

KUF: 9.71x8.31mm

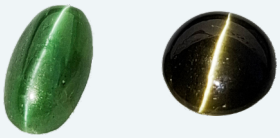

Left: 9.02x5.37mm

# *Methods*

## Classical gemmological instruments

Refractive indices were measured on a refractometer from Schneider Gemmologie. A hydrostatical balance was used to obtain specific gravity and a Mettler Toledo balance to measure the carat weight.
A digital sliding caliper is used to measure the samples dimensions.
short-wave (254 nm) and long-wave (365nm) UV lamps was used to observe luminescence of samples and Leica camera to photograph luminescence.
A ZEISS Stemi 508 Stereo microscope was used for observation of inclusions and of pleochroism by placing a London dichroscope between the sample and objective lens.
For microphotography as well as macrophotography of part of the samples, a Samsung Galaxy A55 cellphone was used.

## Raman spectroscopy

*Raman (Renishaw)*

Most Raman spectra were obtained on a Renishaw InVia confocal Raman microscope equiped (with a 50x objective) with a 514 nm laser excitation. The spectral acquisition time was 10 seconds and laser power adapted.

*Raman T64000*

Part of the Raman scattering spectra were also measured with an Ar+ argon excitation laser at 514.5nm, using a T64000 Horiba Jobin-Yvon spectrometer equipped with a microscope in backscattering configuration.

## Ultraviolet-visible-near infrared (UV-Vis-NIR) spectroscopy

Optical absorption spectra UV-Vis-NIR spectra were acquired on a PerkinElmer UV-Vis-NIR spectrometer Lambda 950s equipped with a deuterium and a halogen lamps (lamp change at 319.20nm) and three detectors PbS, InGaS and PMT (detector change at 814.40 nm). Spectra were acquired over a range from 200 to 1500 nm, the sampling was carried out with a step size of 1 nm and a scanning speed of 306.67 nm/min.

## Fourier-tranform infrared (FTIR) spectroscopy

FTIR spectra were acquired on a Nicolet iS50 FTIR spectrometer, with spectral sampling of 4 $cm^{-1}$ for 128 scans in absorption and reflection modes in the range of 7500-400 $cm^{-1}$.

## Luminescence spectroscopy

The emission spectra, excitation spectra and phosphorescence decay time spectra were aquired on a fluorimeter Horiba Jobin-Yvon Fluorolog 3. Essence. Filters were used to avoid artefacts. Integration time (0.1-0.2 second) and slits (from 2nm to 14nm Bandpass) were adapted to obtain spectra with adequate resolutions.

## Energy-dispersive X-ray fluorescence (EDXRF) analysis

Quantitative EDXRF data were collected using an ARL QUANT'X EDXRF analyzer Thermo Scientific, vacuum atmosphere, with 3.5mm collimator. The parameters were set as routine analyses settings of the DSEF German Gem Lab. Known concentrations given to kornerupines previously to calculation: 3.30wt.-% $B_2O_3$ and 1.00wt.-% of $H_2O$.

## Scanning electron microscope (SEM)

Scanning electron microscope JEOL JSM IT510 working at 15KV for a beam current in the 1nA range, providing sufficient statistics for the acquisition of spectra and maps by the integrated EDS detector. Images were acquired using either an Everhart-Thornley secondary electron detector or a dual PN junction backscattered electron detector.

# Results

## *Classical gemmology*

### Gemmological properties

The density of the twelve kornerupine samples varies from 3.21 to 3.32 g/cm$^3$.

The refractive index (RI) of individual samples are listed in Table 3, including spot reading values for two samples with cabochon cut (KUD7 & KUD8).

Except from one translucent to opaque sample (KUD8), all kornerupine samples are dichroic or trichroic. The speciments of the Green-Blue-Violet series (KTJ1, KTJ2, KUD5, KUD7, KUF and KTM) show distinct plechroism (Fig. 5).

**Table 3** Measurements of twelve kornerupines *sensu lato*

| Sample | Colour | Weight | RI | Density | Pleochroism |
|---|---|---|---|---|---|
| KTJ1 | Green | 0.45 ct. | 1.661-1.673 | 3.21 g/m$^3$ | Yellowish-green/emerald green |
| KTJ2 | Green | 2.39 ct. | 1.661-1.673 | 3.25 g/m$^3$ | Brown/yelowish-green/emerald green |
| KUD5 | Green | 1.39 ct. | 1.661-1.674 | 3.21 g/m$^3$ | Brownish-yellow/yellowish-green/emerald-green |
| KUD7 | Green | 1.53 ct. | ~1.660 | 3.24 g/m$^3$ | Brown/yellow/green |
| KUF | Green-blue | 3.52 ct. | 1.661-1.673 | 3.27 g/m$^3$ | Yellowish-green/purple/violet |
| KTM | Blue-violet | 2.08 ct. | 1.660-1.673 | 3.24 g/m$^3$ | Yellowish-green/purple/violet |
| KUD6 | Yellow-brown | 3.13 ct. | 1.661-1.675 | 3.25 g/m$^3$ | Light-brown/brown |
| KSE4637 | Yellowish-green | 3.88 ct. | 1.665-1.678 | 3.28 g/m$^3$ | Brown/brownish-green |
| KUD3 | Greenish-yellow | 1.83 ct. | 1.662-1.675 | 3.28 g/m$^3$ | Brown/light brown |
| KME3887 | Brownish-green | 1.06 ct. | 1.669-1.681 | 3.32 g/m$^3$ | Brown/bluish-green/yellowish-green |
| KUH | Brownish-green | 1.90 ct. | 1.669-1.682 | 3.30 g/m$^3$ | Brown/green/bluish-green |
| KUD8 | Brown-green | 1.54 ct. | ~1.670 | 3.32 g/m$^3$ | - |

**Fig. 5** Examples of pleochoism in KTJ2, KTM and KUF. Observed under stereo microscope with a dichroscope. From left to right: 9.52x7.40mm, 8.98 x 7.03mm and 9.71 x 8.31mm.

### Inclusions

Inclusions observed under stereo microscope include zircons (Fig. 6), hollow tubes (Fig. 7), fluid inclusions, negative crystals, mineral inclusions, healing cracks, etc..

Raman spectroscopy confirmed the identity of the zircon inclusions (Fig. 6) in the sample KME3887 (Appendix KME3887).

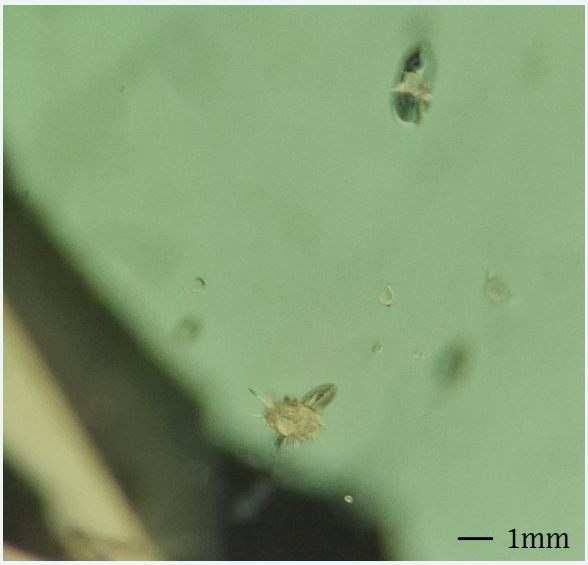


**Fig. 6** Zircon inclusions with tension halos in the sample KME3887.

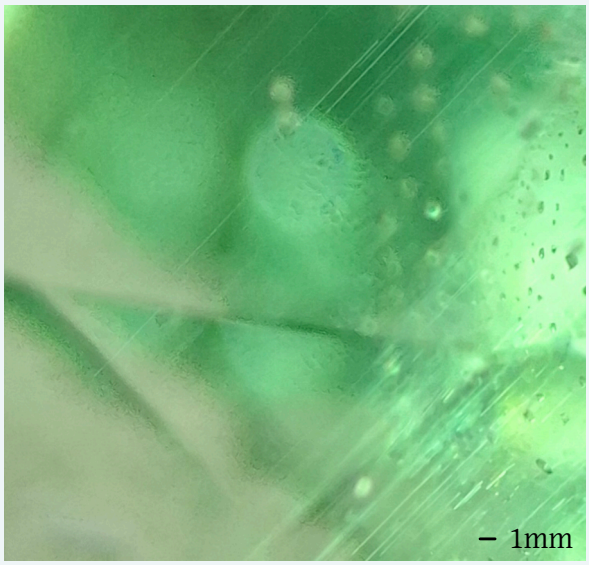


**Fig. 7** Hollow tubes and two-phase inclusions in the sample KTJ1.

## Luminescence

The six kornerupine samples of the Green-Blue-Violet series show distinct luminescence under short-wave UV (SWUV) and long-wave UV (LWUV) light, with LWUV > SWUV, unlike the andalusite sample, which shows a stronger SW luminescence and a very weak LW luminescence. (Table 4, Fig. 8)

*Under fluorescent light*

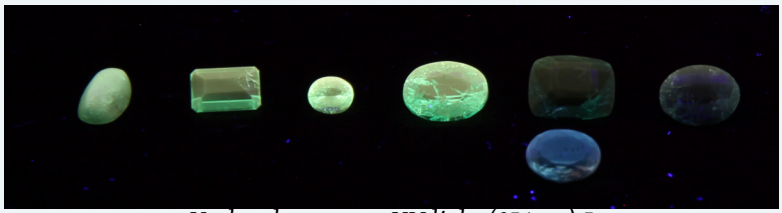

*Under short-wave UV light (254nm) 5s*

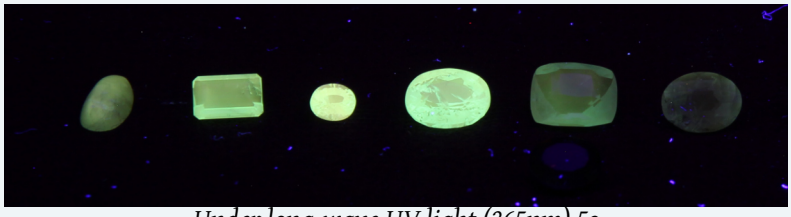

*Under long-wave UV light (365nm) 5s*

**Fig. 8** Luminescence of six kornerupine samples and one andalusite (in the front) (First sample on the left: 9.02 x 5.37 mm)

**Table 4** Luminescence of kornerupine samples

| Sample | Weight | SWUV Luminescence | LWUV Luminescence | SWUV vs LWUV |
|---|---|---|---|---|
| KTJ1 | 0.45 ct. | Yellow-green | Greenish-yellow | < |
| KTJ2 | 2.39 ct. | Yellowish-green | Yellowish-green | < |
| KUD5 | 1.39 ct. | Yellowish-green | Yellow-green | < |
| KUD7 | 1.53 ct. | Yellowish-green | Yellow-green | < |
| KUF | 3.52 ct. | Weak green | Yellowish-green | < |
| KTM | 2.08 ct. | Weak yellowish-green | Yellowish-green | < |
| KUD6 | 3.13 ct. | Weak orange | Orange | < |
| KUD3 | 3.88 ct. | Very weak brown | Greenish-brown | < |
| KSE4637 | 1.83 ct. | Very weak brown | Brown | < |
| KUH | 1.06 ct. | Inert | Inert | - |
| KME3887 | 1.90 ct. | Inert | Inert | - |
| KUD8 | 1.54 ct. | Inert | Inert | - |

# *Laboratory gemmology*

## Scanning Electron Microscopy

SEM provides possibilities of accurate identification of material with high magnification (Fig. 9). Besides inclusions already reported in the literature, SEM analysis of the sample KTJ1 identified further inclusions which have not yet been described in the literature:

- kornerupine as inclusion within the host kornerupine (**inclusion A**, Fig. 10-11),
- sphalerite (**inclusion B**, Fig. 12-13)
- and pyrite (**inclusion C**, Fig. 14-15).

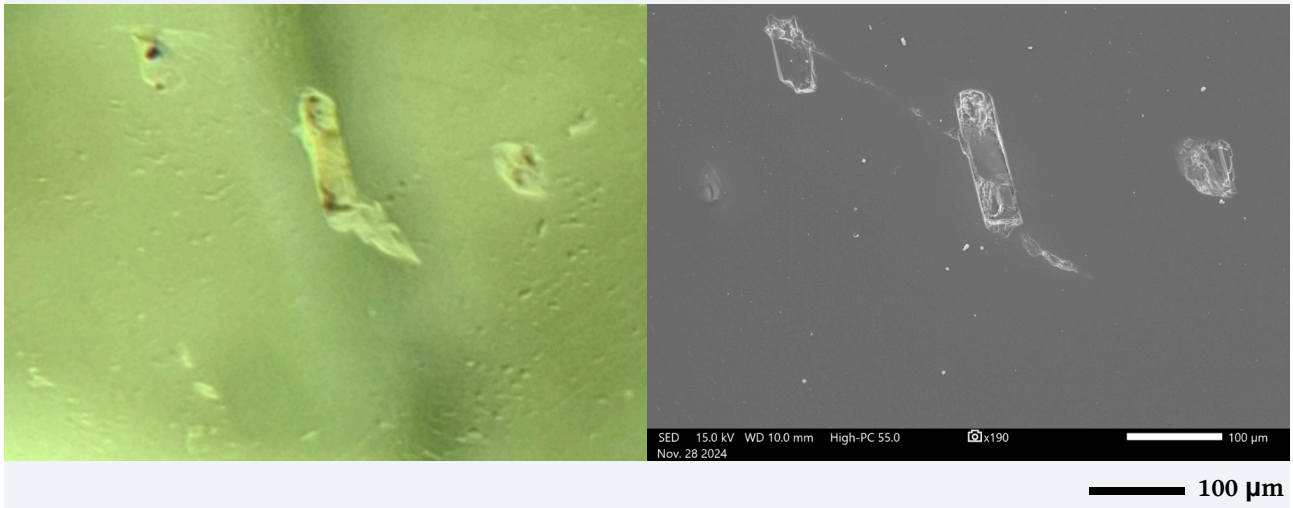


**Fig. 9** **Top**: Images of inclusions in the sample KTJ1, taken from a stereo microscope (left) and by Scanning Electron Microscope (right) using secondary electron detector (SED).
**Bottom left**: sample KTJ1 prepared for SEM analysis.

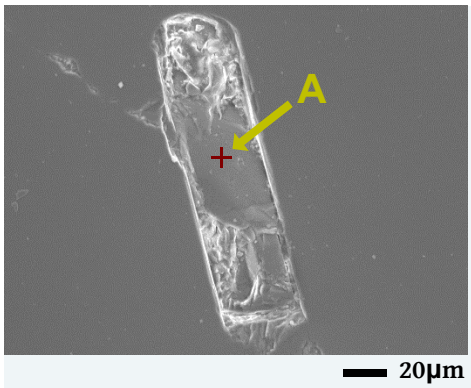


**Fig. 10**

**Left**: SEM image of a prismatic inclusion - inclusion A, taken with secondary electron detector (SED). Inclusion A was analysed at the position indicated by the arrow.

**Below**: chemical composition of inclusion A, identified as kornerupine.

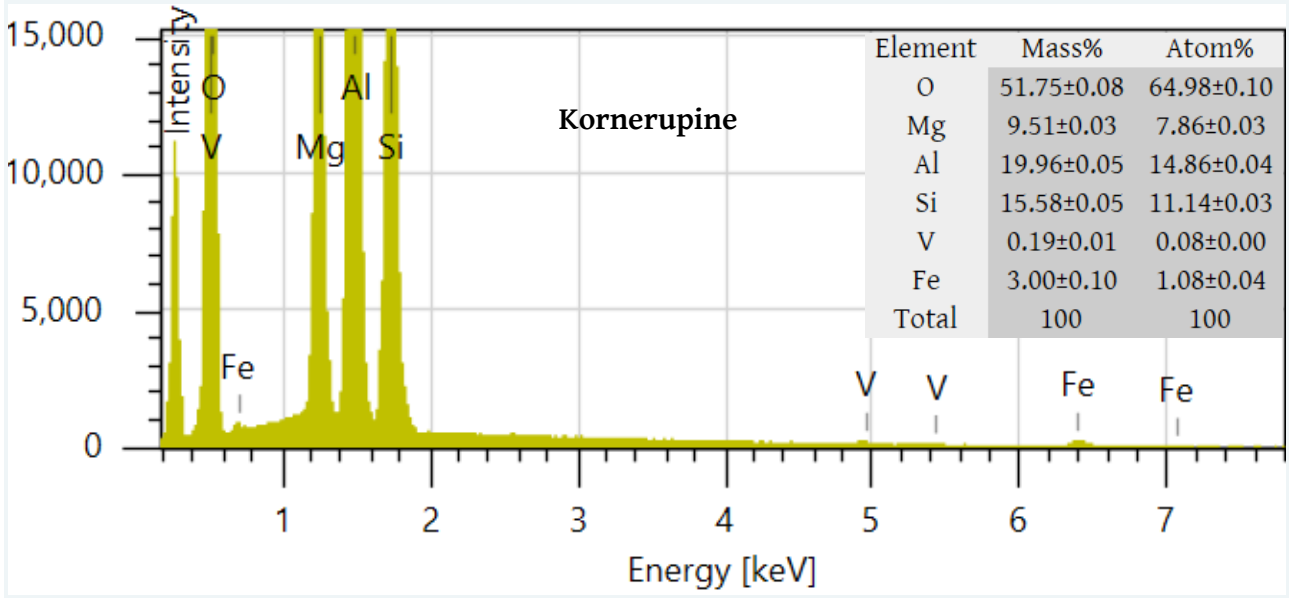


| Element | Mass% | Atom% |
|---|---|---|
| O | 51.75±0.08 | 64.98±0.10 |
| Mg | 9.51±0.03 | 7.86±0.03 |
| Al | 19.96±0.05 | 14.86±0.04 |
| Si | 15.58±0.05 | 11.14±0.03 |
| V | 0.19±0.01 | 0.08±0.00 |
| Fe | 3.00±0.10 | 1.08±0.04 |
| Total | 100 | 100 |

The chemistry of the inclusion A (SEM analysis, Fig. 10) was compared with that of the host kornerupine KTJ1 (EDXRF analysis, Fig. 11). Despite the difference of calculation methods between the two analytic instruments, it is obvious that the kornerupine inclusion (inclusion A) has significantly higher iron concentration than the host kornerupine KTJ1. The eventuality of inclusion A being a negative crystal is excluded: placed between crossed polarisation filters under microscope, it shines as a birefringent mineral inclusion; futhermore, inclusion A hosts further solid inclusions (Fig. 12).

| Compound | m/m% | StdErr | El | m/m% | StdErr |
|---|---|---|---|---|---|
| Al2O3 | 46.00 | 0.30 | Al | 24.34 | 0.16 |
| SiO2 | 29.39 | 0.22 | Si | 13.74 | 0.10 |
| MgO | 19.48 | 0.20 | Mg | 11.75 | 0.12 |
| CaO | 0.162 | 0.008 | Ca | 0.116 | 0.006 |
| TiO2 | 0.155 | 0.015 | Ti | 0.0927 | 0.0091 |
| V2O5 | 0.145 | 0.009 | V | 0.0812 | 0.0050 |
| MnO | 0.112 | 0.009 | Mn | 0.0868 | 0.0066 |
| Fe2O3 | 0.099 | 0.011 | Fe | 0.0694 | 0.0077 |
| SO3 | 0.060 | 0.022 | Sx | 0.0239 | 0.0090 |
| Sc2O3 | 0.0585 | 0.0033 | Sc | 0.0381 | 0.0021 |
| Cr2O3 | 0.0147 | 0.0015 | Cr | 0.0101 | 0.0010 |
| ZnO | 0.0119 | 0.0008 | Zn | 0.0096 | 0.0006 |
| K2O | 0.0062 | 0.0021 | K | 0.0051 | 0.0017 |
| Ga2O3 | 0.0054 | 0.0006 | Ga | 0.0040 | 0.0004 |

**Fig. 11** EDXRF analysis of sample KTJ1

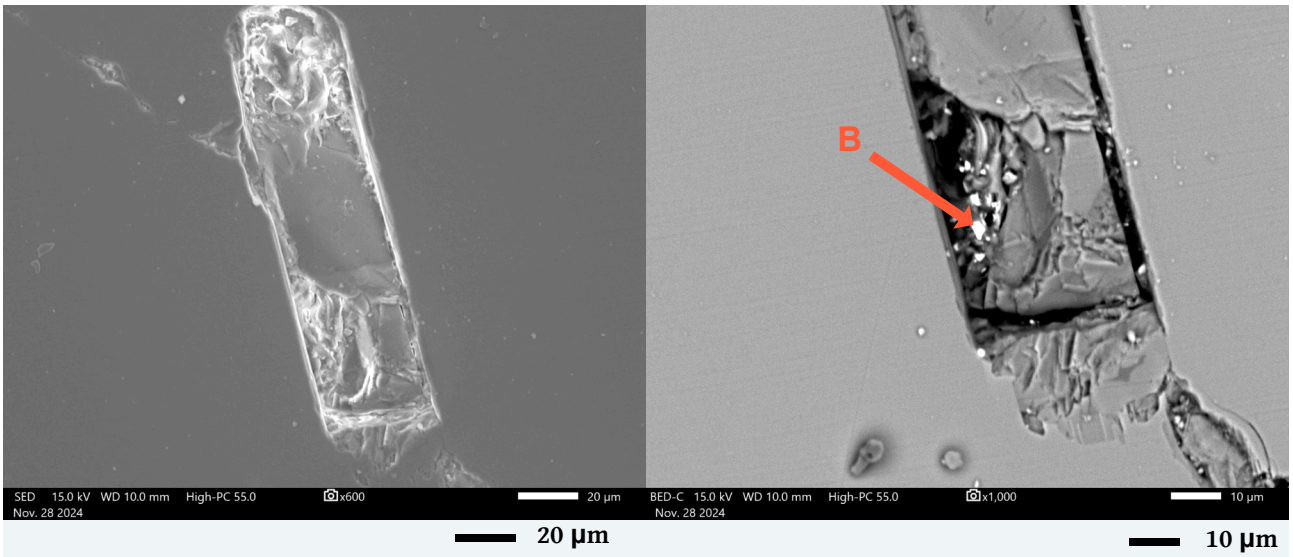


**Fig. 12** Image taken with SED (left) and BED (right) of a prismatic inclusion identified as kornerupine (inclusion A) hosting the inclusion B.

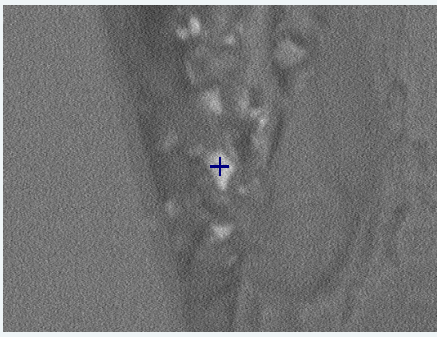


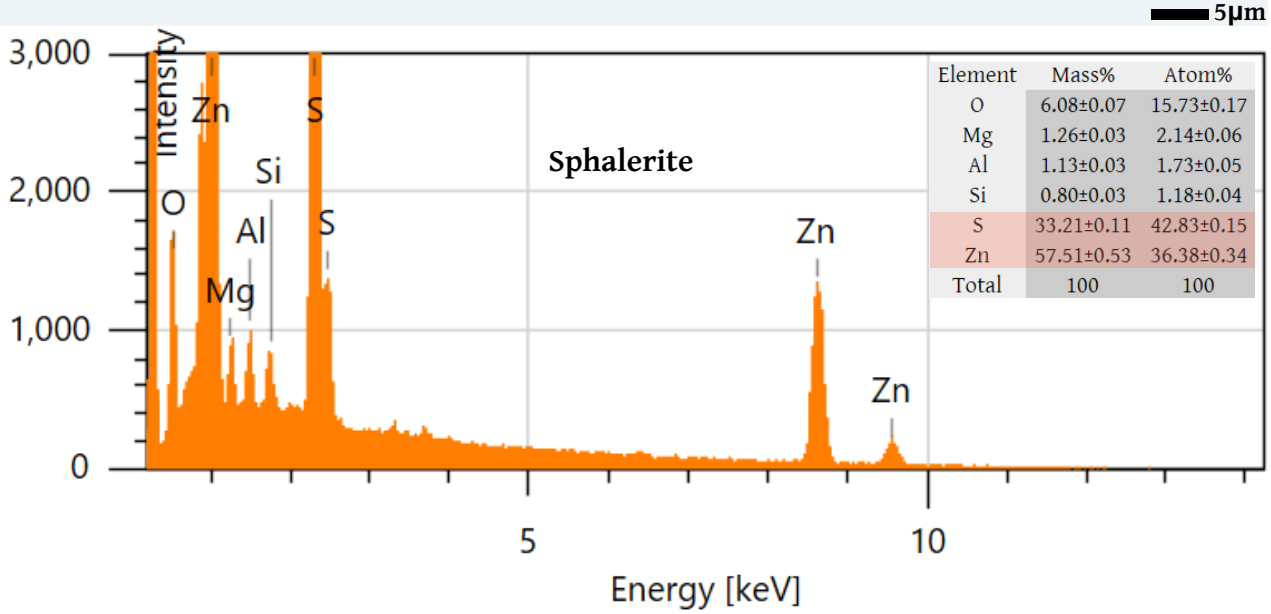


**Fig. 13** BED image (right) and chemical composition (bottom) of inclusion B, identified as sphalerite.

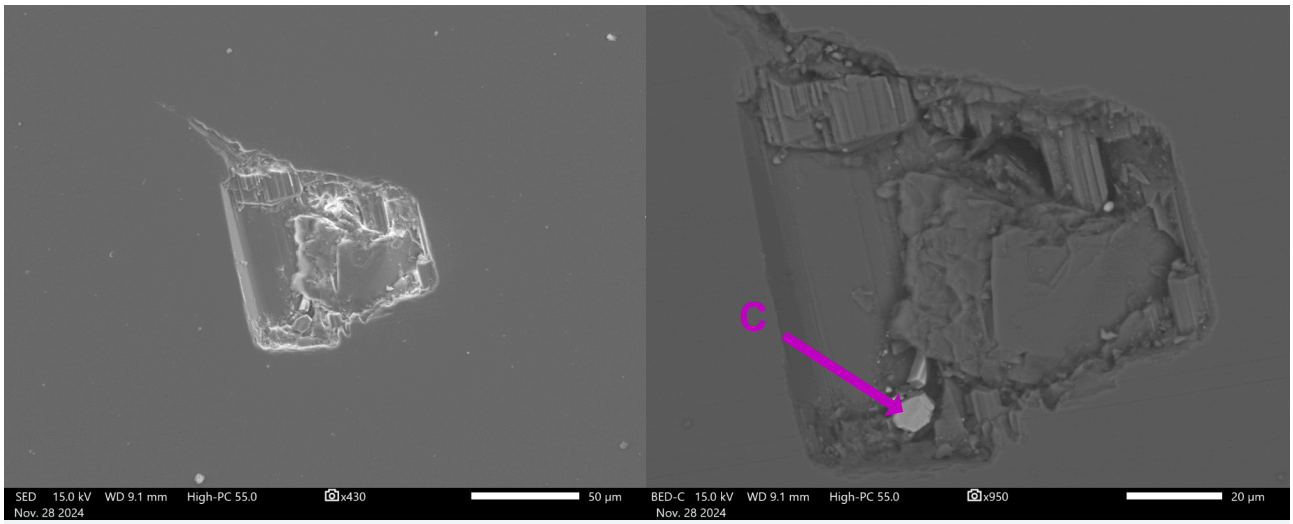


**Fig. 14** SED (left) and BED (right) images of the inclusion C within its hosting inclusion.

**Fig. 15** BED image (right) and chemical composition (bottom) of inclusion C, identified as pyrite.

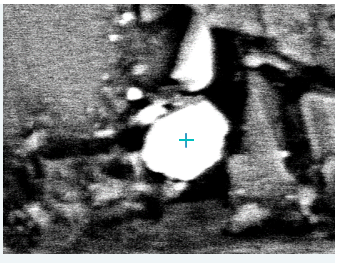


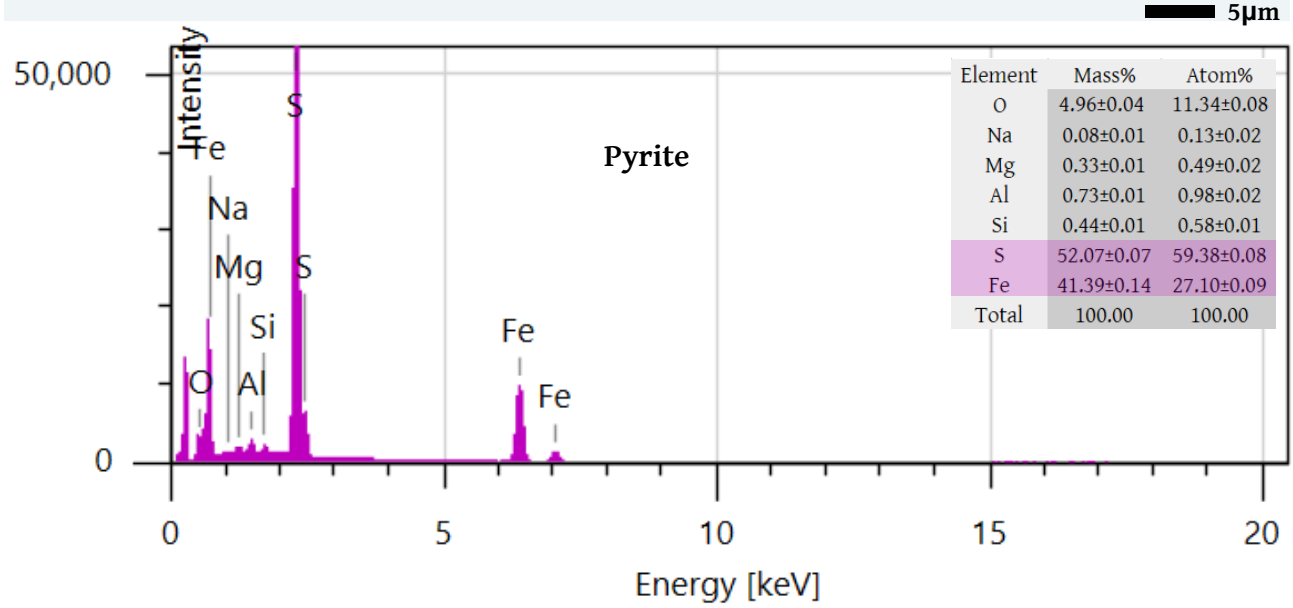


| Element | Mass% | Atom% |
|---|---|---|
| O | 4.96±0.04 | 11.34±0.08 |
| Na | 0.08±0.01 | 0.13±0.02 |
| Mg | 0.33±0.01 | 0.49±0.02 |
| Al | 0.73±0.01 | 0.98±0.02 |
| Si | 0.44±0.01 | 0.58±0.01 |
| S | 52.07±0.07 | 59.38±0.08 |
| Fe | 41.39±0.14 | 27.10±0.09 |
| Total | 100.00 | 100.00 |

## Raman spectroscopy

Acquired Raman spectra were imported in CystalSleuth to compare with the reference data. All 12 kornerupines spectra match to the RRUFF reference spectra of kornerupine *sensu lato*. Fig. 16 shows two examples of search results.

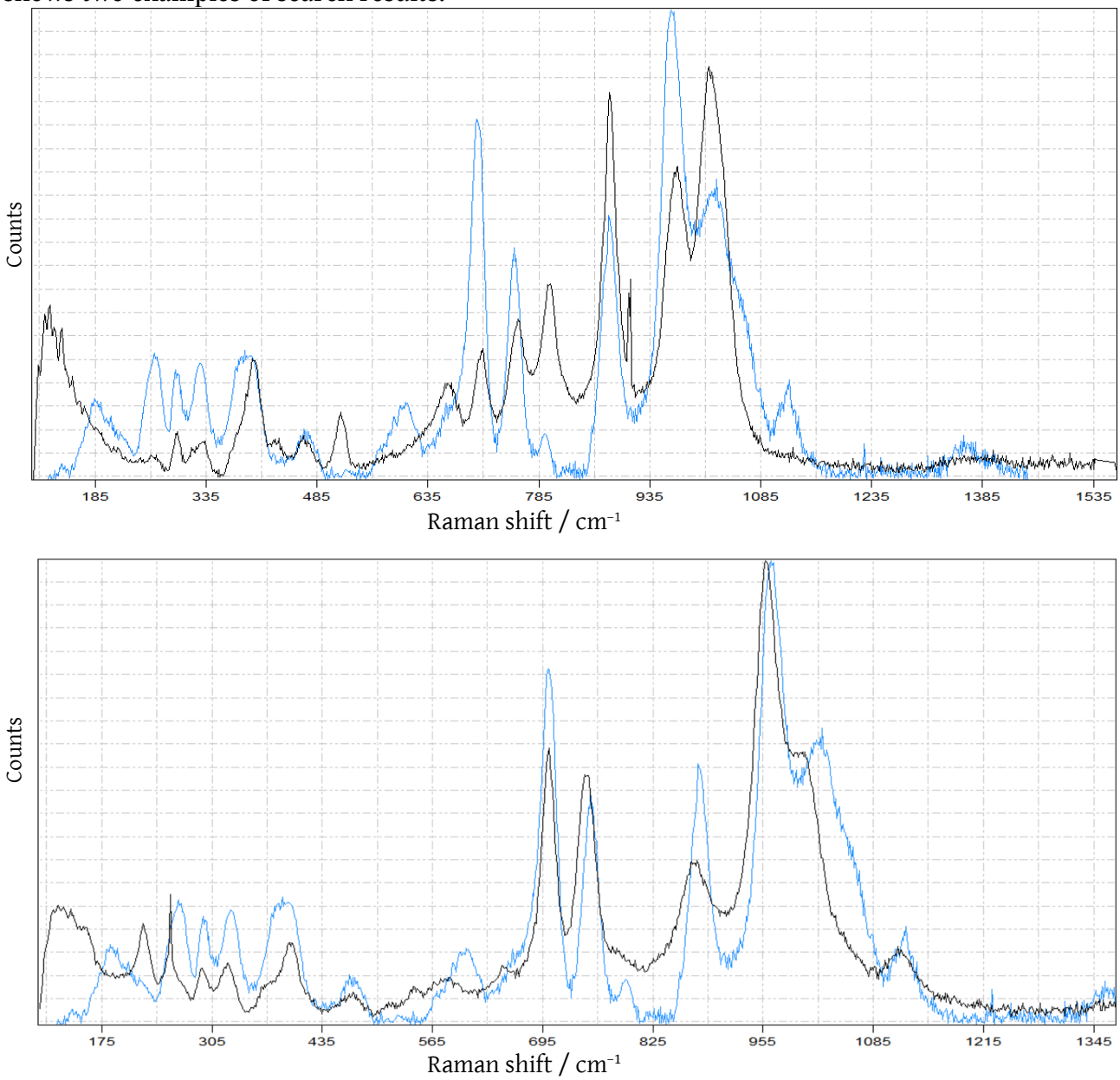


**Fig. 16** Raman spectra (in black colour) of KUD3 (top) and KUD6 (bottom) match to those of kornerupine in RRUFF reference data (blue).

The distinction between kornerupine *sensu stricto* and prismatine among the kornerupine samples was made according to the method of Wopenka et al.(1999)(Fig. 2).

The Raman spectra of all twelve samples were analysed. The spectrum of one sample (KUD6) shows no peak at ~803 $\Delta cm^{-1}$ and a weak peak at ~881 $\Delta cm^{-1}$, all other samples shows peak at ~803 $\Delta cm^{-1}$ and strong peak at ~881 $\Delta cm^{-1}$. Sample KUD6 is identified as kornerupine *sensu stricto* and all other samples as prismatines (Table 5). Fig. 17 displays the Raman spectra of the kornerupine *sensu stricto* (KUD6) and two prismatine samples (KTJ2 & KUD3).

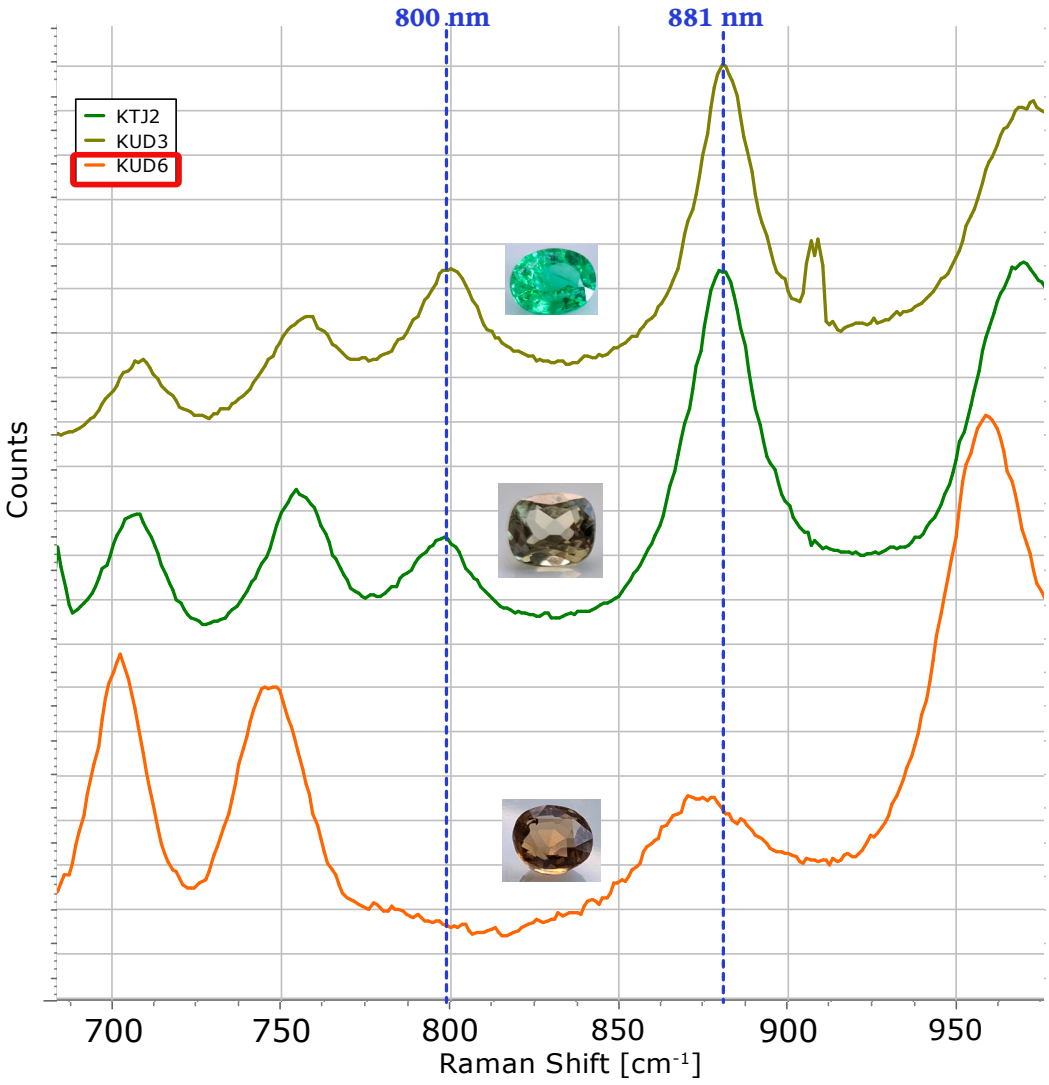


**Fig. 17** Raman spectra of three kornerupine samples

**Table 5** Result of Raman spectroscopy analysis

| Sample | Weight | Result |
|---|---|---|
| KTJ1 | 0.45 ct. | Prismatine |
| KTJ2 | 2.39 ct. | Prismatine |
| KUD5 | 1.39 ct. | Prismatine |
| KUD7 | 1.53 ct. | Prismatine |
| KUF | 3.52 ct. | Prismatine |
| KTM | 2.08 ct. | Prismatine |
| KUD6 | 3.13 ct. | Kornerupine *sensu stricto* |
| KUD3 | 3.88 ct. | Prismatine |
| KSE4637 | 1.83 ct. | Prismatine |
| KUH | 1.06 ct. | Prismatine |
| KME3887 | 1.90 ct. | Prismatine |
| KUD8 | 1.54 ct. | Prismatine |

## Energy-dispersive X-ray fluorescence (EDXRF) analysis

The EDXRF analysis was completed on all thirteen samples. Table 6 exposes the representative data, the complete data can be found in Appendix.

**Table 6** Result of EDXRF analysis

| Site | AND4100 | KTJ1 | KTJ2 | KUD5 | KUD7 | KUF | KTM | KUD6 | KSE4637 | KUD3 | KME3887 | KUH | KUD8 |
|---|---|---|---|---|---|---|---|---|---|---|---|---|---|
| Al2O3 | 61.92 | 46.00 | 44.57 | 45.02 | 44.78 | 44.43 | 43.93 | 43.31 | 42.99 | 42.54 | 43.06 | 43.79 | 40.54 |
| SiO2 | 36.80 | 29.39 | 29.89 | 29.87 | 30.43 | 30.26 | 30.25 | 27.92 | 30.13 | 29.92 | 29.07 | 28.46 | 29.01 |
| MgO | 0.93 | 19.48 | 20.56 | 19.99 | 19.32 | 20.27 | 21.04 | 19.75 | 20.33 | 19.91 | 19.22 | 17.63 | 15.14 |
| CaO | 0.00 | 0.16 | 0.07 | 0.06 | 0.25 | 0.06 | 0.04 | 0.10 | 0.06 | 0.15 | 0.04 | 0.04 | 1.87 |
| TiO2 | 0.01 | 0.16 | 0.11 | 0.01 | 0.13 | 0.05 | 0.03 | 0.15 | 0.05 | 0.03 | 0.03 | 0.00 | 0.30 |
| V2O5 | 0.01 | 0.15 | 0.18 | 0.23 | 0.17 | 0.08 | 0.01 | 0.02 | 0.03 | 0.01 | 0.00 | 0.00 | 0.06 |
| MnO | 0.00 | 0.11 | 0.17 | 0.20 | 0.27 | 0.12 | 0.06 | 0.01 | 0.02 | 0.02 | 0.15 | 0.11 | 0.19 |
| Fe2O3 | 0.22 | 0.10 | 0.06 | 0.05 | 0.06 | 0.17 | 0.08 | 1.38 | 2.04 | 3.05 | 4.04 | 5.57 | 8.05 |
| BaO | 0.00 | 0.00 | 0.03 | 0.00 | 0.03 | 0.00 | 0.00 | 0.00 | 0.00 | 0.00 | 0.00 | 0.00 | 0.00 |
| SO3 | 0.00 | 0.06 | 0.00 | 0.00 | 0.00 | 0.00 | 0.00 | 0.00 | 0.00 | 0.00 | 0.00 | 0.00 | 0.22 |
| Sc2O3 | 0.00 | 0.06 | 0.02 | 0.02 | 0.05 | 0.00 | 0.02 | 0.00 | 0.00 | 0.00 | 0.01 | 0.00 | 0.00 |
| Cr2O3 | 0.00 | 0.01 | 0.02 | 0.01 | 0.02 | 0.22 | 0.25 | 0.01 | 0.00 | 0.00 | 0.00 | 0.00 | 0.10 |
| ZnO | 0.00 | 0.01 | 0.01 | 0.00 | 0.00 | 0.01 | 0.00 | 0.00 | 0.00 | 0.01 | 0.01 | 0.02 | 0.06 |
| K2O | 0.01 | 0.01 | 0.01 | 0.00 | 0.02 | 0.01 | 0.00 | 0.01 | 0.01 | 0.01 | 0.01 | 0.00 | 0.04 |
| Cl | 0.00 | 0.00 | 0.00 | 0.01 | 0.02 | 0.02 | 0.00 | 0.01 | 0.00 | 0.01 | 0.01 | 0.01 | 0.04 |
| Co3O4 | 0.00 | 0.00 | 0.00 | 0.00 | 0.00 | 0.00 | 0.00 | 0.00 | 0.01 | 0.00 | 0.04 | 0.04 | 0.07 |
| Ga2O3 | 0.01 | 0.01 | 0.00 | 0.00 | 0.00 | 0.01 | 0.01 | 0.00 | 0.00 | 0.01 | 0.00 | 0.01 | 0.01 |
| P2O5 | 0.08 | 0.00 | 0.00 | 0.00 | 0.00 | 0.00 | 0.00 | 0.00 | 0.00 | 0.00 | 0.00 | 0.00 | 0.00 |
| B2O3 (fixed) | 3.30 | 3.30 | 3.30 | 3.30 | 3.30 | 3.30 | 3.30 | 3.30 | 3.30 | 3.30 | 3.30 | 3.30 | 3.30 |
| H2O (fixed) | 1.00 | 1.00 | 1.00 | 1.00 | 1.00 | 1.00 | 1.00 | 1.00 | 1.00 | 1.00 | 1.00 | 1.00 | 1.00 |

## Ultraviolet-Visible-Near Infrared (UV-Vis-NIR) spectroscopy

The absorption spectra of samples of the Brown-Yellow-Green series share common features with two main absorption bands in the range of 315nm to 382nm and 1024nm to 1049nm, weaker absorption at 445nm, 500nm. The spectrum of KUD8 shows an extra band at 681nm and a shoulder at 760nm, and the spectrum of KUD6 shows an extra shoulder at 454nm.

The absorption spectra of the green kornerupine samples (KTJ1, KTJ2, KUD5 and KUD7) share common features with two main absorption bands at 418nm, 675nm and a weak shoulder at 454nm.

The absorption spectra of the blue to violet samples (KUF and KTM) share common bands/ shoulders at 384nm, 434nm, 526nm, 578nm, 681nm and 760nm.

UV-Vis-NIR spectra of the samples are interpreted and further discussed in the section Disscusion.

## Fourier-Transform Infrared (FTIR) spectroscopy

FTIR absorption spectra were acquired for all kornerupine samples. A certain similarity of the spectral pattern could be observed among kornerupines of the Brown-Yellow-Green series and those of the Green-Blue-Violet series (Fig. 19-20). As all the FTIR absorption spectra show total absorption between 2000cm$^{-1}$ and 400cm$^{-1}$, FTIR reflection spectra of two samples (KUD5&KUD6) were acquired to further explore this region (Fig. 21).

Fig. 18 illustrates the FTIR absorption spectrum of sample KUD5. The broad absorption bands observed between 3630cm$^{-1}$ and 3000cm$^{-1}$ is related to stretching of O-H. The sharp bands between 6000cm$^{-1}$ and 4000cm$^{-1}$ could be the combination of stretching and bending of water including fluids and water in the structure. The strong absorption bands around 7000cm$^{-1}$ is related to stretching of O-H.

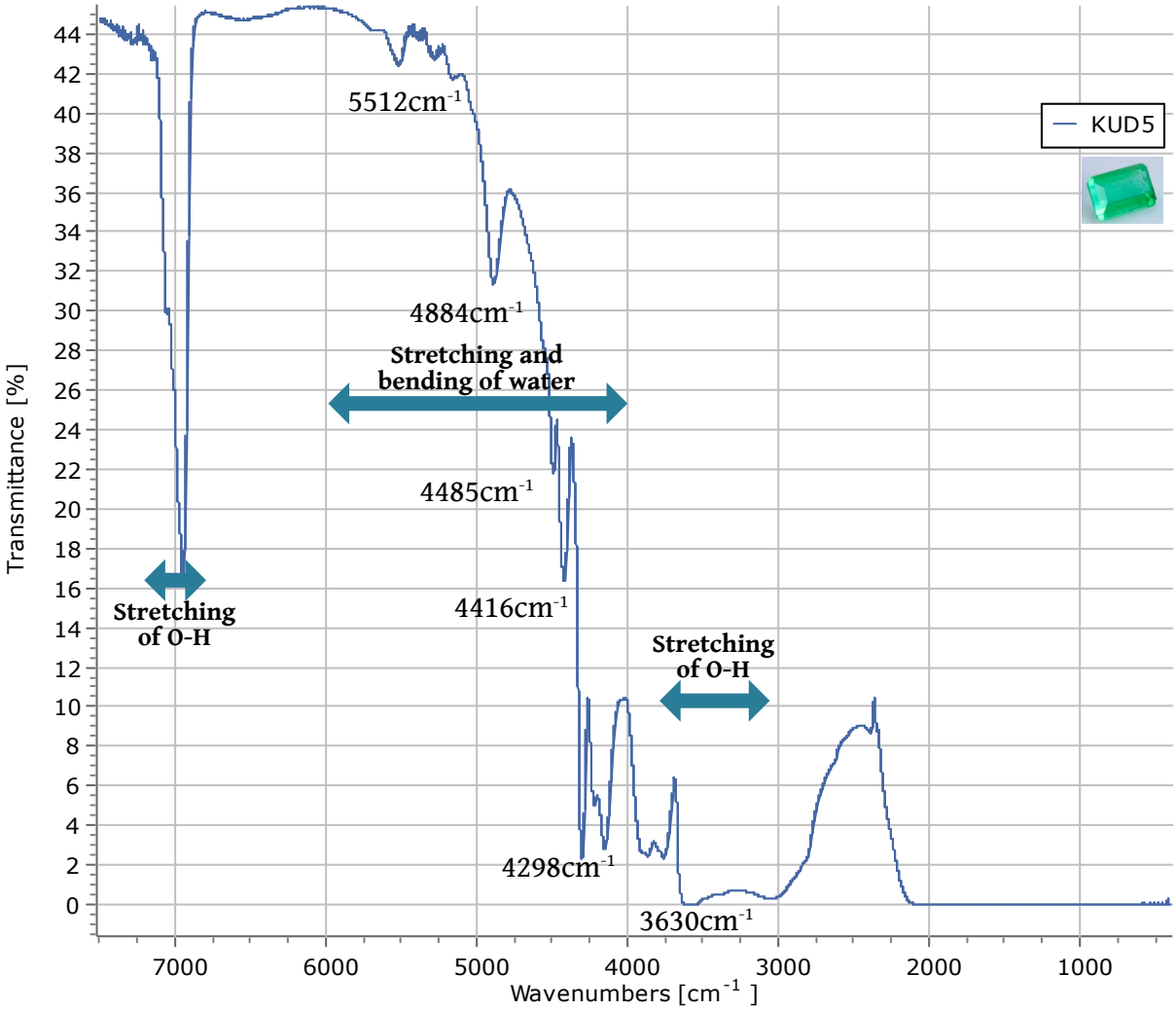


**Fig. 18** FTIR absorption spectrum of sample KUD5

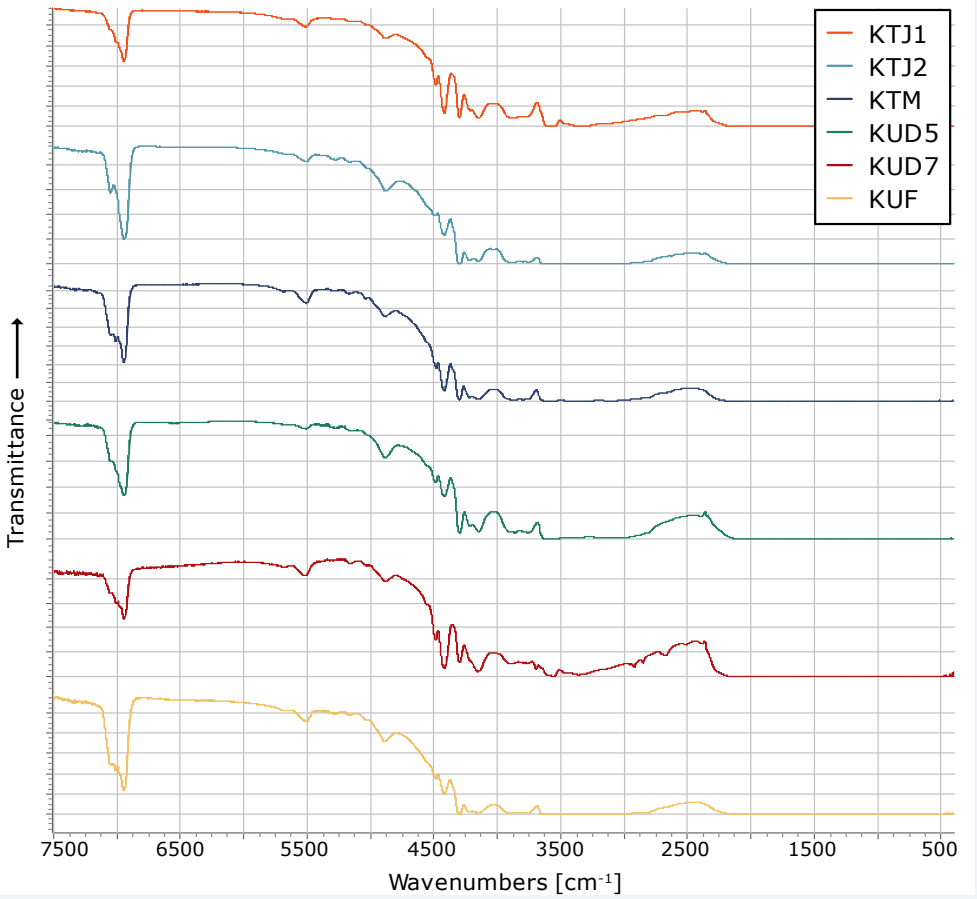


**Fig. 19**
FTIR absorption spectra of Green-Blue-Violet series

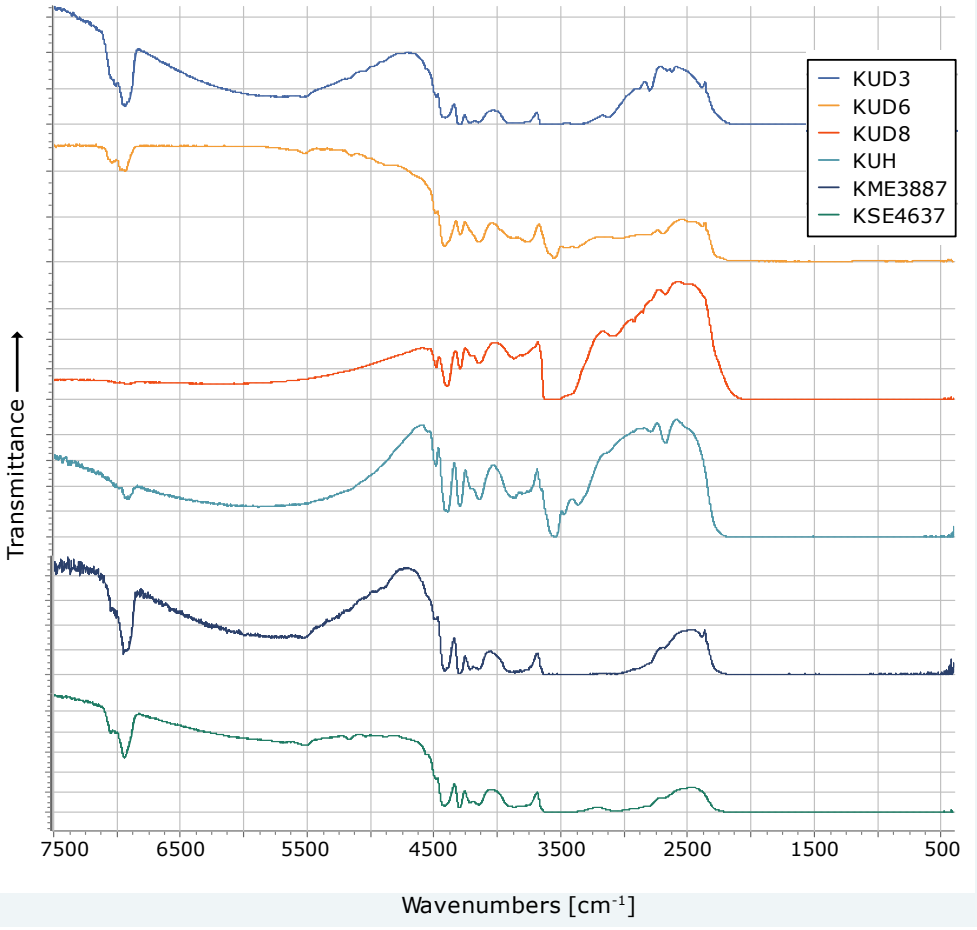


**Fig. 20**
FTIR absorption spectra of Brown-Yellow-Green series

Moenke researched on the recognition of $BO_3$ and $BO_4$ in different boron silicates including kornerupine through FTIR spectra. According to Moenke, the absorption bands in the fingerprint region of the FTIR spectrum show vibrations of tetrahedral boron in kornerupine (Fig. 21). Subsequent X-ray structural analyses and infrared studies confirmed the implications of these assignments for borosilicate structures. (1974).

FTIR reflection spectra of samples KUD5 and KUD6 are illustrated in Fig. 22. It turns out that, except from some minor shift which might be partly related to the stretching and bending of Si-O, the positions of major bands (Fig. 22) match to those in Fig. 21. As samples KUD5 and KUD6 have been identified respectively as prismatine and kornerupine *sensu stricto*, the difference or the correlation of fingerprint region of FTIR spectra between korunerupine *sensu stricto* and prismatine deserves further investigation.

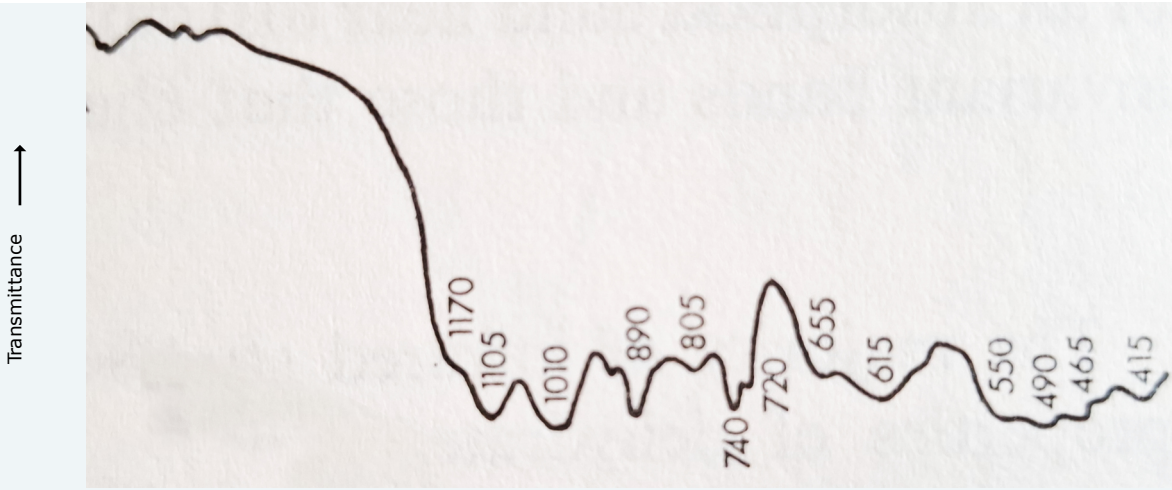


**Fig. 21** Recognition of $BO_4$ in kornerupine (Moenke, 1974)

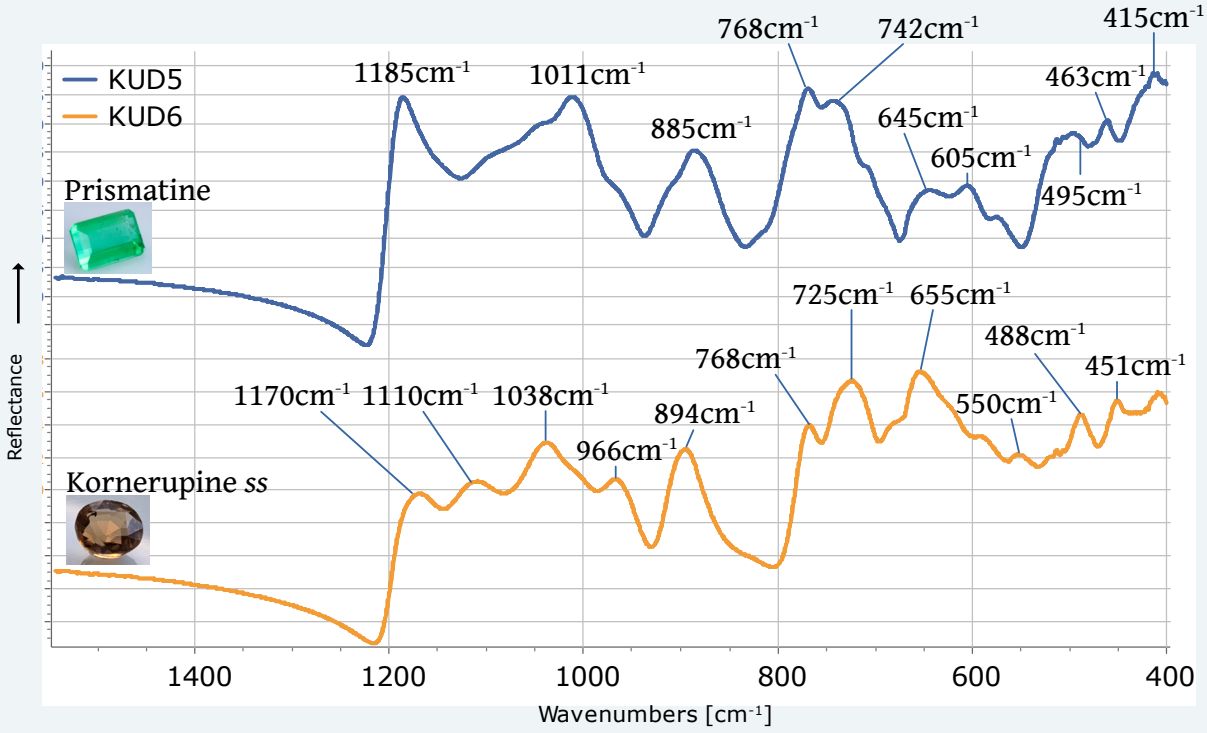


**Fig. 22** FTIR reflection spectra of samples KUD5 and KUD6

# Discussion

## *Colouring agents*

Colours of kornerupine *sensu lato,* caused by traces of the elements iron, chromium and vanadium, have been described in the literature. Iron-bearing and thus Fe-coloured kornerupines range in colour from brown to yellow to green. $V^{3+}$-coloured green kornerupines of gem quality have been found in Kenya since the early 1970s. Schmetzer describes the colour variation in vanadium- and chromium-bearing East African kornerupines as follows:

- V> Cr => green,
- V≈Cr => blue-green,
- Cr>V => blue.

(Schmetzer et al., 1974; Schmetzer, 1977; Schmetzer, 1982; Henn, 1985; Milisenda and Wehr, 2009; Henn, 2019)

EDXRF analysis result (Table 7) of the twelve kornerupine samples shows:

- Iron concentration is predominant (9,660–56,300 ppmw) in the samples of Brown-Yellow-Green series (illustrated in brown) - KUD6, KSE4637, KUD3, KME3887, KUH and KUD8.
- Vanadium concentration is predominant (812–1260 ppmw) in the green samples (illustrated in green) - KTJ1, KTJ2, KUD5 and KUD7, with lower concentration of iron (349–694 ppmw) and significantly lower concentration of chromium (92–146 ppmw).
- Chromium concentration is predominant (1480–1720 ppmw) in the green-blue and blue-violet samples (illustrated in blue) - KUF and KTM, with a lower concentration of iron (532–1,170 ppmw) and significantly lower concentration of vanadium (35–439 ppmw).

**Table 7** Concentration of V, Cr and Fe in the twelve kornerupine samples (EDXRF analysis)

| Sample | Element (ppmw) | | |
|---|---|---|---|
| | V | Cr | Fe |
| KTJ1 | 812 | 101 | 694 |
| KTJ2 | 1,010 | 146 | 418 |
| KUD5 | 1,260 | 92 | 349 |
| KUD7 | 946 | 143 | 387 |
| KUF | 439 | 1,480 | 1,170 |
| KTM | 35 | 1,720 | 532 |
| KUD6 | 85 | 86 | 9,660 |
| KSE4637 | 147 | ND | 14,300 |
| KUD3 | 53 | ND | 21,300 |
| KME3887 | ND | ND | 28,300 |
| KUH | ND | ND | 39,000 |
| KUD8 | 308 | 681 | 56,300 |

The following terms are used for samples with similar colouring agents (Fig. 23):

- Iron kornerupine – high concentration of iron, ND or significantly lower concentration of chromium and vanadium;
- Vanadium kornerupine – high concentration of vanadium, significantly lower concentration of chromium and iron;
- Chromium kornerupine – high concentration of chromium, lower concentration of iron, significant lower concentration of vanadium.


**Fig. 23** Kornerupine samples according to colouring agents

The UV-Vis-NIR Absorption spectra acquired are mainly unpolarised due to the fact that the samples are all cut stones.

Fig. 24 illustrates the UV-Vis-NIR spectra of three kornerupine samples belonging respectively to vanadium kornerupine (KTJ1), chromium kornerupine(KTM) and iron kornerupine (KUH).

- The green colour of sample KTJ1 originates from:
  - absorption bands related to $V^{3+}$ at 454nm and 675nm
  - and transmission window with maximum at 528nm in the green range of visible region.
- The blue-violet colour of sample KTM is due to:
  - absorption bands related to $Cr^{3+}$ at 384nm, 434nm, 526nm and 578nm,
  - transmission window with maximum at 470nm in the violet-blue range of visible range.
- The brownish-green colour of sample KUH results from:
  - absorption of $Fe^{3+}$ at 445nm and 500nm,
  - weak transmission at 480nm in the blue range and a continuum starting from transmission at 525nm in the green range toward absorption of $Fe^{2+}$ in the near infrared region.
- Absorption bands in the region 1420-1450nm are related to water.
- Absorption band at 1050nm of sample KUH is related to $Fe^{2+}$.

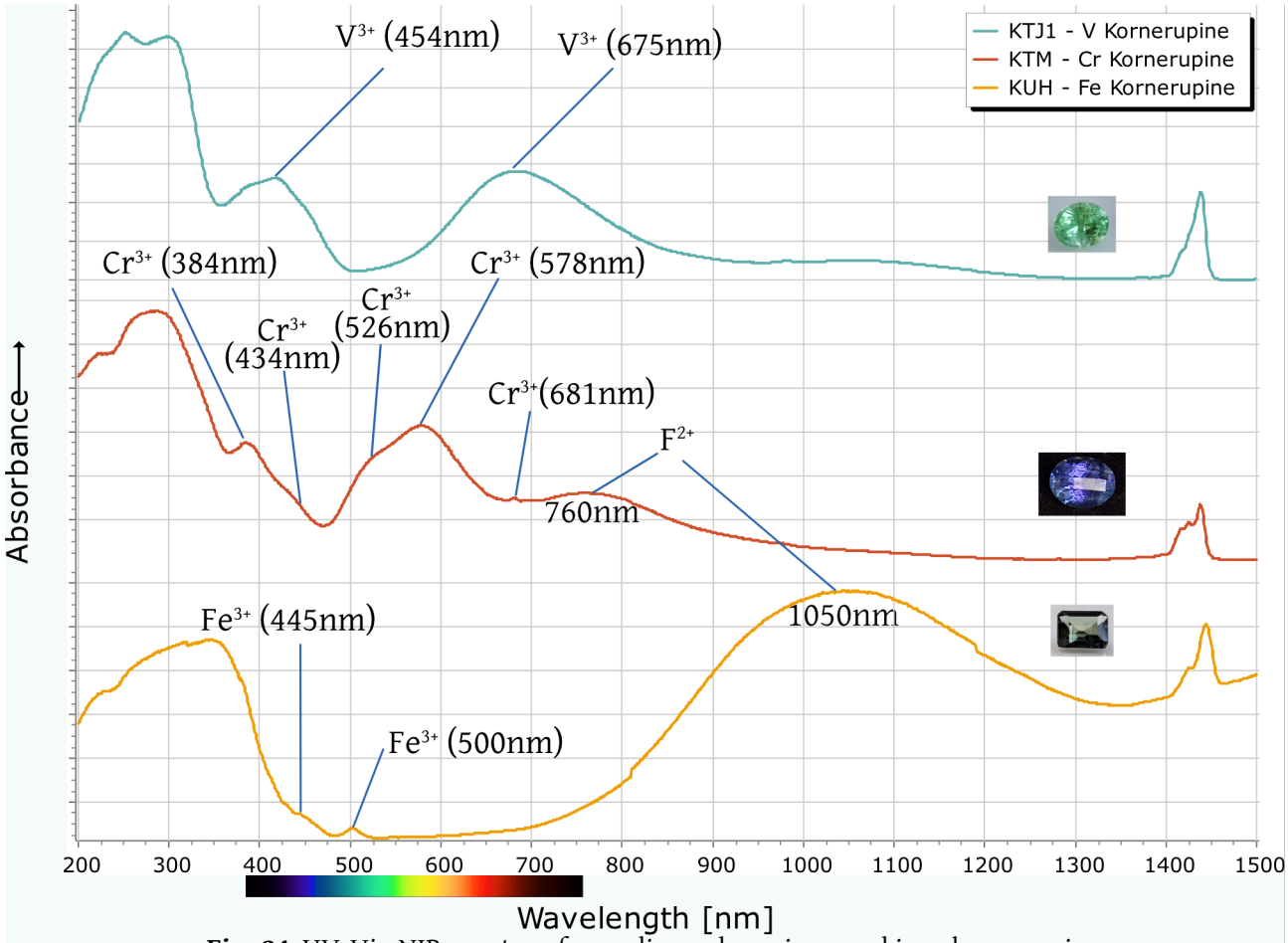


**Fig. 24** UV-Vis-NIR spectra of vanadium, chromium and iron kornerupines

Polarised UV-Vis-NIR spectra were acquired for sample KUD7 (Fig. 25), a green kornerupine with cat's-eye effect. The measurement of polarised spectra for this sample was possible due to the orientation of hollow tubes which are not only responsible to the cat's-eye effect but also helps to give a hint on the crystal axes. The polarised spectra show the absorption bands which are predominantly related to $V^{3+}$ and secondarily related to $C^{3+}$, two colouring agents responsible to the green colour of the sample KUD7.

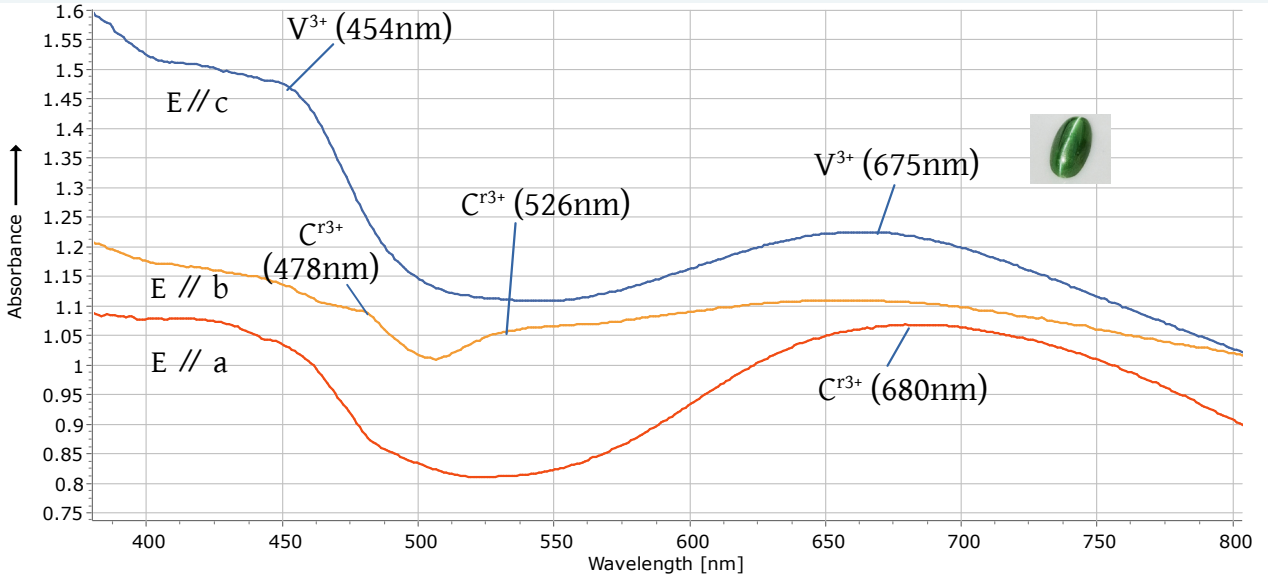


**Fig. 25** Polarised UV-Vis-NIR spectra of sample KUD7

## *Luminescence*

Distinct luminescence was observed in the andalusite sample and six kornerupine samples of the Green-Blue-Violet series (Fig. 8). The emission and excitation maxima of all seven samples are located at similar areas, which explain their luminescence colours in the range of yellow and green (Table 4).

Fig. 26 illustrates the emission and excitation spectra of sample KUD5 under respectively 254nm excitation and 565nm emission:

- Emission spectrum under short-wave 254nm excitation displays an intensive broad band emission with maximum at 559nm, with full width at half maximum (FWHM) ~150nm;
- Excitation spectrum under 565nm emission peaks at 273nm in the short-wave to middle-wave range, with FWHM ~70nm.

Luminescence decay time of sample KUD5 (see appendix) is:

- 22 microseconds under λex = 265nm and λem = 550nm;
- 14 microseconds under λex = 325nm and λem = 550nm.

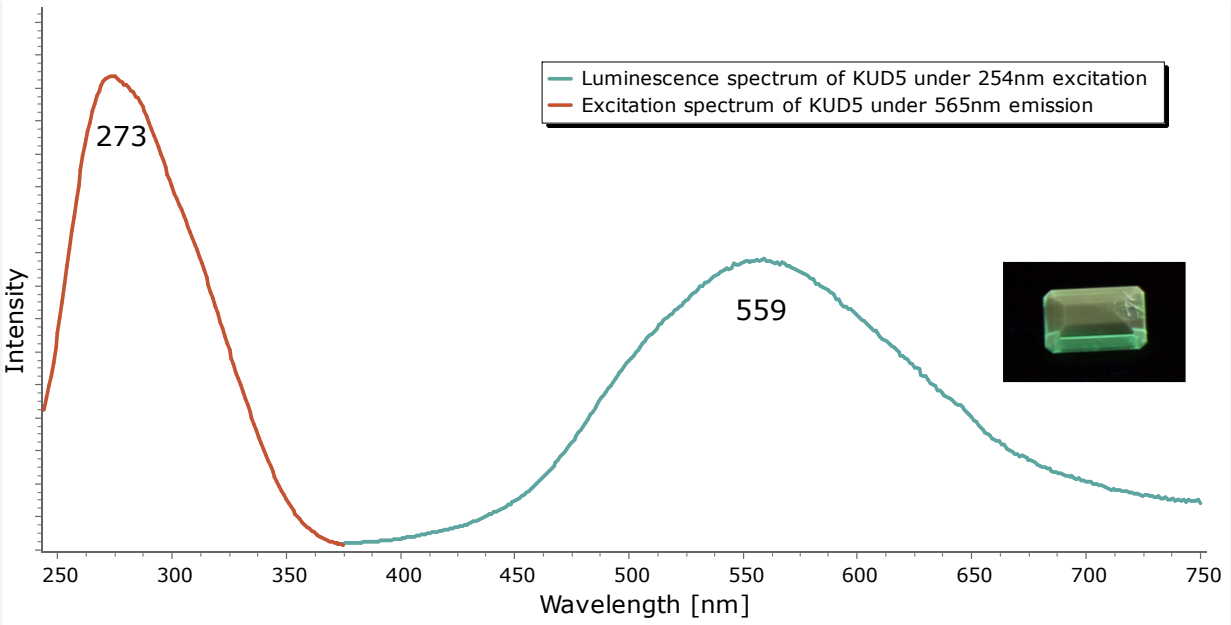


**Fig. 26** Luminescence spectrum (on the right) and excitation spectrum (on the left) of sample KUD5

**Table 8** Emission and excitation maxima of the andalusite sample and kornerupine samples of the Green-Blue-Violet series at room temperature.

| Sample | Emission Maxima | | Excitation Maxima |
|---|---|---|---|
| | λex = 254 nm | λex = 365 nm | |
| AUE4100 | 441 | 437 | 257 |
| KTJ1 | 552 | 567 | 289 |
| KTJ2 | 557 | 551 | 271 |
| KUD5 | 559 | 551 | 273 |
| KUD7 | 575 | 575 | 261 |
| KUF | 541 | 551 (λex =318nm) | 317 |
| KTM | 568 | 435 | 292 |

Similar spectroscopic characteristics are observed in the luminescent samples (Fig. 27-28):

- All emission spectra display a broad band
  - centred between 441nm and 575nm under short-wave excitation and between 437nm and 575nm under long-wave excitation
  - with an average full width at half maximum (FWHM) of ~150nm.
- All excitation spectra display an asymmetric band
  - centred between 257nm and 317nm
  - with an average FWHM of ~70nm

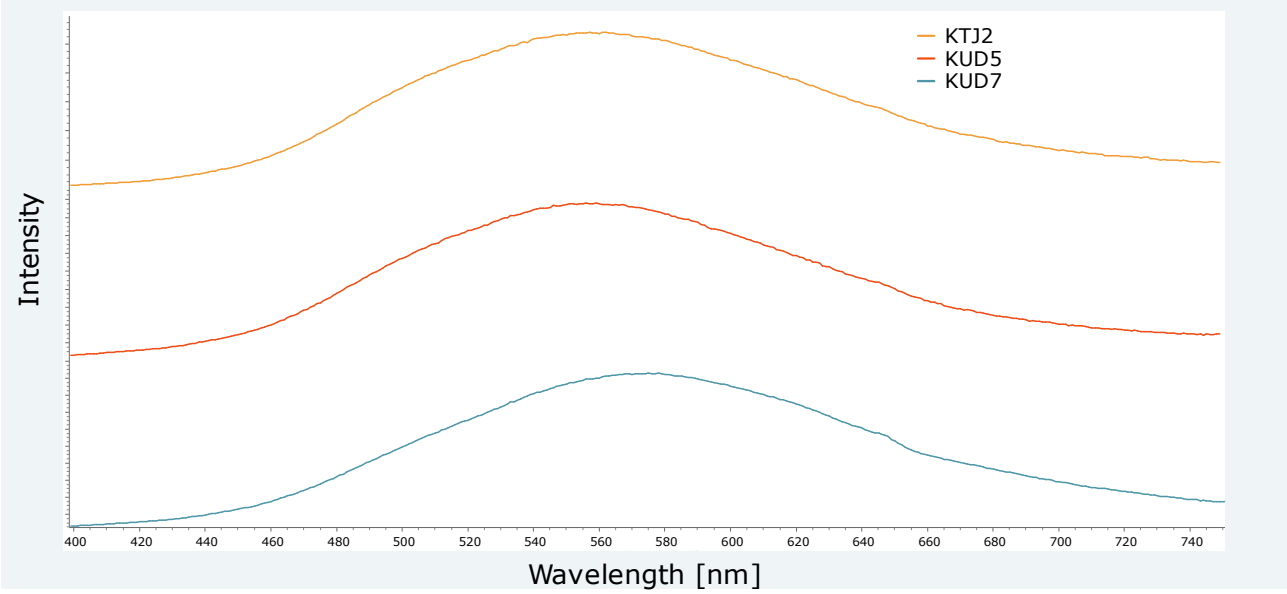


**Fig. 27** Emission spectra of three green kornerupine samples under λ ex = 254 nm at room temperature

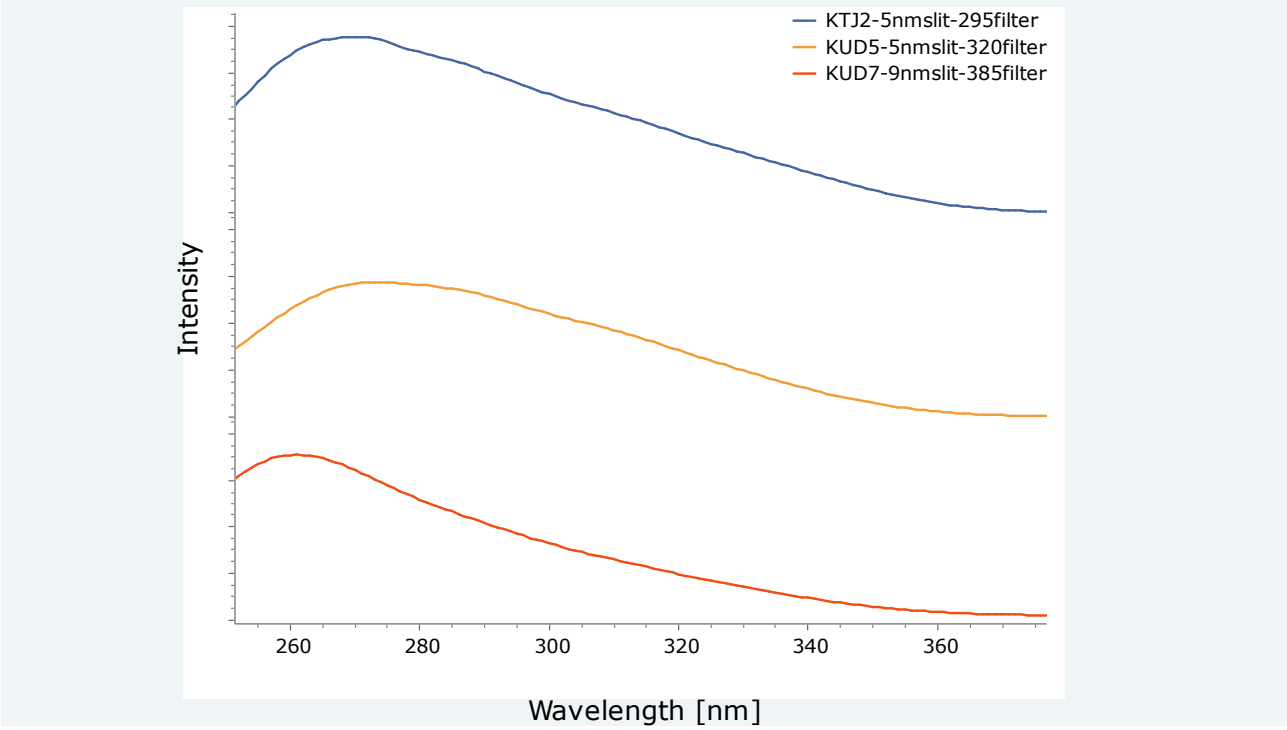


**Fig. 28** Excitation spectra of three green kornerupine samples under λ em = 550 nm for sample KTJ2, λ em=565 nm for sample KUD5 and λ em=570 nm forKUD7 at room temperature

Luminescence decay time was measured for fours samples and it varies from 8 to 28 microseconds.

The above mentioned luminescence characteristics of the seven samples are similar to those of titanate emission described by Gaft et al. (2015) and Vigier et al. (2023):

- A broad emission short-wave UV with
  - maximum 420-480 nm
  - FWHM ~100 nm
- Excitation spectrum
  - peaking in the short-wave UV to middle-wave UV range
  - FWHM ~50 nm
- Luminescence decay time is about 20 microseconds in average.

An example of intrinsic luminescence emission spectra of benitoite, titanium-bearing mineral $BaTiSi_3O_9$, show the above mentioned characteristics (Fig. 29).

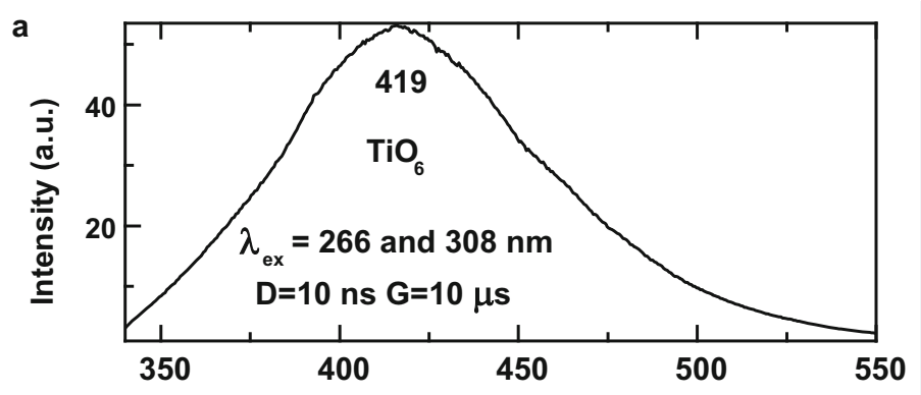


**Fig. 29** Laser-induced time-resolved luminescence spectra of benitoite demonstrating $TiO_6$ centre (Gaft et al., 2015)

**Table 9** Concentration of Ti and Fe from EDXRF analysis

| Sample | | Element (ppmw) | |
|---|---|---|---|
| | | Ti | Fe |
| Luminescent | AUE4100 | 82 | 1,550 |
| | KTJ1 | 927 | 694 |
| | KTJ2 | 649 | 418 |
| | KUD5 | 761 | 349 |
| | KUD7 | 786 | 387 |
| | KUF | 270 | 1,170 |
| | KTM | 260 | 532 |
| Faintly Luminescent | KUD6 | 902 | 9,660 |
| | KSE4637 | 314 | 14,300 |
| | KUD3 | 152 | 21,300 |
| Inert | KME3887 | 308 | 28,300 |
| | KUH | ND | 39,000 |
| | KUD8 | 1,800 | 56,300 |

The chemistry of the luminescent samples (Table 9) provides a further support to a possible correlation between intensity of luminescence and concentration of titanium in kornerupine: under both SWUV and LWUV light, the yellow-green range luminescence of the samples with higher concentration of titanium, unless quenched by a high concentration of iron, seems to be more intense than those with lower concentration of titanium.

Many titanium-containing minerals are known to have blue-to-blue-green short-wave-excited luminescence but titanate related luminescence is not restricted to blue short-wave ultraviolet luminescence. Some minerals emit a green to a yellow luminescence with the same excitation spectrum and similar lifetimes to blue short-wave luminescence. This is recorded for natural minerals such as andalusite, topaz, cassiterite, lorenzite, talc, uvarovite, baghdadite , chrysoberyl: alexandrite and enstatites. (Vigier et al., 2023)

Although one andalusite sample was included for this research work, it would be helpful to collect more andalusite samples and especially those display a distinct so called “mustard-coloured” luminescence, with the aim of a more effective comparison to korneruprine on luminescence.

Analysis of luminescence parameters combined with chemistry of the luminescent kornerupine samples suggests a possible luminescence activator in kornerupine *sensu lato*: titanate.

# Conclusion

Minerals of the Kornerupine Group/Kornerupine *sensu lato* include kornerupine *sensu stricto* and prismatine, members of an isomorphic series differing in boron content. Analytical technology such as Laser Ablation Inductively Coupled Plasma Mass Spectrometry (LA-ICP-MS) allows detection of the boron content in the mineral. Raman spectroscopy turns out to be an effective method for the separation between kornerupine *sensu stricto* and prismatine.

Pyrite, sphalerite and kornerupine were detected as inclusions in minerals of the kornerupine group.

$V^{3+}$, $Cr^{3+}$ and $Fe^{3+}$ are the colouring agents of kornerupine *sensu lato.*The correlation between vanadium, chromium and iron within the sample has direct impact on the colour and pleochroism of kornerupine.

Titanate could be the luminescence activator of kornerupine *sensu lato.*

The assumption stays still exploratory at this stage. Further research needs to be carried out.

# Appendix

## *Sample KTJ1*

*KTJ1*

*5.06 x 4.13 x 2.97 mm*

Raman spectrum

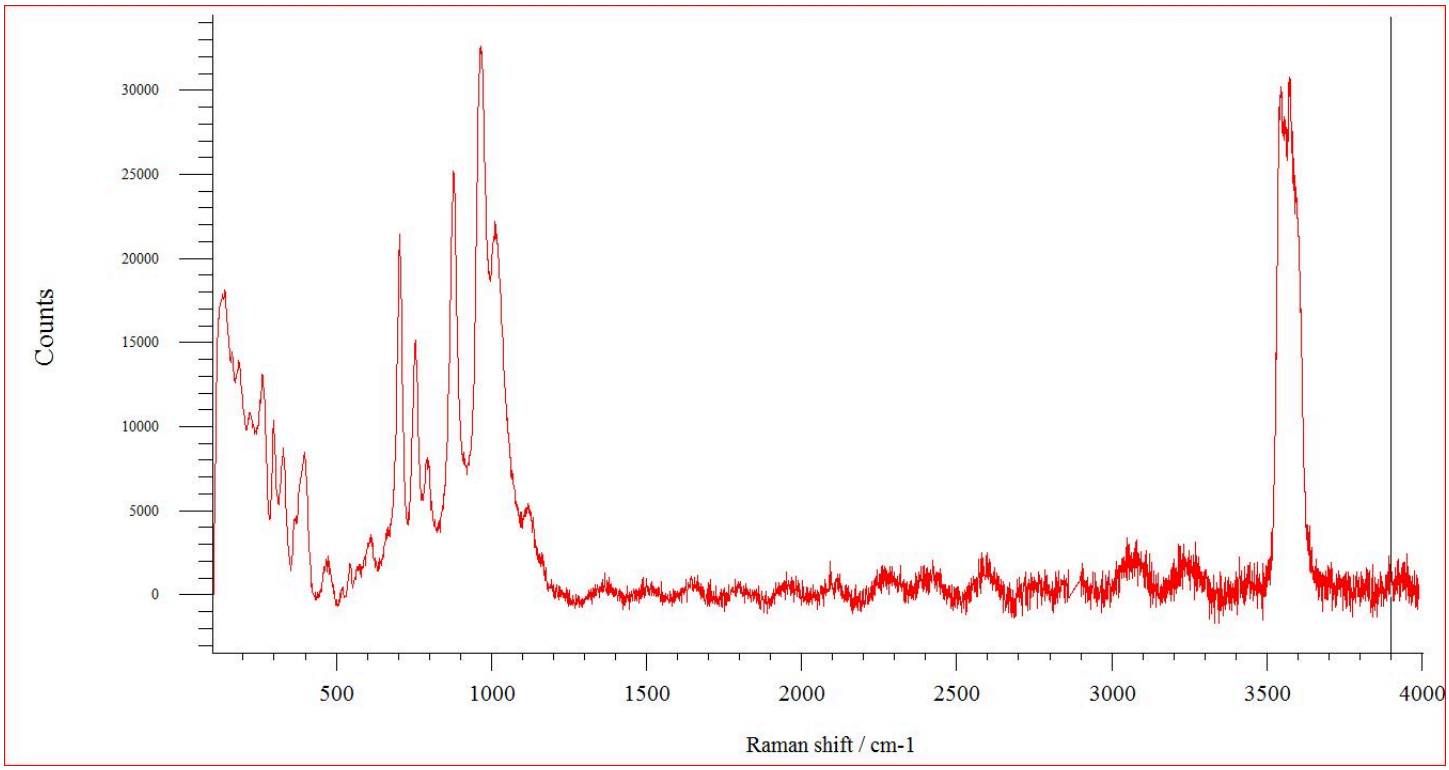


UV-Vis-NIR spectrum

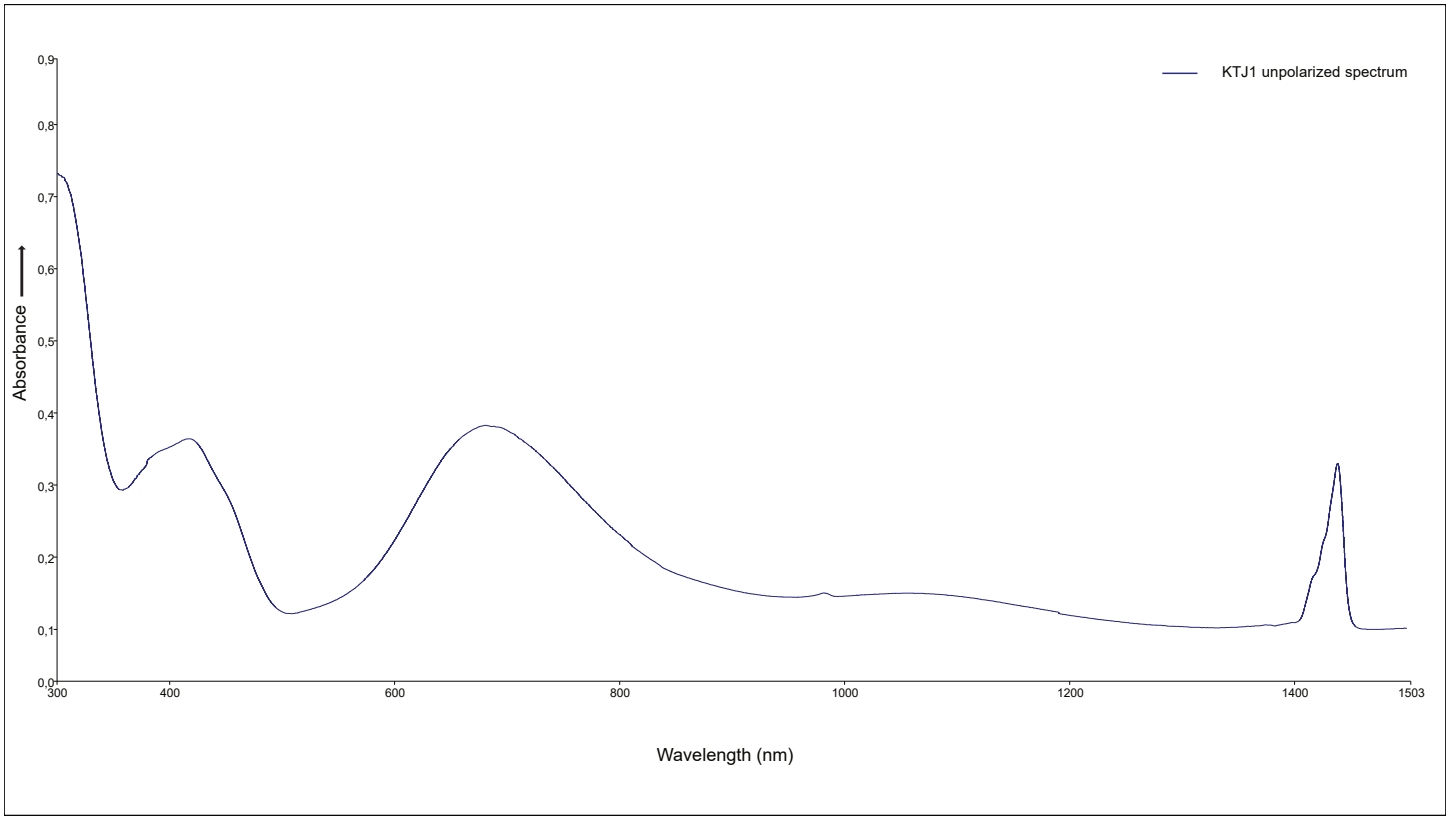

*KTJ1*

*5.06 x 4.13 x 2.97 mm*

## FTIR spectrum

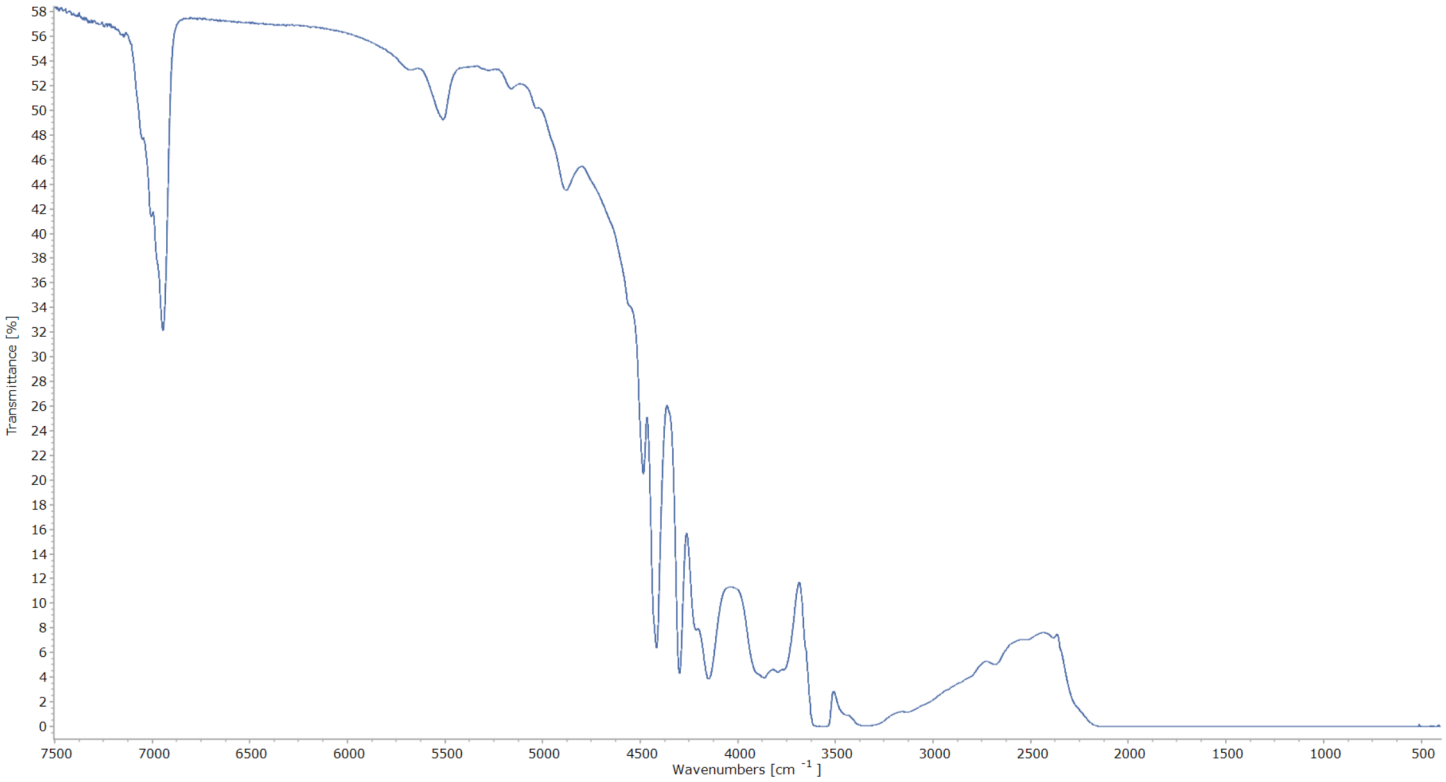


## EDXRF analysis

| Compound | m/m% | StdErr | El | m/m% | StdErr |
|---|---|---|---|---|---|
| Al2O3 | 46.00 | 0.30 | Al | 24.34 | 0.16 |
| SiO2 | 29.39 | 0.22 | Si | 13.74 | 0.10 |
| MgO | 19.48 | 0.20 | Mg | 11.75 | 0.12 |
| CaO | 0.162 | 0.008 | Ca | 0.116 | 0.006 |
| TiO2 | 0.155 | 0.015 | Ti | 0.0927 | 0.0091 |
| V2O5 | 0.145 | 0.009 | V | 0.0812 | 0.0050 |
| MnO | 0.112 | 0.009 | Mn | 0.0868 | 0.0066 |
| Fe2O3 | 0.099 | 0.011 | Fe | 0.0694 | 0.0077 |
| SO3 | 0.060 | 0.022 | Sx | 0.0239 | 0.0090 |
| Sc2O3 | 0.0585 | 0.0033 | Sc | 0.0381 | 0.0021 |
| Cr2O3 | 0.0147 | 0.0015 | Cr | 0.0101 | 0.0010 |
| ZnO | 0.0119 | 0.0008 | Zn | 0.0096 | 0.0006 |
| K2O | 0.0062 | 0.0021 | K | 0.0051 | 0.0017 |
| Ga2O3 | 0.0054 | 0.0006 | Ga | 0.0040 | 0.0004 |

KnownConc= 3.30 B2O3 REST= 1.00 H2O D/S= 0
Sum Conc's before normalisation to 100% : 59.0 %

## Emission spectra

*KTJ1*

*5.06 x 4.13 x 2.97 mm*

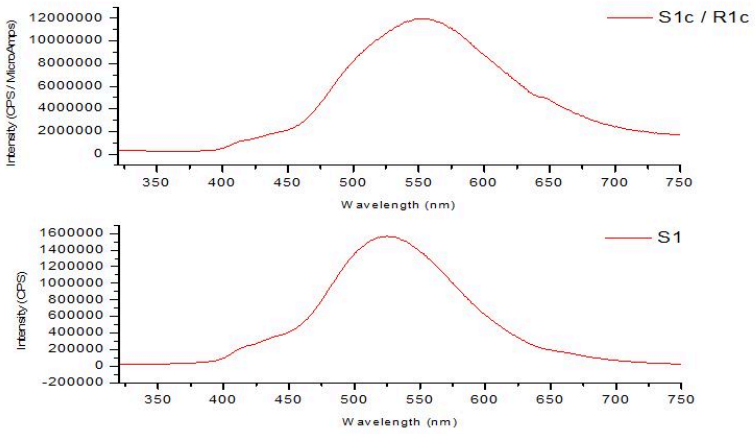


*Emission spectra*
*under λex = 254nm at*
*room temperature*

*S1: measured*
*S1c/R1c: corrected*

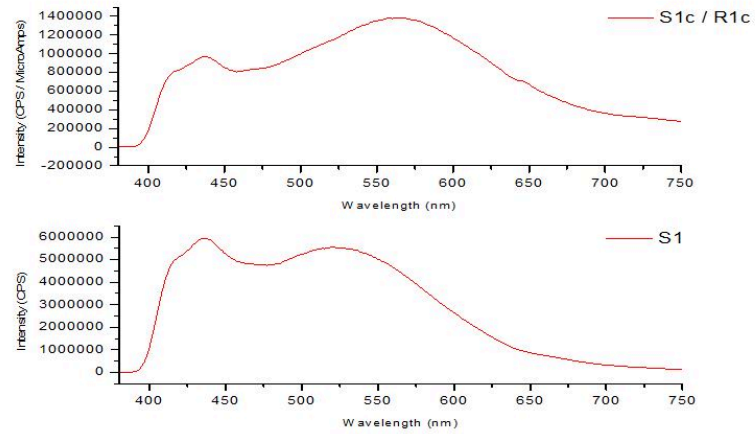


*Emission spectra*
*under λex = 365nm at*
*room temperature*

*S1: measured*
*S1c/R1c: corrected*

## Exitation spectra

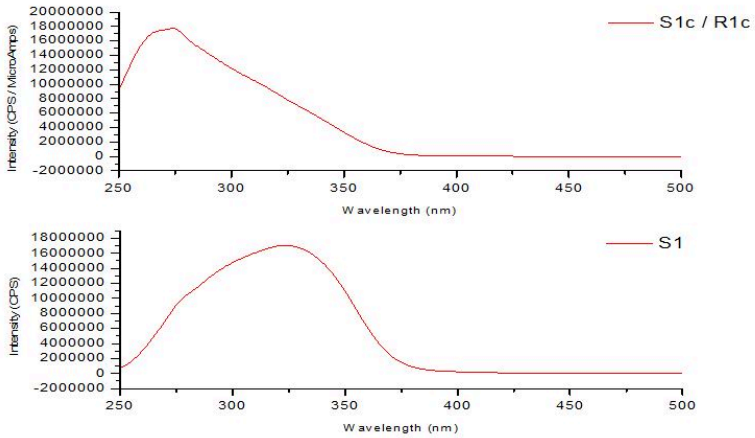


*Excitation spectra*
*under λem = 550nm at*
*room temperature*

*S1: measured*
*S1c/R1c: corrected*

## Phosphorescence decay time spectra

*KTJ1*

*5.06 x 4.13 x 2.97 mm*

- *λex = 265nm*
- *λem = 550nm*
- *10nm slit*

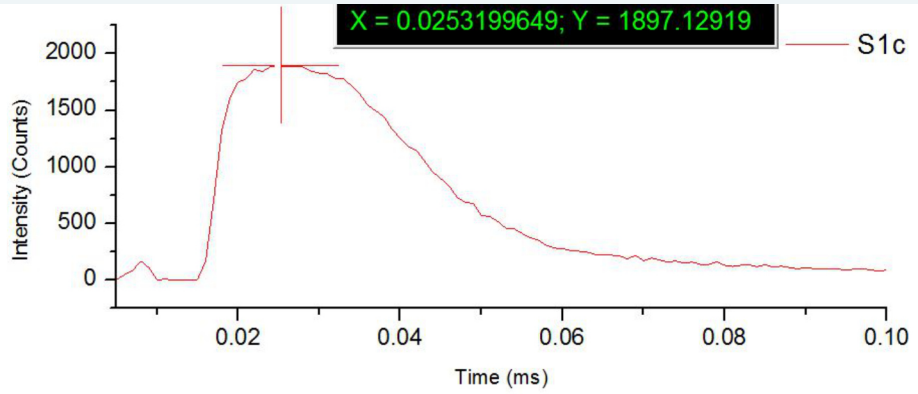


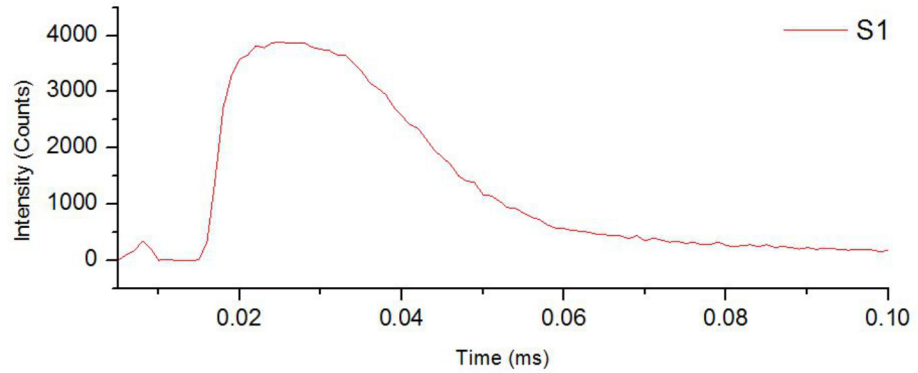


- *λex = 325nm*
- *λem = 550nm*
- *10nm slit*

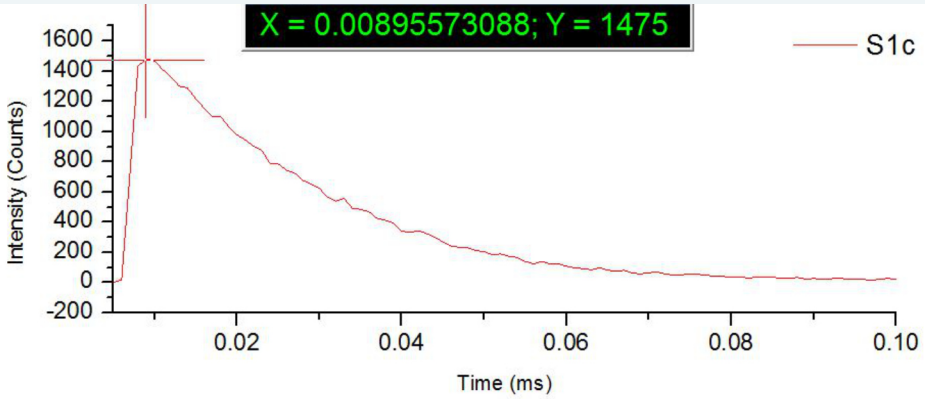


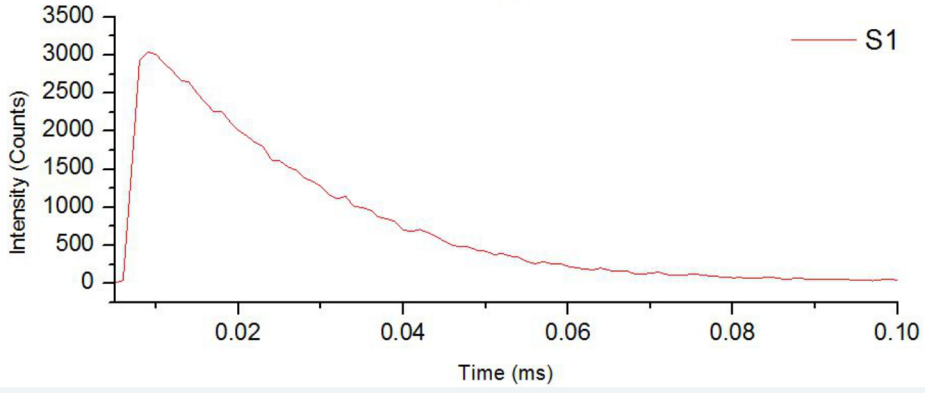

# Appendix

## *Sample KTJ2*

*KTJ2*

*9.52 x 7.40 x 4.61 mm*

Raman spectrum

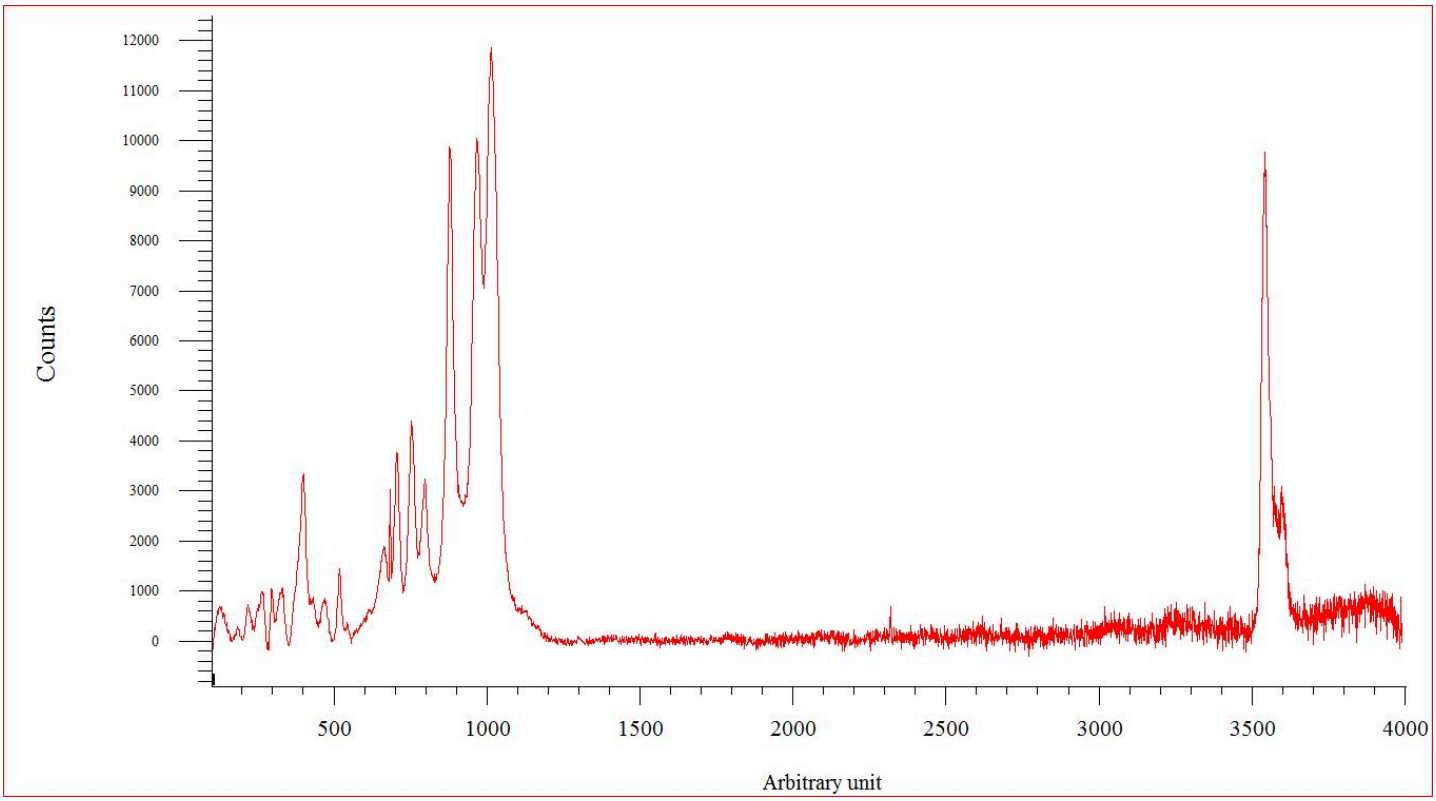


UV-Vis-NIR spectrum

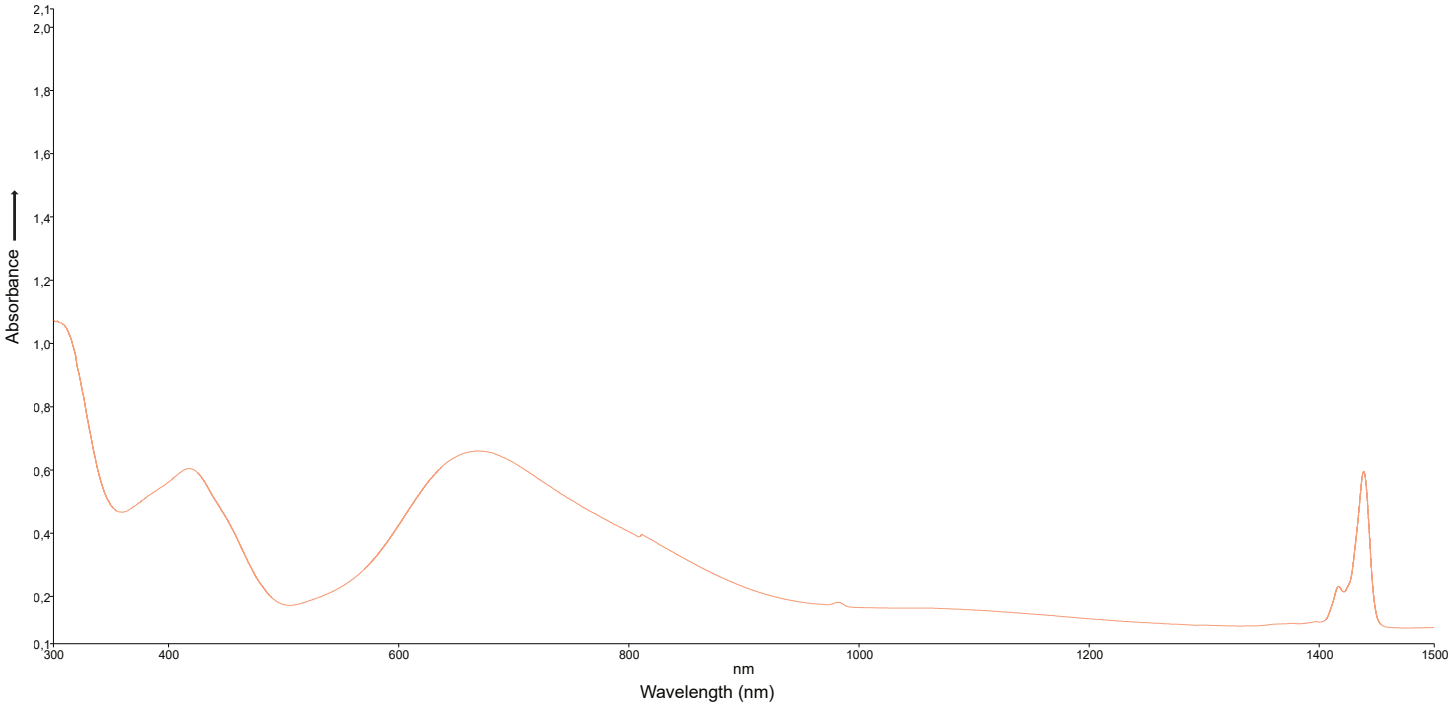

*KTJ2*

*9.52 x 7.40 x 4.61 mm*

## FTIR spectrum

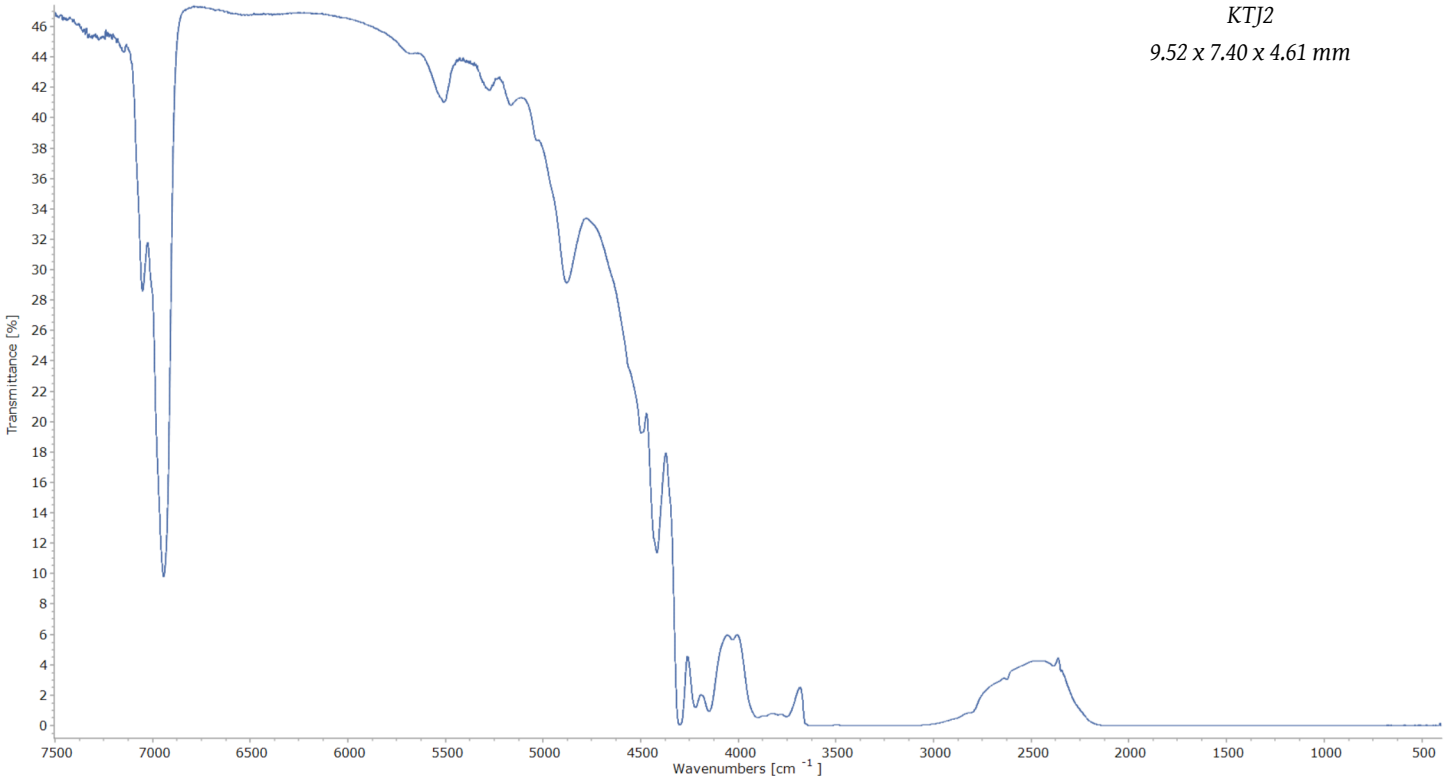


## EDXRF analysis

| Compound | m/m% | StdErr | El | m/m% | StdErr |
|---|---|---|---|---|---|
| Al2O3 | 44.57 | 0.26 | Al | 23.59 | 0.14 |
| SiO2 | 29.89 | 0.22 | Si | 13.97 | 0.10 |
| MgO | 20.56 | 0.20 | Mg | 12.40 | 0.12 |
| V2O5 | 0.180 | 0.011 | V | 0.101 | 0.006 |
| MnO | 0.167 | 0.013 | Mn | 0.129 | 0.010 |
| TiO2 | 0.108 | 0.011 | Ti | 0.0649 | 0.0064 |
| CaO | 0.0656 | 0.0033 | Ca | 0.0469 | 0.0023 |
| Fe2O3 | 0.0598 | 0.0066 | Fe | 0.0418 | 0.0046 |
| BaO | 0.0286 | 0.0082 | Ba | 0.0256 | 0.0074 |
| Sc2O3 | 0.0217 | 0.0018 | Sc | 0.0141 | 0.0012 |
| Cr2O3 | 0.0213 | 0.0017 | Cr | 0.0146 | 0.0012 |
| K2O | 0.0103 | 0.0017 | K | 0.0086 | 0.0014 |
| ZnO | 0.0095 | 0.0006 | Zn | 0.0076 | 0.0004 |

KnownConc= 3.30 B2O3 REST= 1.00 H2O D/S= 0
Sum Conc's before normalisation to 100% : 86.3 %

## Emission spectra

*KTJ2*
*9.52 x 7.40 x 4.61 mm*

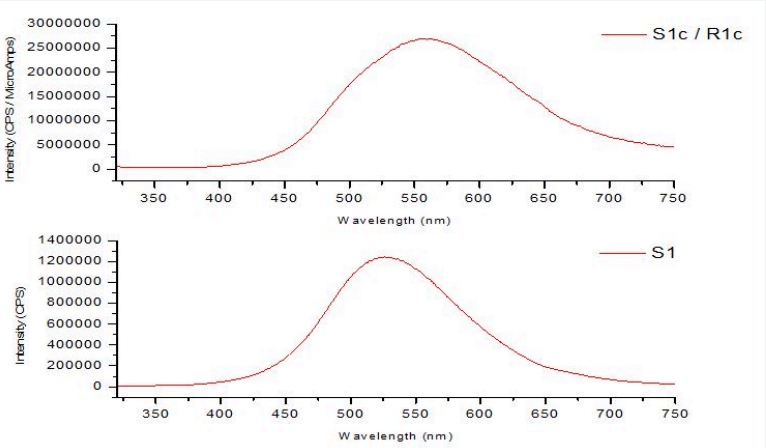


*Emission spectra under λex = 254nm at room temperature*
*S1: measured*
*S1c/R1c: corrected*

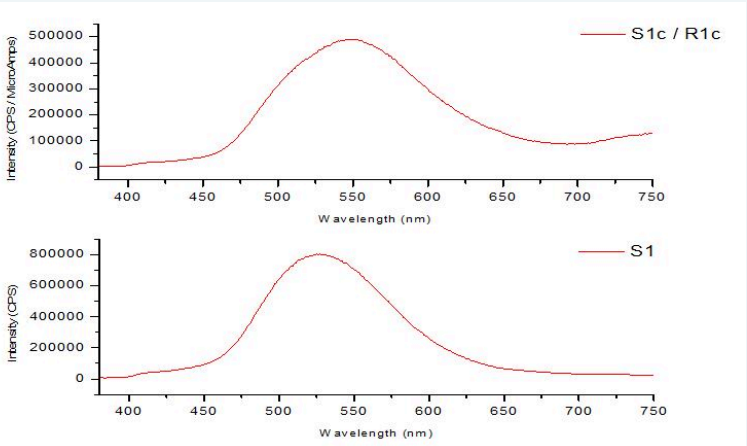


*Emission spectra under λex = 365nm at room temperature*
*S1: measured*
*S1c/R1c: corrected*

## Exitation spectra

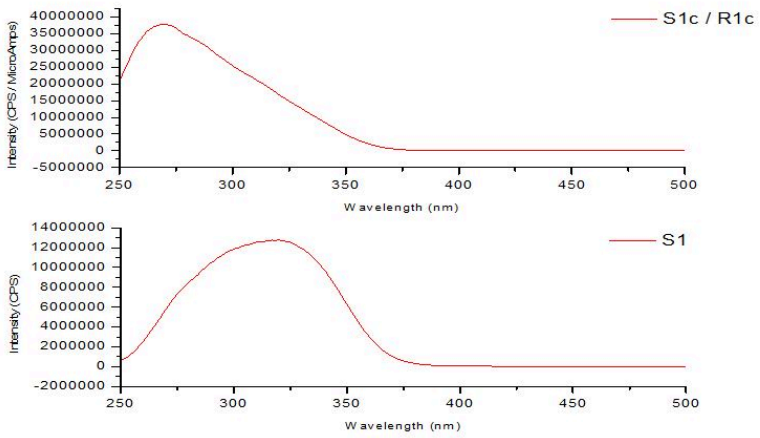


*Excitation spectra under λem = 550nm at room temperature*
*S1: measured*
*S1c/R1c: corrected*

# *Appendix*

## *Sample KUD5*

*KUD5*

Raman spectrum

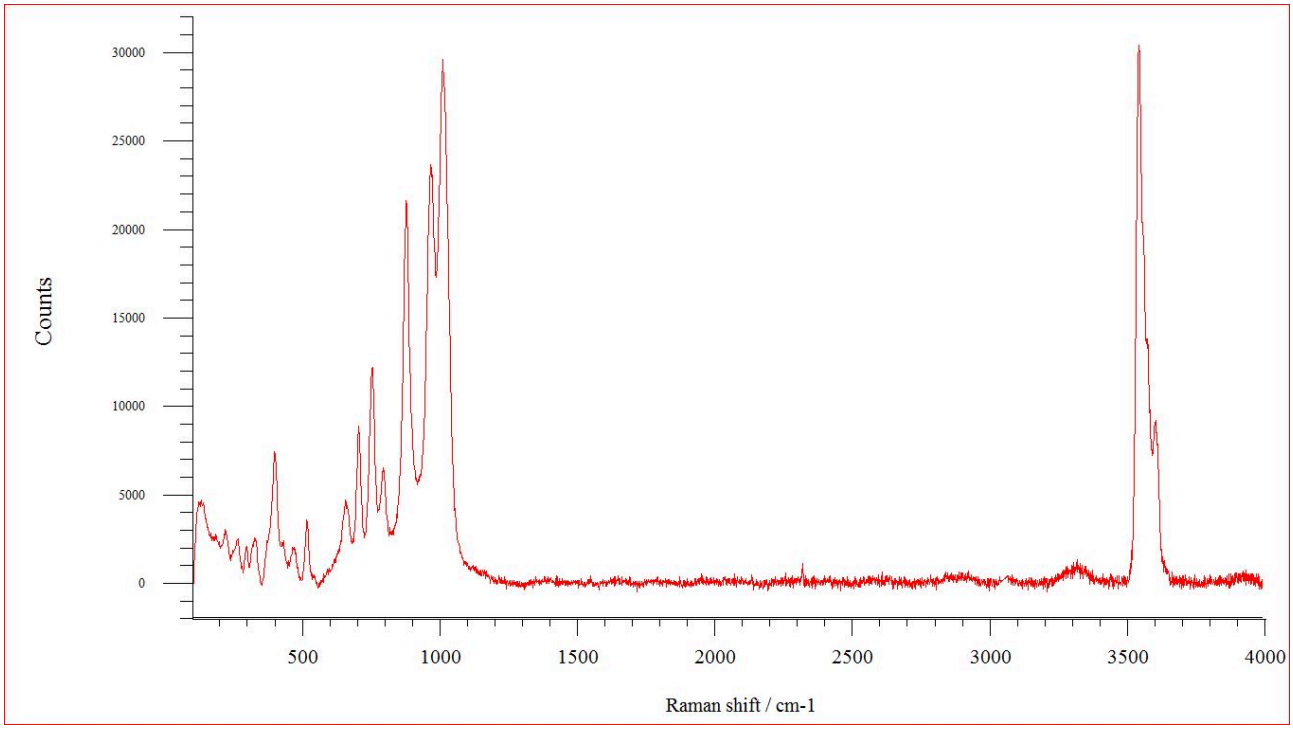


UV-Vis-NIR spectrum

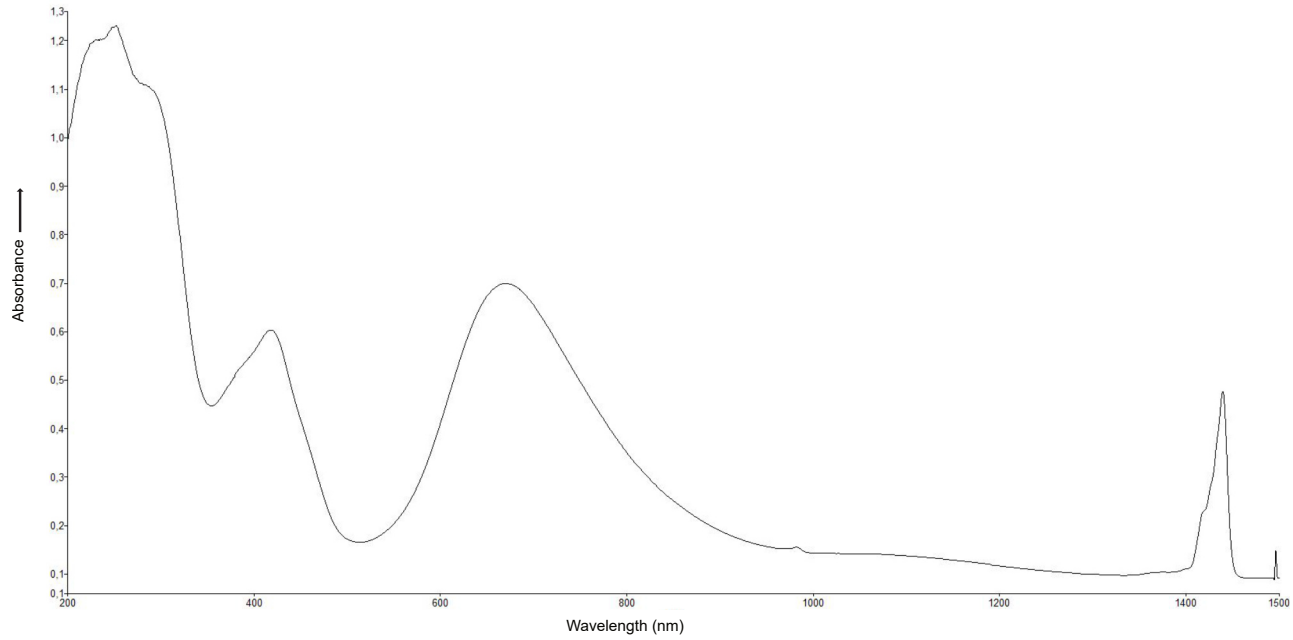

## FTIR spectra (absorption & reflectance)

*KUD5*

*7.64 x 5.54 x 3.44 mm*

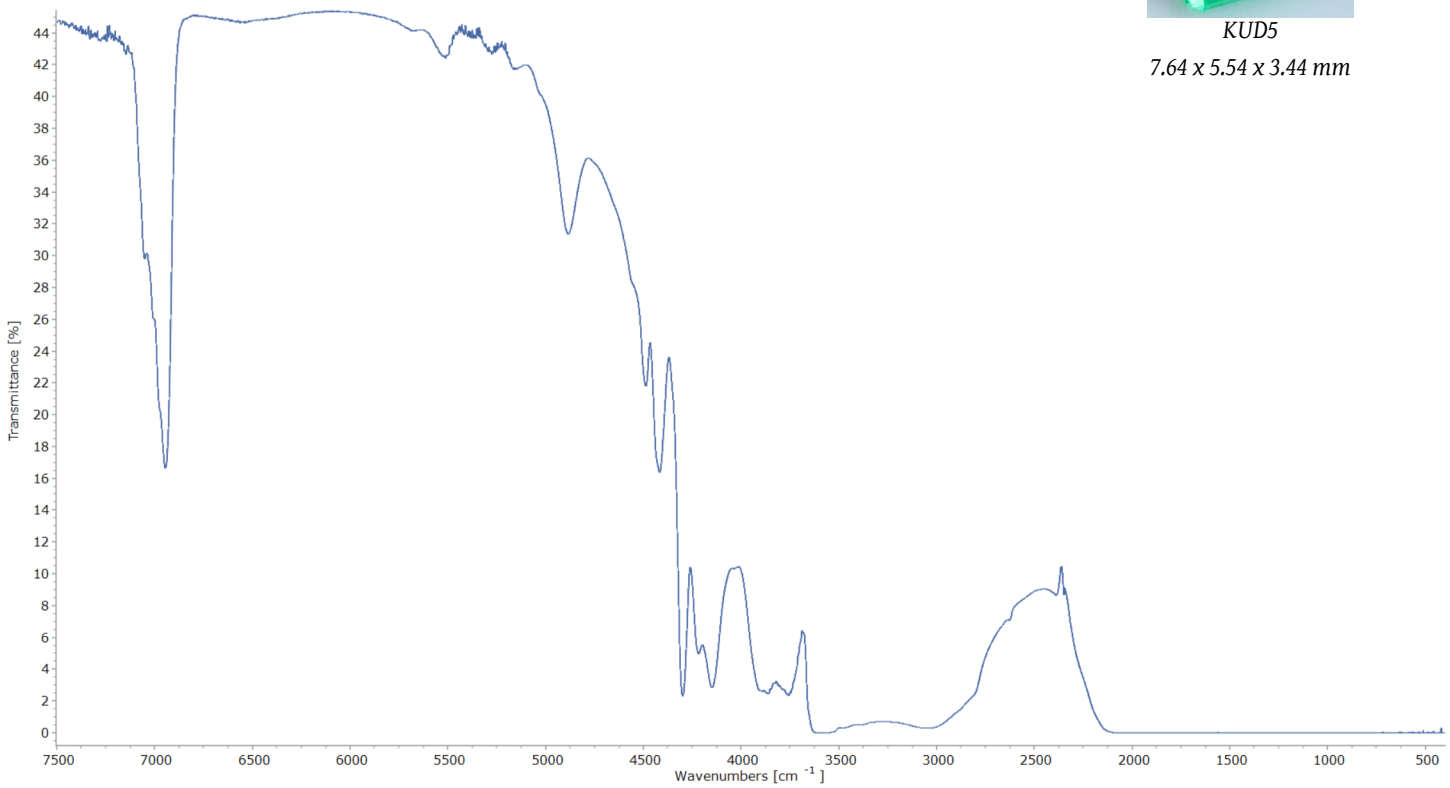


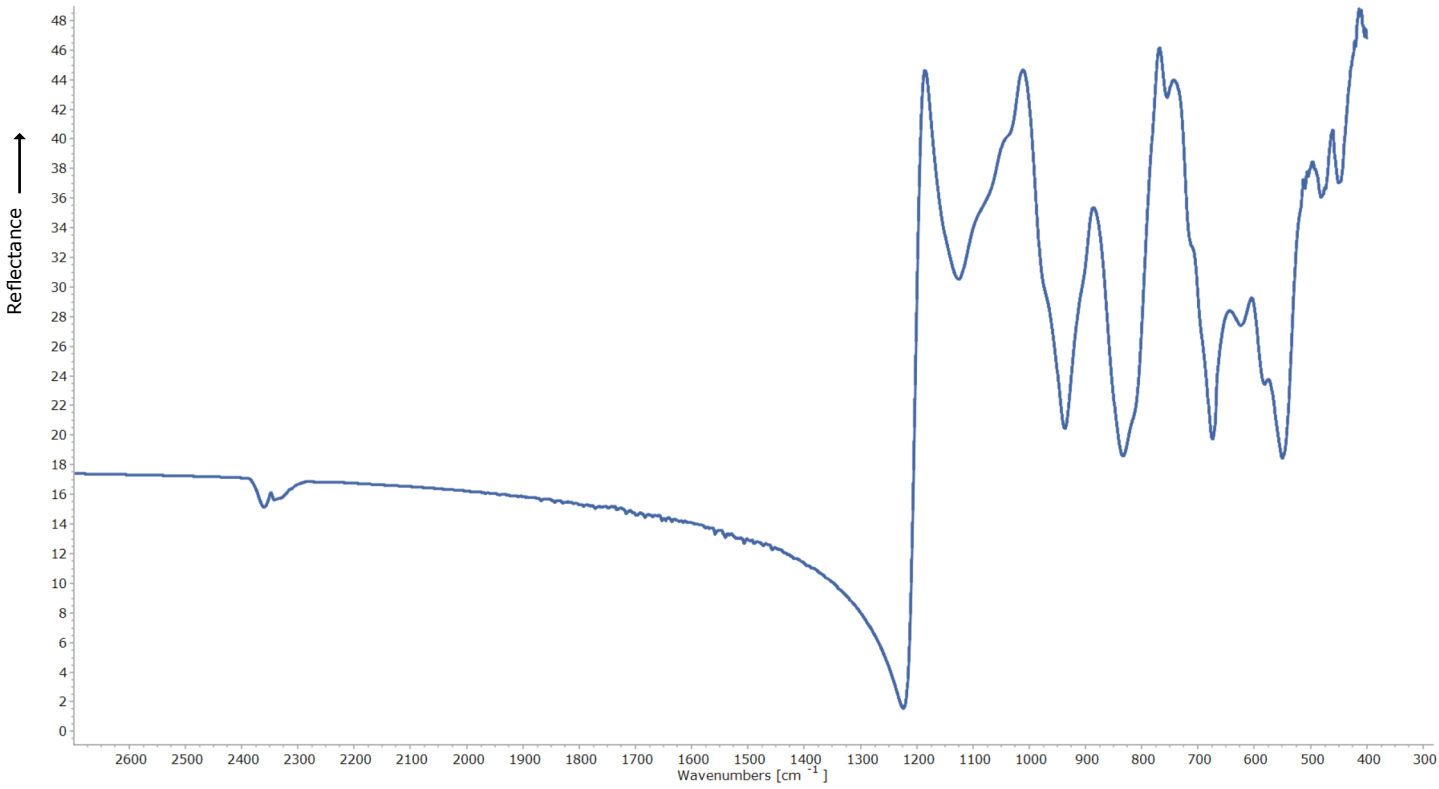

*KUD5*

*7.64 x 5.54 x 3.44 mm*

## EDXRF analysis

| Compound | m/m% | StdErr | El | m/m% | StdErr |
|---|---|---|---|---|---|
| Al2O3 | 45.02 | 0.26 | Al | 23.82 | 0.14 |
| SiO2 | 29.87 | 0.22 | Si | 13.97 | 0.10 |
| MgO | 19.99 | 0.20 | Mg | 12.06 | 0.12 |
| V2O5 | 0.225 | 0.014 | V | 0.126 | 0.008 |
| MnO | 0.220 | 0.017 | Mn | 0.171 | 0.013 |
| TiO2 | 0.127 | 0.012 | Ti | 0.0761 | 0.0075 |
| SO3 | 0.085 | 0.018 | Sx | 0.0340 | 0.0072 |
| CaO | 0.0587 | 0.0030 | Ca | 0.0420 | 0.0021 |
| Fe2O3 | 0.0499 | 0.0055 | Fe | 0.0349 | 0.0039 |
| Sc2O3 | 0.0245 | 0.0019 | Sc | 0.0160 | 0.0013 |
| Cr2O3 | 0.0135 | 0.0022 | Cr | 0.0092 | 0.0015 |
| Cl | 0.0090 | 0.0030 | Cl | 0.0090 | 0.0030 |

KnownConc= 3.30 B2O3 REST= 1.00 H2O D/S= 0
Sum Conc's before normalisation to 100% : 76.3 %

## Emission spectra

*KUD5*

*7.64 x 5.54 x 3.44 mm*

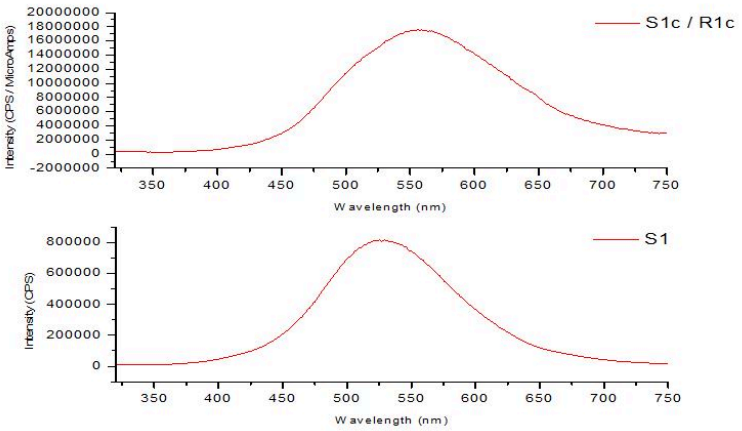


*Emission spectra under λex = 254nm at room temperature*

*S1: measured*
*S1c/R1c: corrected*

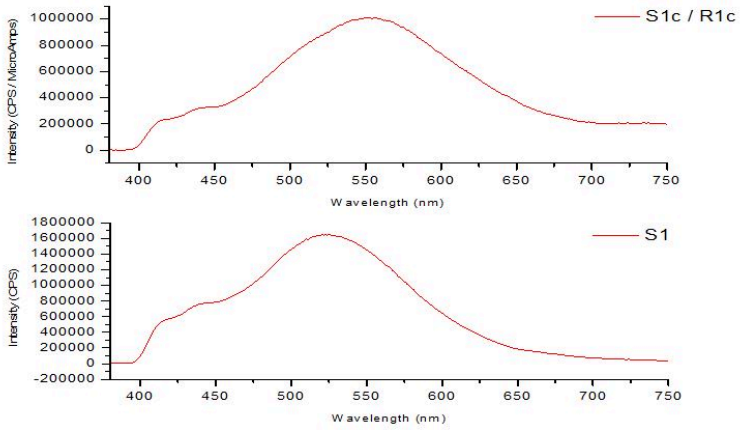


*Emission spectra under λex = 365nm at room temperature*

*S1: measured*
*S1c/R1c: corrected*

## Exitation spectra

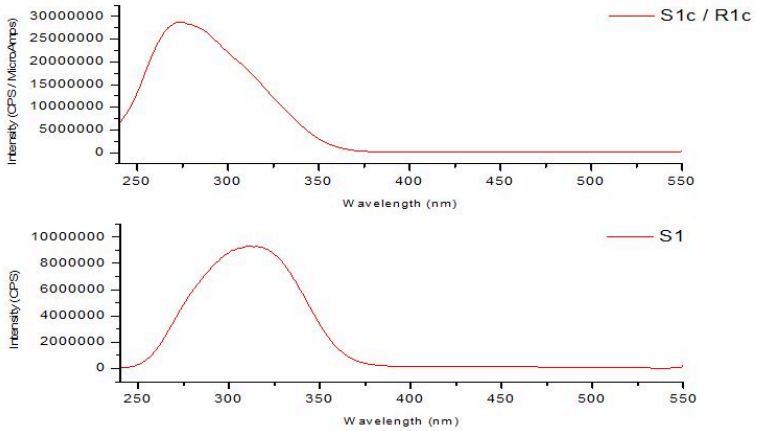


*Excitation spectra under λem = 565nm at room temperature*

*S1: measured*
*S1c/R1c: corrected*

## Phosphorescence decay time spectra

*KUD5*

*7.64 x 5.54 x 3.44 mm*

- *λex = 265nm*
- *λem = 550nm*
- *10nm slit*

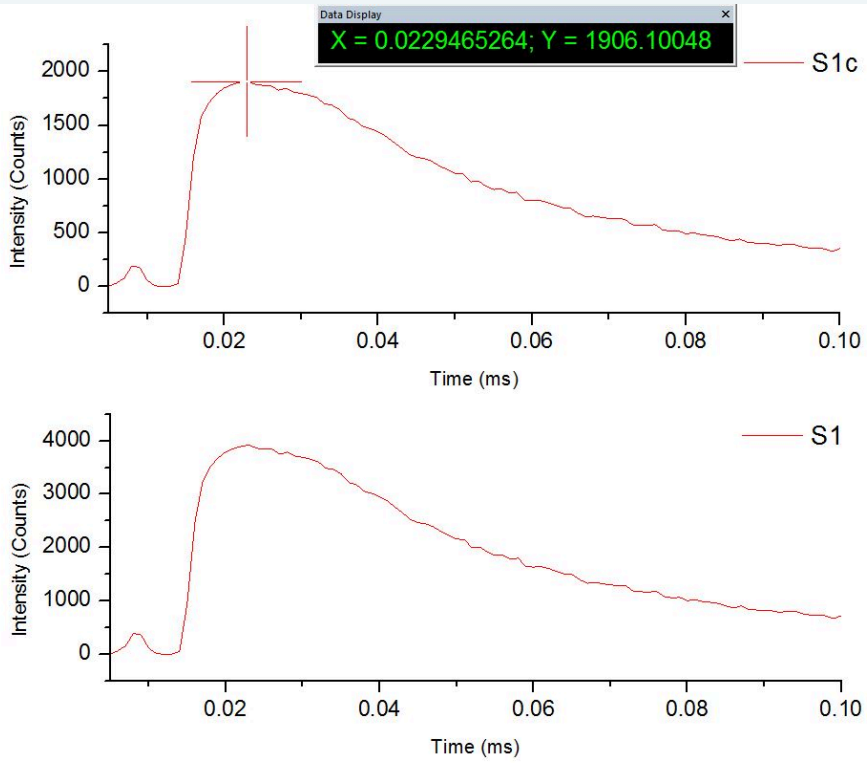


- *λex = 325nm*
- *λem = 550nm*
- *10nm slit*

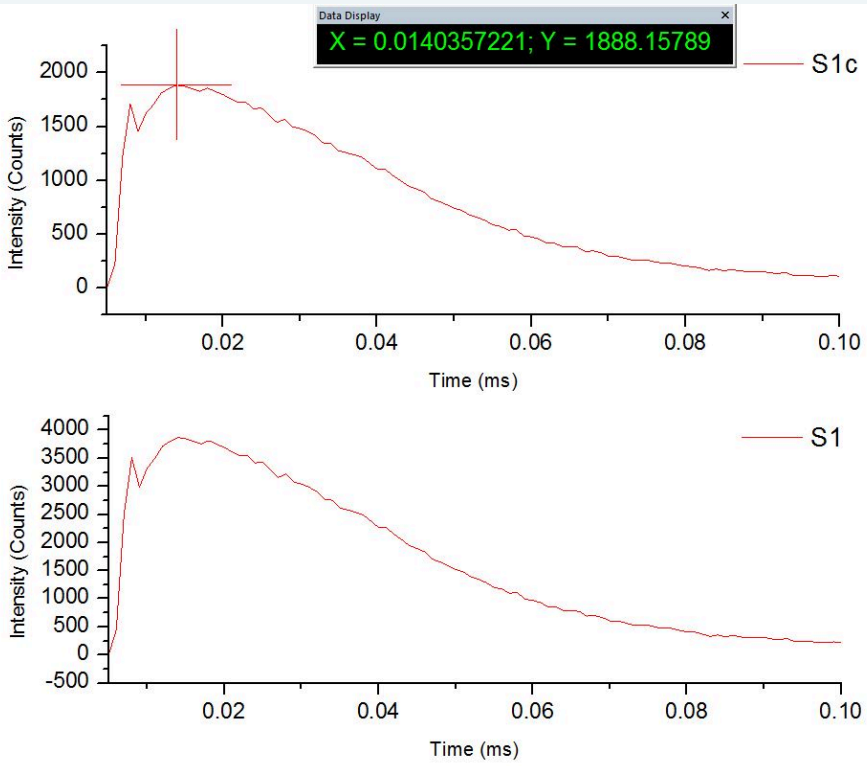

# Appendix

## *Sample KUD7*

*KUD7*

*9.02 x 5.37 x 3.46 mm*

Raman spectrum

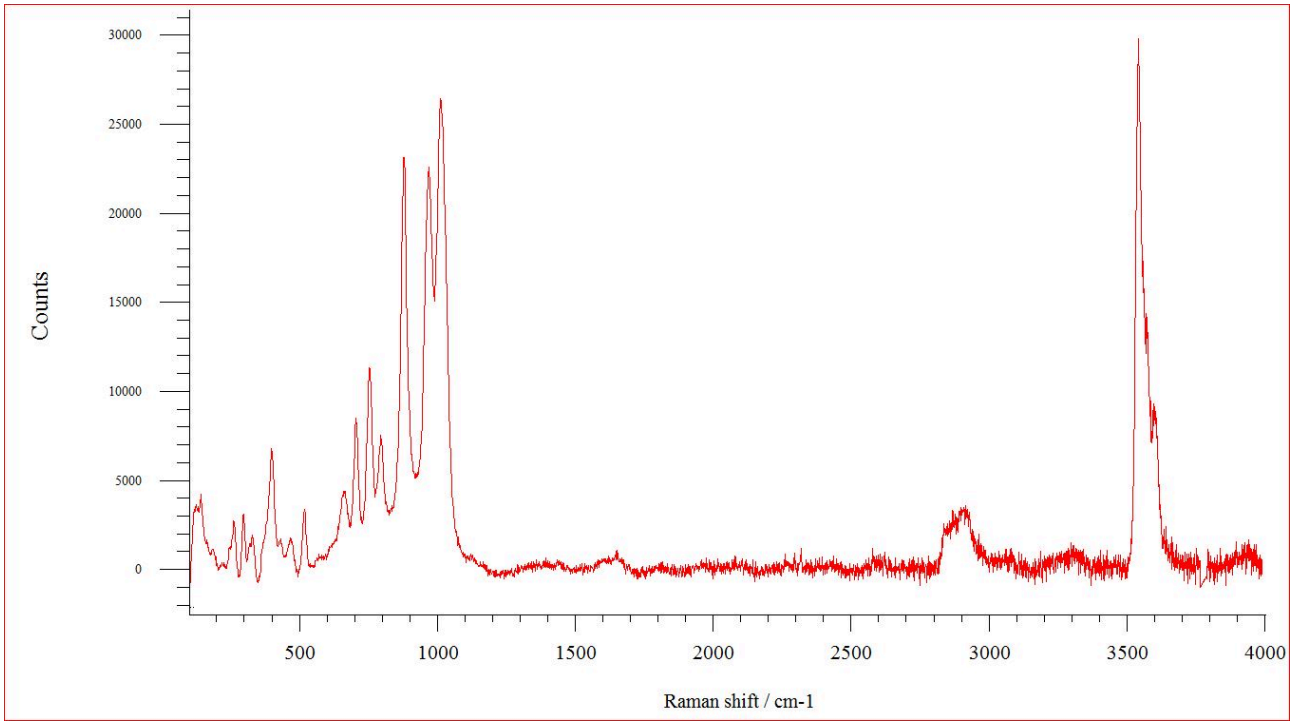


UV-Vis-NIR spectrum (polarised)

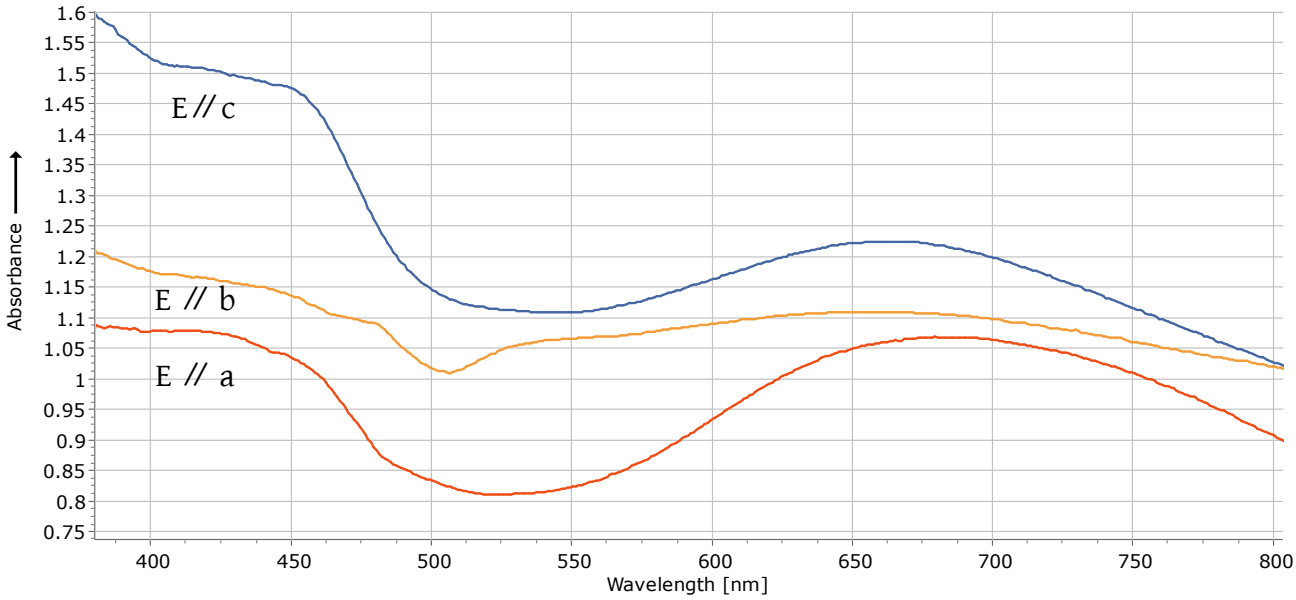

## FTIR spectra

*KUD7*

*9.02 x 5.37 x 3.46 mm*

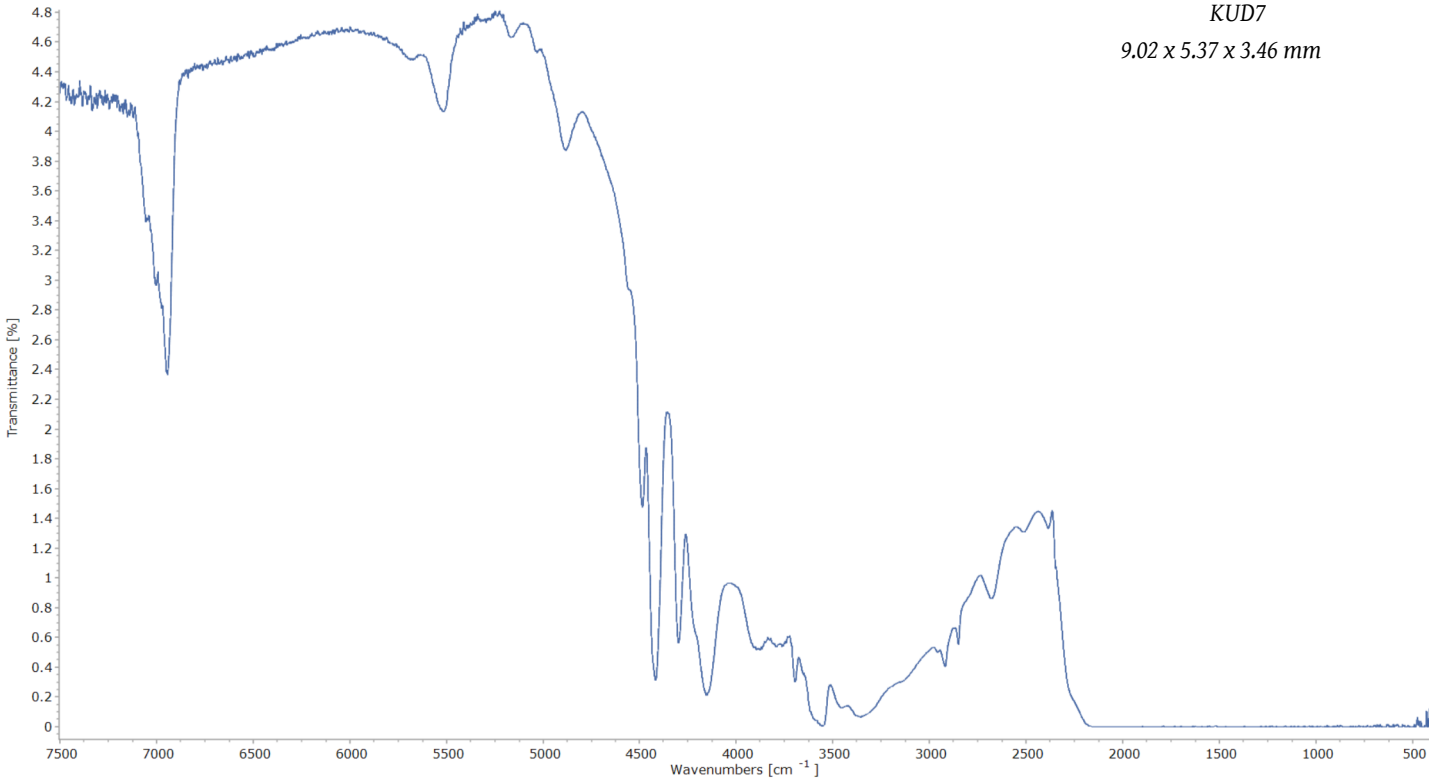

## Emission spectra

*KUD7*

*9.02 x 5.37 x 3.46 mm*

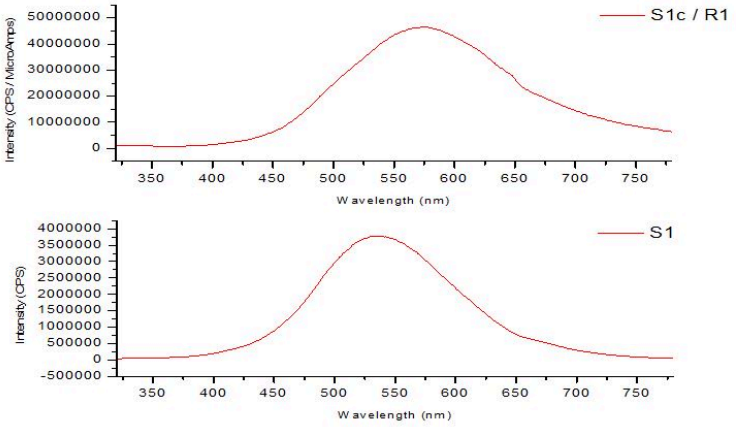


*Emission spectra under λex = 254nm at room temperature*

*S1: measured*
*S1c/R1c: corrected*

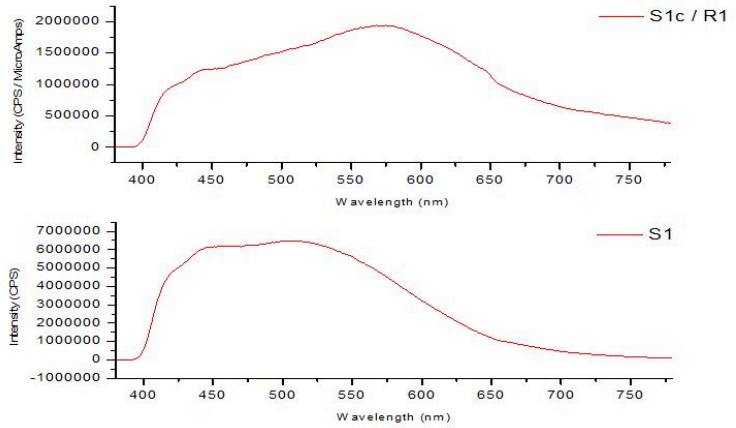


*Emission spectra under λex = 365nm at room temperature*

*S1: measured*
*S1c/R1c: corrected*

## Exitation spectra

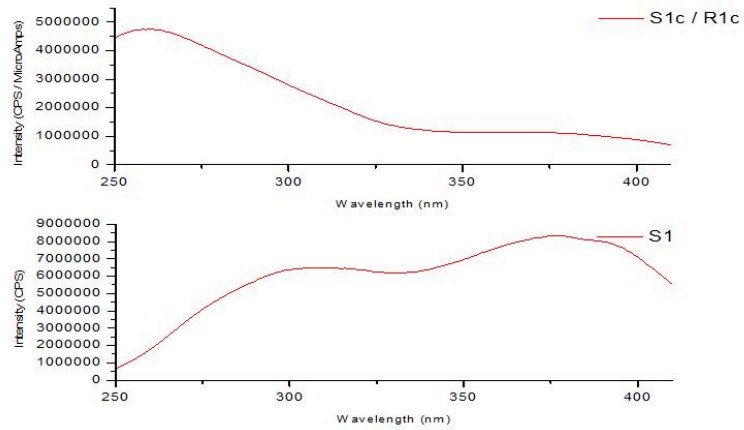


*Excitation spectra under λem = 445nm at room temperature*

*S1: measured*
*S1c/R1c: corrected*

## Excitation spectra

*KUD7*

*9.02 x 5.37 x 3.46 mm*

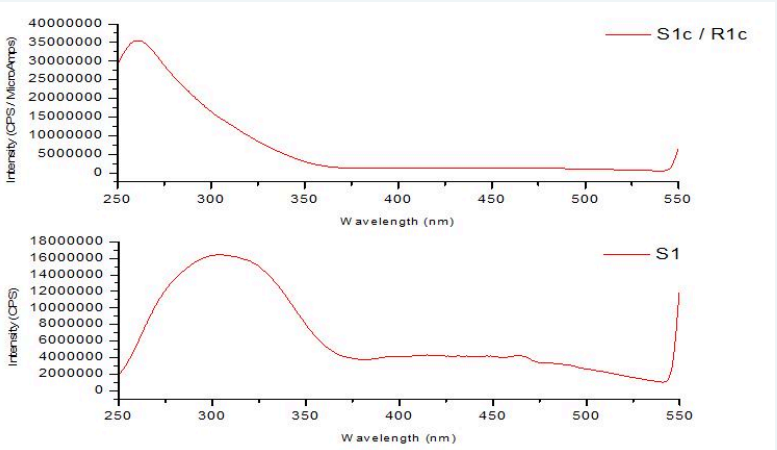


*Excitation spectra under λem = 570nm at room temperature*

*S1: measured*
*S1c/R1c: corrected*

## Phosphorescence decay time spectra

- *λex = 265nm*
- *λem = 550nm*
- *10nm slit*

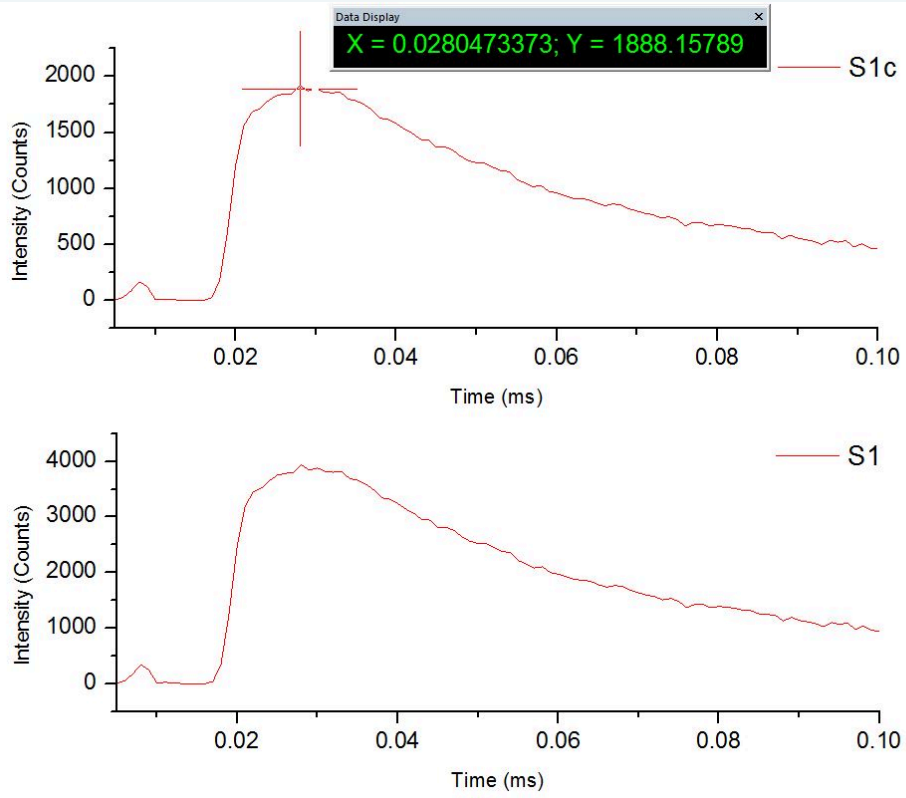

- *λex = 325nm*
- *λem = 550nm*
- *10nm slit*

*KUD7*

*9.02 x 5.37 x 3.46 mm*

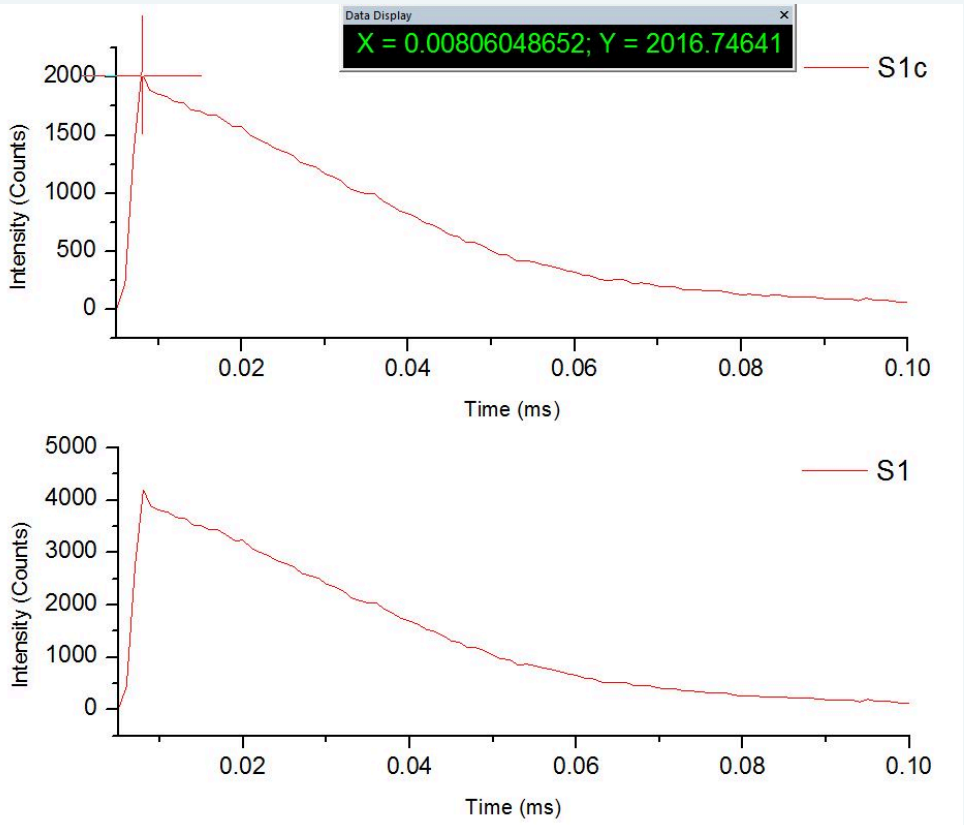


## EDXRF analysis

| Compound | m/m% | StdErr | El | m/m% | StdErr |
|---|---|---|---|---|---|
| Al2O3 | 44.78 | 0.27 | Al | 23.70 | 0.14 |
| SiO2 | 30.43 | 0.23 | Si | 14.23 | 0.11 |
| MgO | 19.32 | 0.20 | Mg | 11.65 | 0.12 |
| MnO | 0.270 | 0.021 | Mn | 0.209 | 0.016 |
| CaO | 0.249 | 0.012 | Ca | 0.178 | 0.009 |
| V2O5 | 0.169 | 0.010 | V | 0.0946 | 0.0058 |
| SO3 | 0.163 | 0.025 | Sx | 0.0654 | 0.0100 |
| TiO2 | 0.131 | 0.013 | Ti | 0.0786 | 0.0077 |
| Fe2O3 | 0.0553 | 0.0061 | Fe | 0.0387 | 0.0043 |
| Sc2O3 | 0.0456 | 0.0028 | Sc | 0.0297 | 0.0019 |
| BaO | 0.0265 | 0.0089 | Ba | 0.0237 | 0.0079 |
| Cr2O3 | 0.0209 | 0.0018 | Cr | 0.0143 | 0.0012 |
| Cl | 0.0165 | 0.0041 | Cl | 0.0165 | 0.0041 |
| K2O | 0.0158 | 0.0024 | K | 0.0131 | 0.0020 |

KnownConc= 3.30 B2O3 REST= 1.00 H2O D/S= 0
Sum Conc's before normalisation to 100% : 72.8 %

# Appendix

## *Sample KUF*

*KUF*
*9.71 x 8.31 x 5.61 mm*

Raman spectrum

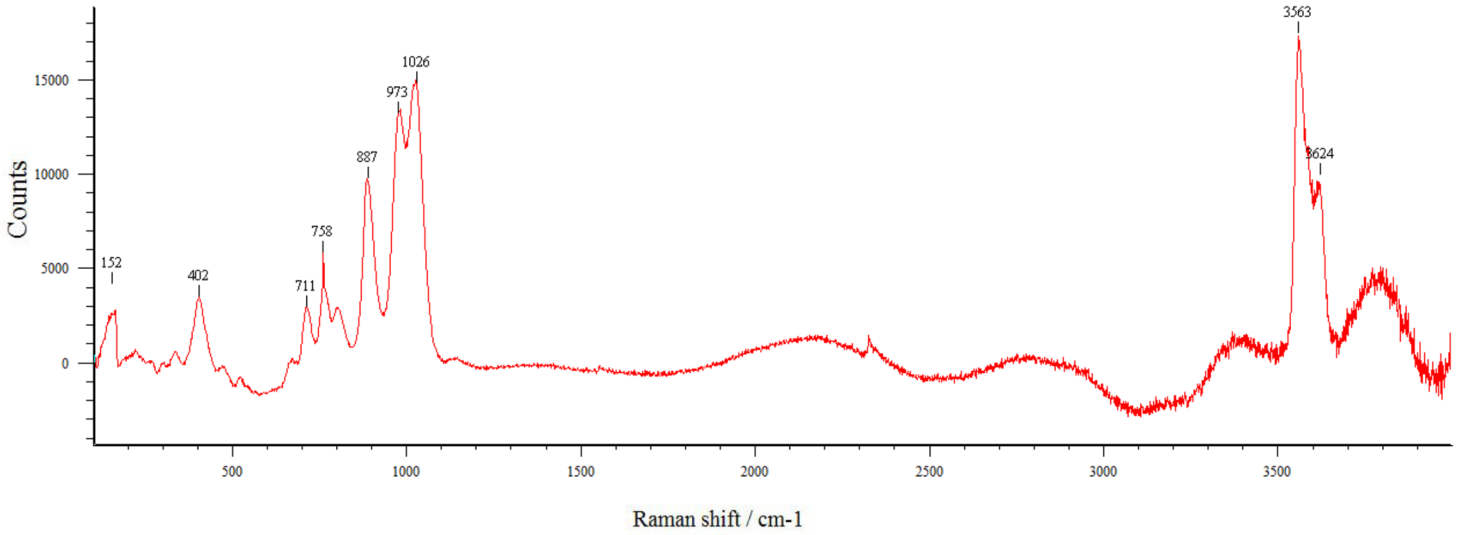


UV-Vis-NIR spectrum

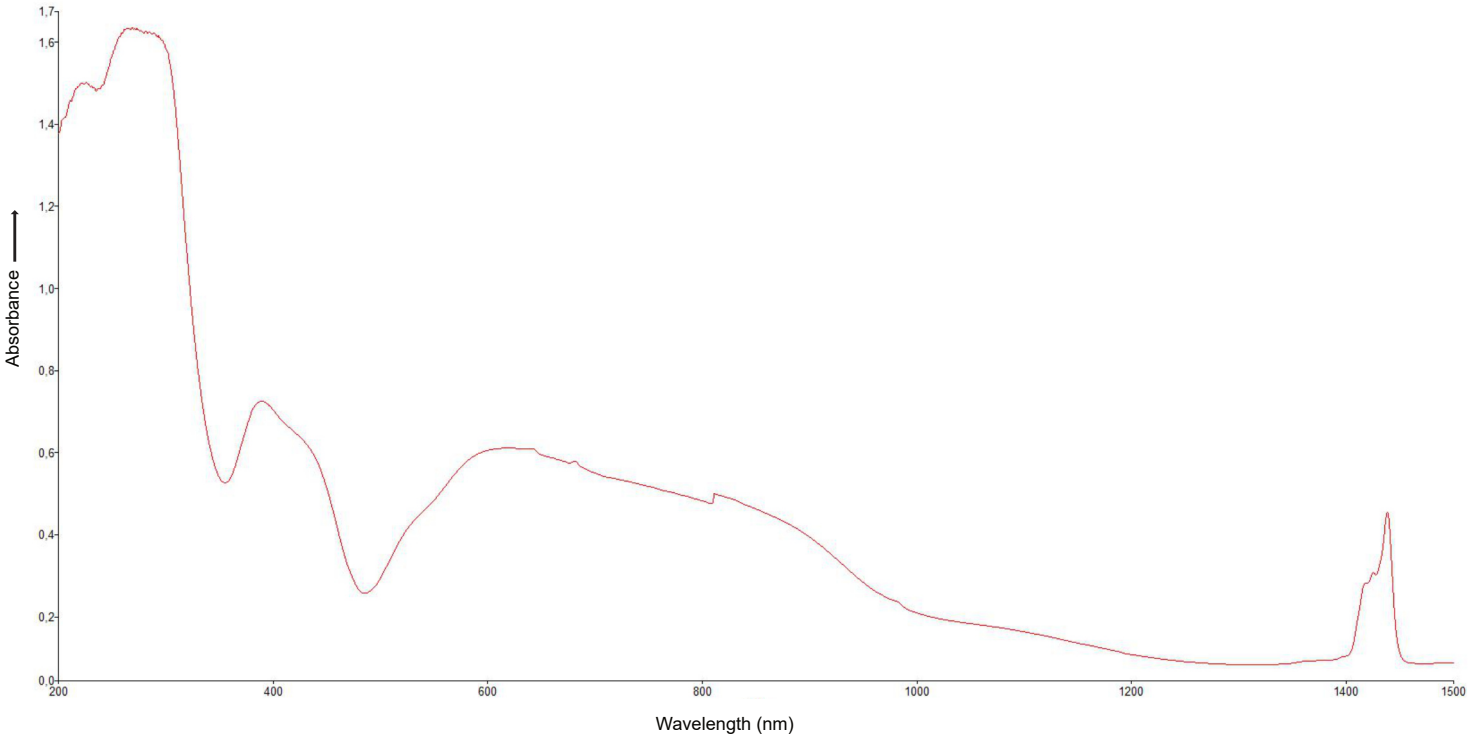

## FTIR spectra

*KUF*
*9.71 x 8.31 x 5.61 mm*

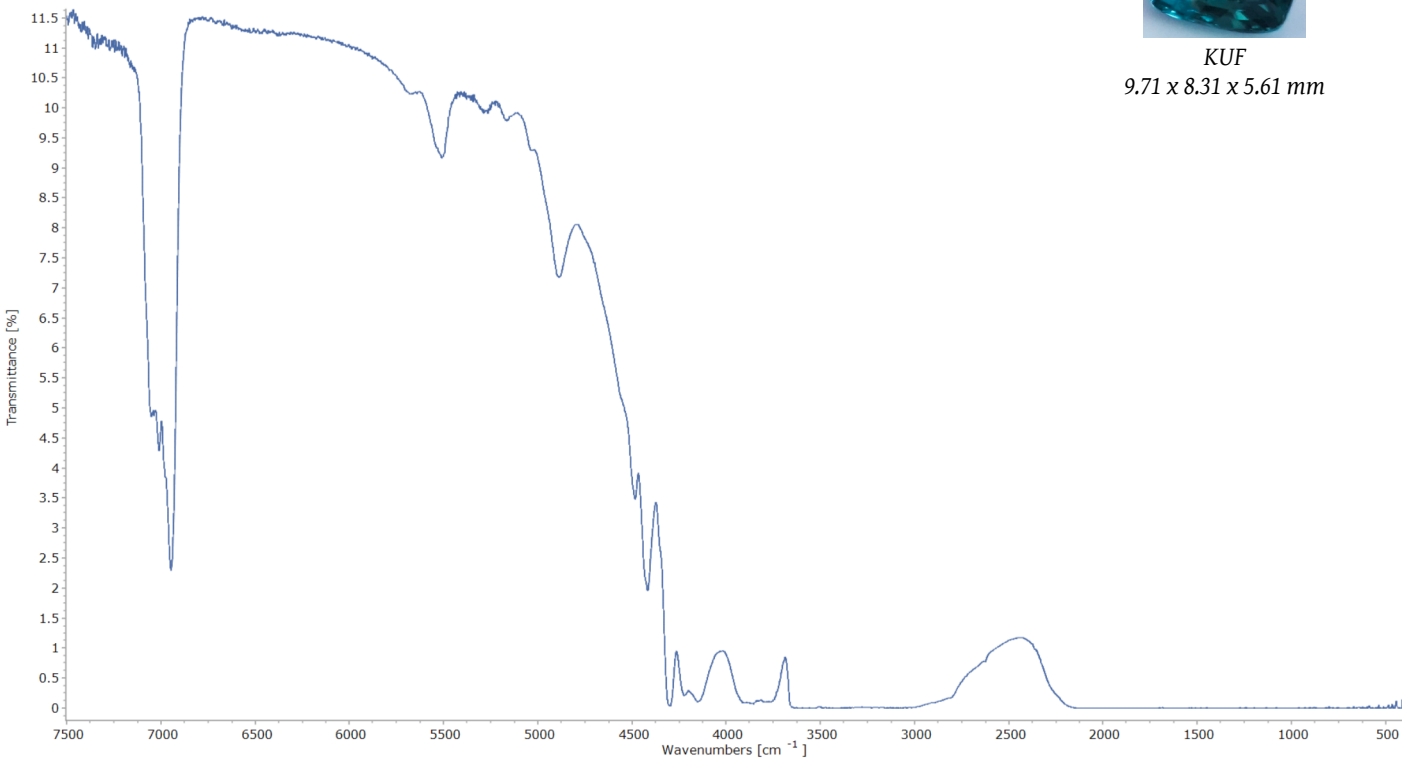


## EDXRF analysis

| Compound | m/m% | StdErr | El | m/m% | StdErr |
|---|---|---|---|---|---|
| Al2O3 | 44.43 | 0.30 | Al | 23.51 | 0.16 |
| SiO2 | 30.26 | 0.23 | Si | 14.15 | 0.11 |
| MgO | 20.27 | 0.20 | Mg | 12.23 | 0.12 |
| Cr2O3 | 0.216 | 0.014 | Cr | 0.148 | 0.010 |
| Fe2O3 | 0.167 | 0.018 | Fe | 0.117 | 0.013 |
| MnO | 0.115 | 0.009 | Mn | 0.0892 | 0.0068 |
| V2O5 | 0.0784 | 0.0048 | V | 0.0439 | 0.0027 |
| CaO | 0.0566 | 0.0036 | Ca | 0.0405 | 0.0026 |
| TiO2 | 0.0451 | 0.0044 | Ti | 0.0270 | 0.0026 |
| Cl | 0.0162 | 0.0046 | Cl | 0.0162 | 0.0046 |
| K2O | 0.0145 | 0.0025 | K | 0.0120 | 0.0020 |
| ZnO | 0.0135 | 0.0009 | Zn | 0.0108 | 0.0007 |
| Ga2O3 | 0.0101 | 0.0007 | Ga | 0.0075 | 0.0005 |

KnownConc= 3.30 B2O3 REST= 1.00 H2O D/S= 0
Sum Conc's before normalisation to 100% : 54.2 %

*KUF*
*9.71 x 8.31 x 5.61 mm*

## Emission spectra

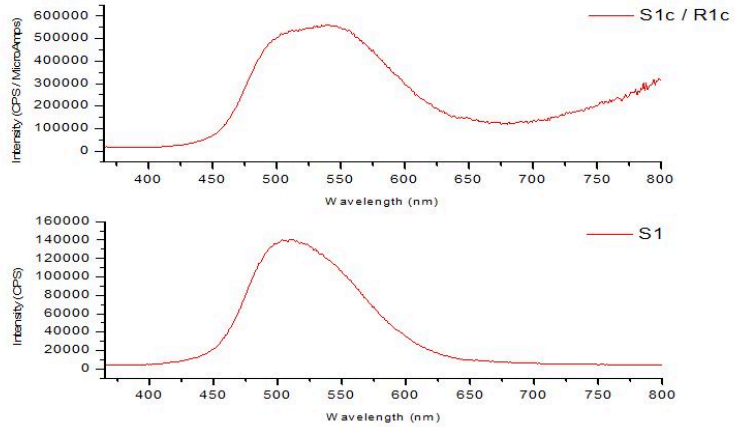


*Emission spectra*
*under λex = 254nm at*
*room temperature*

*S1: measured*
*S1c/R1c: corrected*

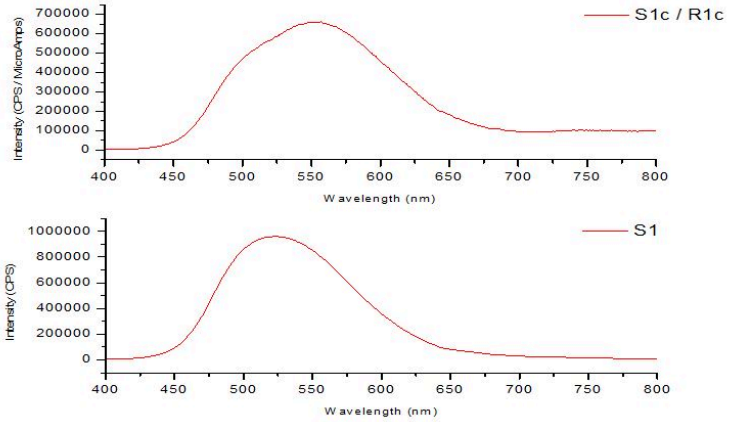


*Emission spectra*
*under λex = 318nm at*
*room temperature*

*S1: measured*
*S1c/R1c: corrected*

## Exitation spectra

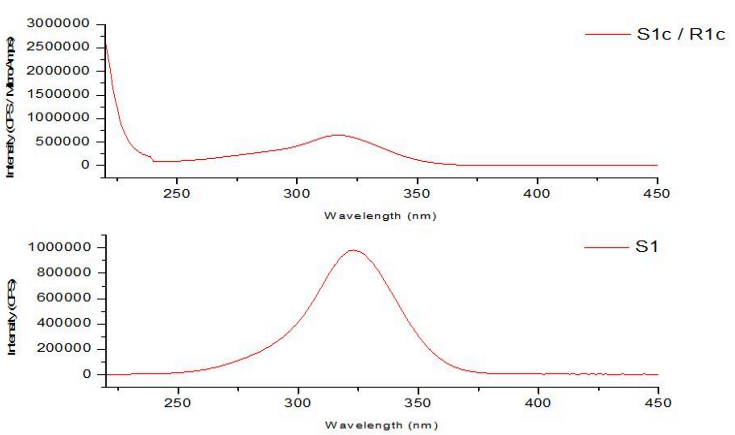


*Excitation spectra*
*under λem = 540nm at*
*room temperature*

*S1: measured*
*S1c/R1c: corrected*

# Appendix

## *Sample KTM*

*KTM*
*8.98 x 7.03 x 5.23 mm*

Raman spectrum

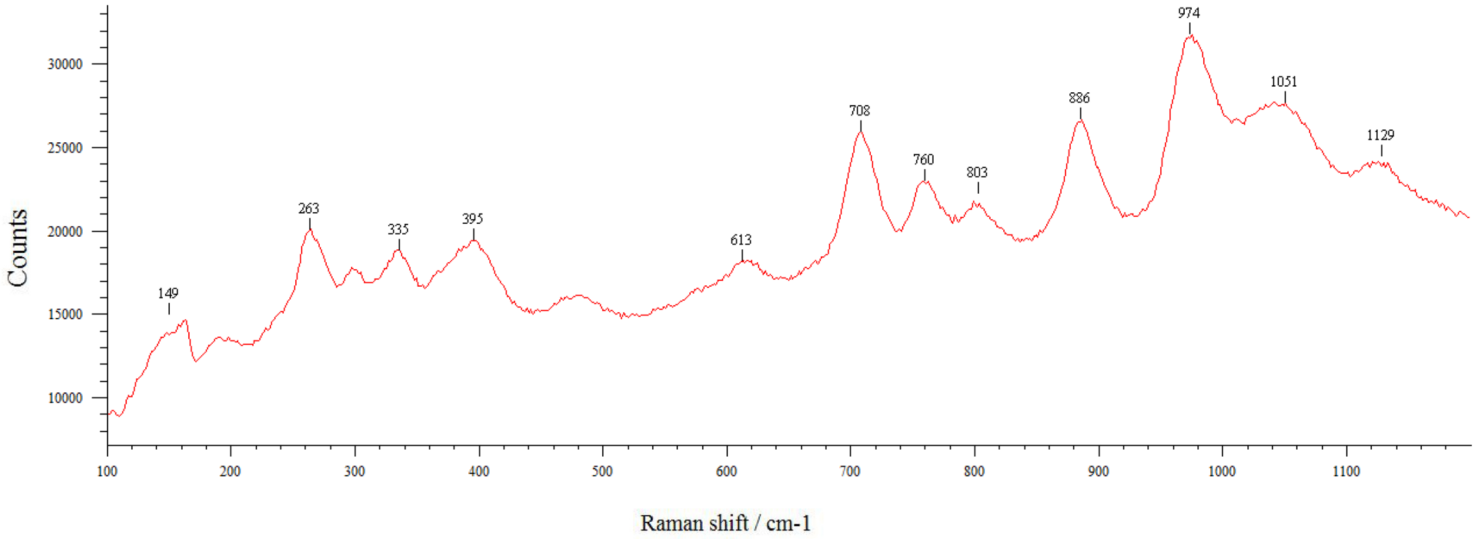


UV-Vis-NIR spectrum

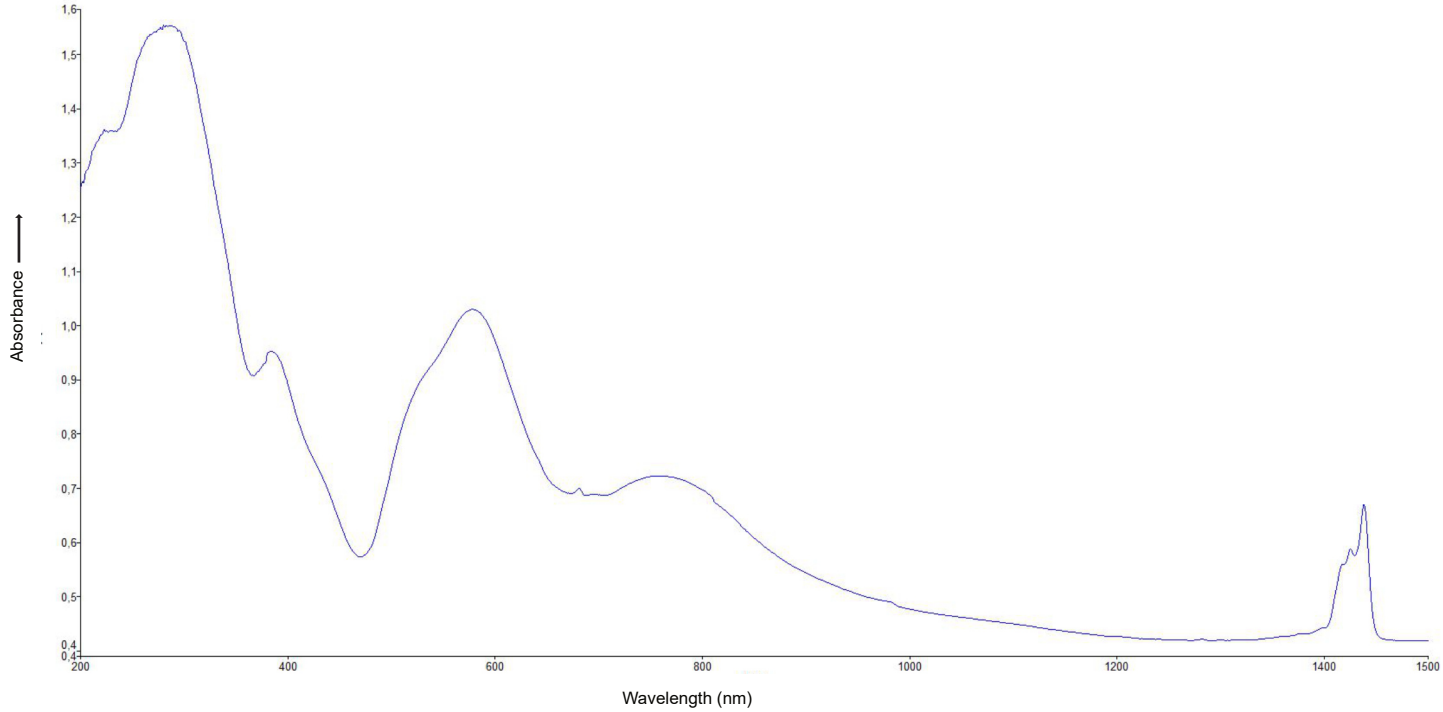

## FTIR spectrum

*KTM*
*8.98 x 7.03 x 5.23 mm*

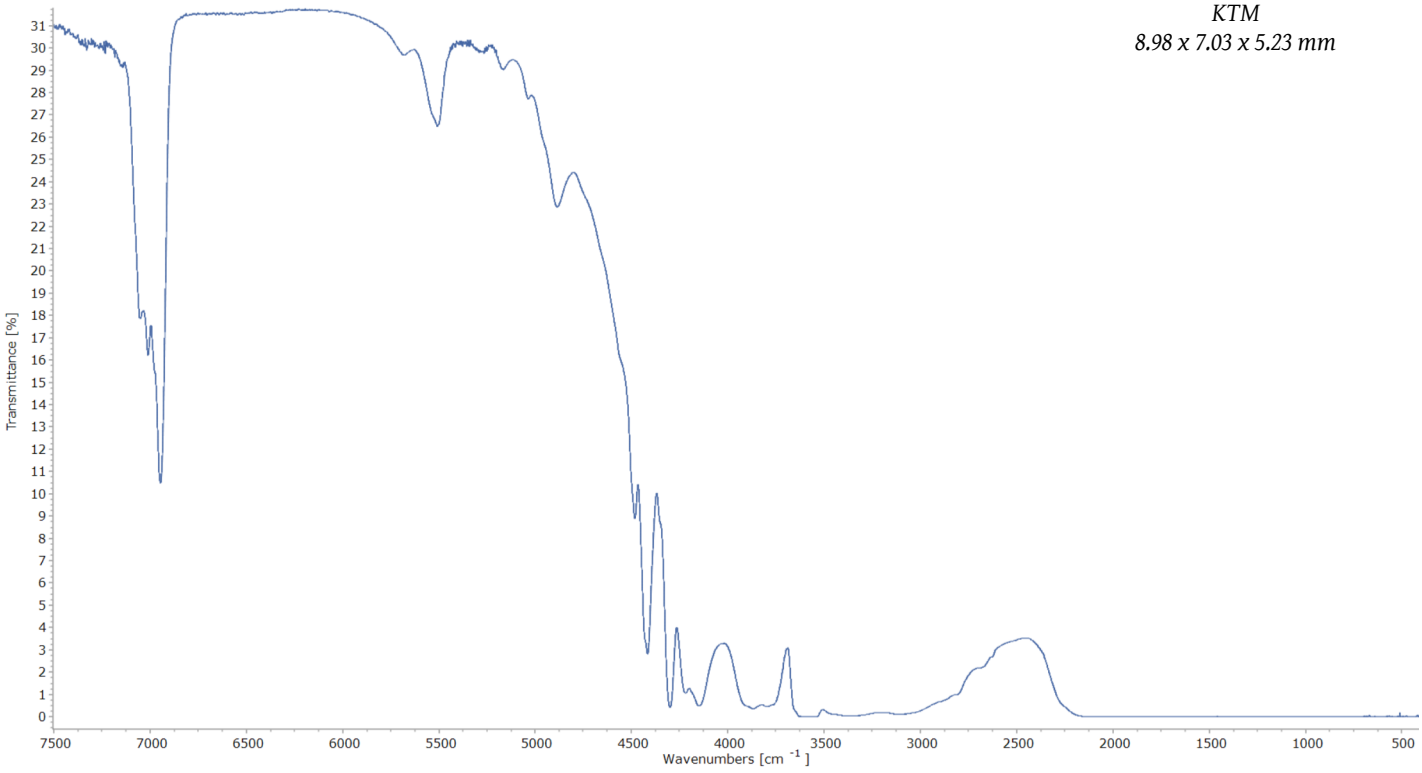


## EDXRF analysis

| Compound | m/m% | StdErr | El | m/m% | StdErr |
|---|---|---|---|---|---|
| Al2O3 | 43.93 | 0.26 | Al | 23.25 | 0.14 |
| SiO2 | 30.25 | 0.23 | Si | 14.14 | 0.11 |
| MgO | 21.04 | 0.20 | Mg | 12.69 | 0.12 |
| Cr2O3 | 0.251 | 0.017 | Cr | 0.172 | 0.011 |
| Fe2O3 | 0.0760 | 0.0084 | Fe | 0.0532 | 0.0059 |
| MnO | 0.0632 | 0.0048 | Mn | 0.0489 | 0.0037 |
| CaO | 0.0392 | 0.0025 | Ca | 0.0280 | 0.0018 |
| TiO2 | 0.0260 | 0.0025 | Ti | 0.0156 | 0.0015 |
| Sc2O3 | 0.0194 | 0.0018 | Sc | 0.0126 | 0.0012 |
| V2O5 | 0.0063 | 0.0011 | V | 0.0035 | 0.0006 |
| Ga2O3 | 0.0051 | 0.0005 | Ga | 0.0038 | 0.0004 |

KnownConc= 3.30 B2O3 REST= 1.00 H2O D/S= 0
Sum Conc's before normalisation to 100% : 77.5 %

## Emission spectra

*KTM*
*8.98 x 7.03 x 5.23 mm*

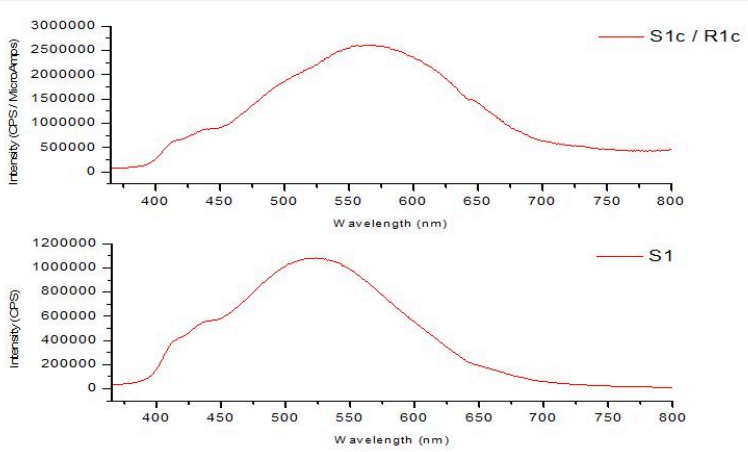


*Emission spectra under λex = 254nm at room temperature*

*S1: measured*
*S1c/R1c: corrected*

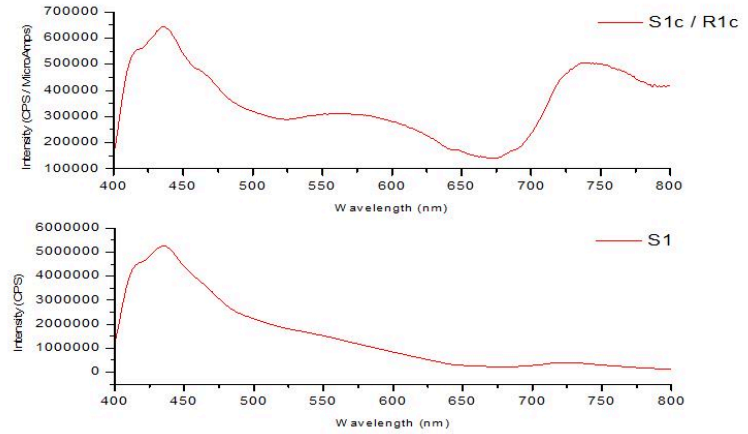


*Emission spectra under λex = 365nm at room temperature*

*S1: measured*
*S1c/R1c: corrected*

## Exitation spectra

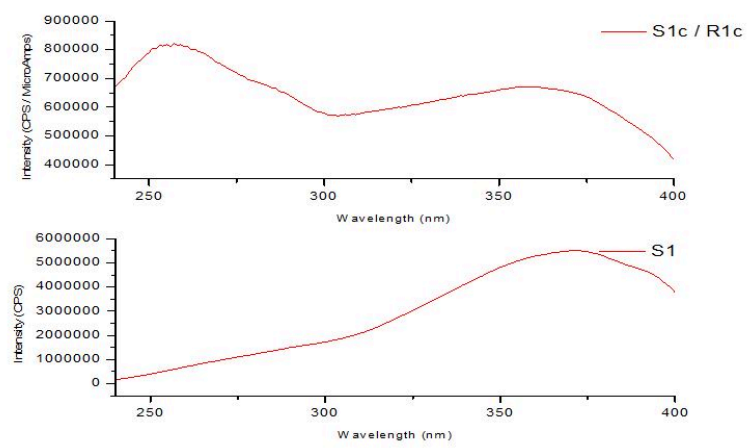


*Excitation spectra under λem = 435nm at room temperature*

*S1: measured*
*S1c/R1c: corrected*

*KTM*
*8.98 x 7.03 x 5.23 mm*

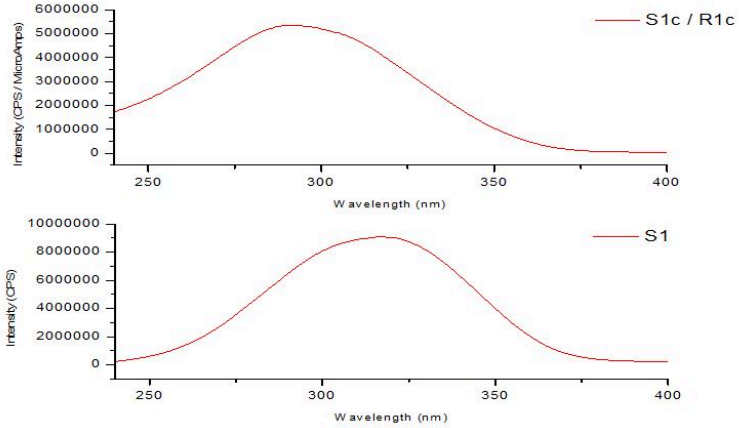


*Excitation spectra under λem = 565nm at room temperature*

*S1: measured*
*S1c/R1c: corrected*

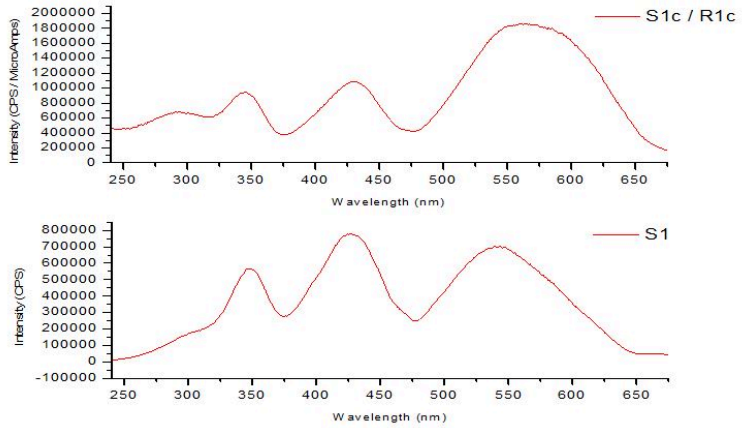


*Excitation spectra under λem = 740nm at room temperature*

*S1: measured*
*S1c/R1c: corrected*

# Appendix

## *Sample KUD6*

*KUD6*
*8.66 x 7.96 x 5.57 mm*

Raman spectrum

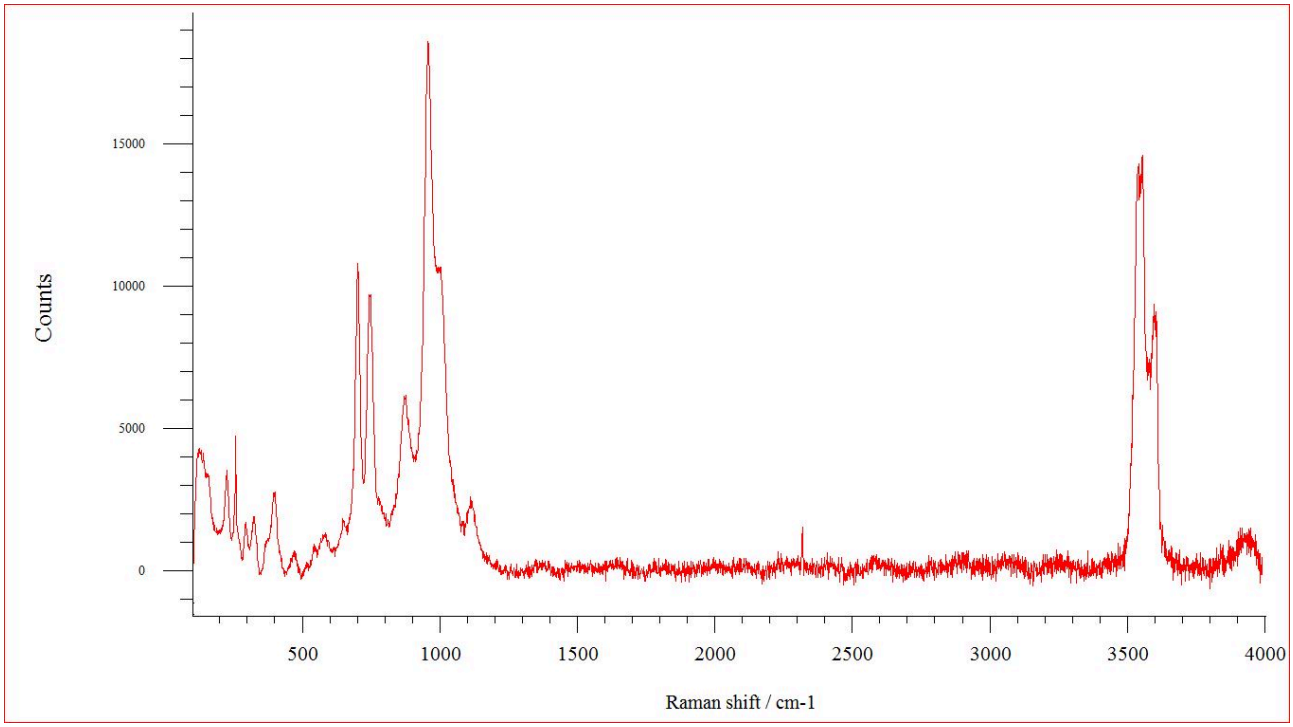


UV-Vis-NIR spectrum

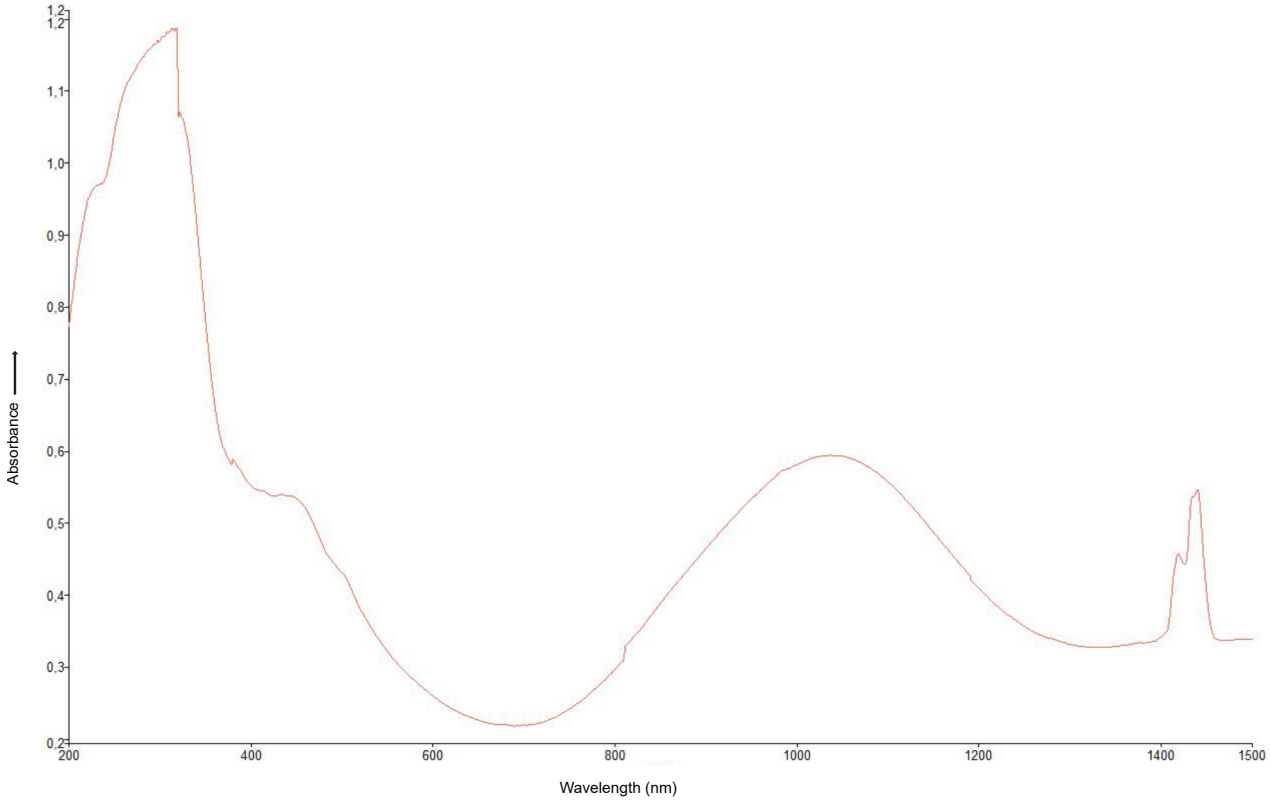

## FTIR spectra (absorption & reflectance)

*KUD6*
*8.66 x 7.96 x 5.57 mm*

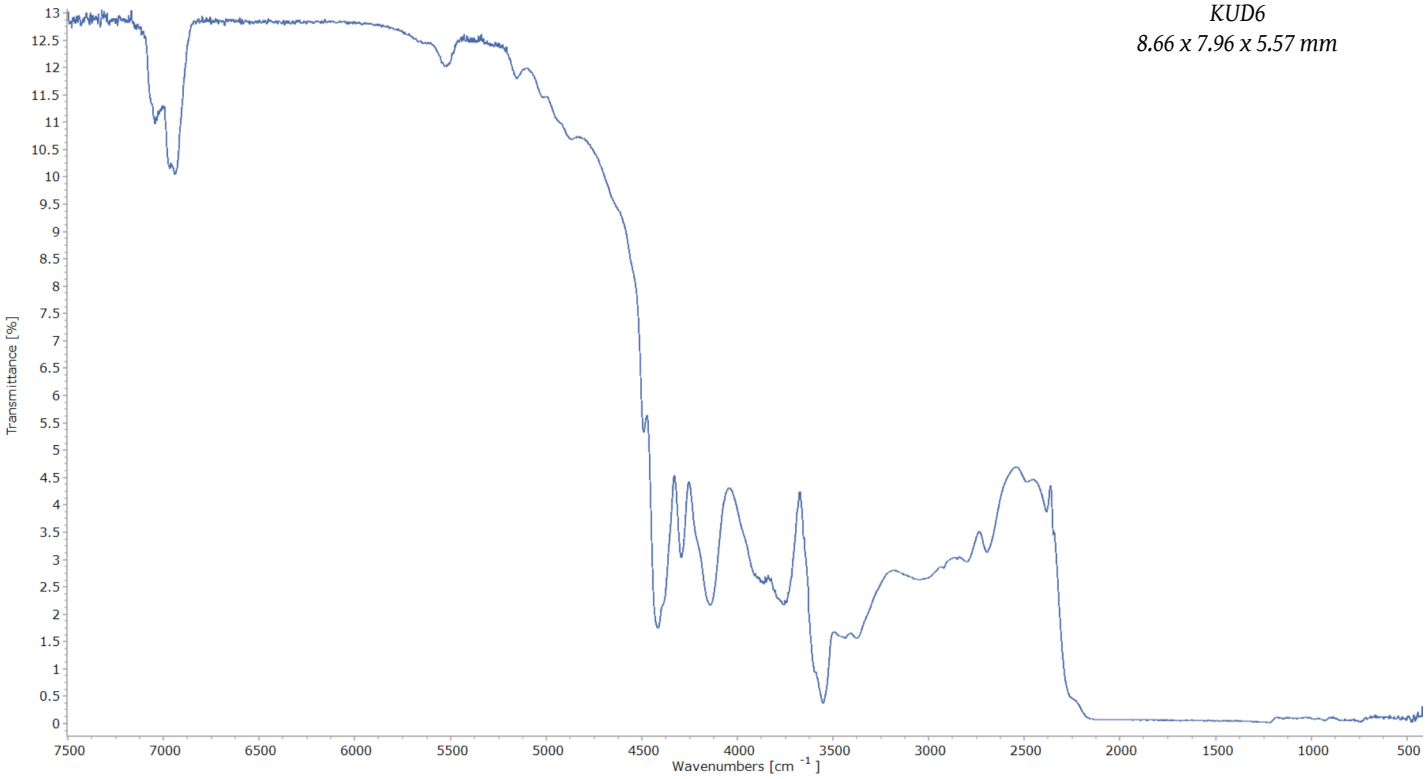


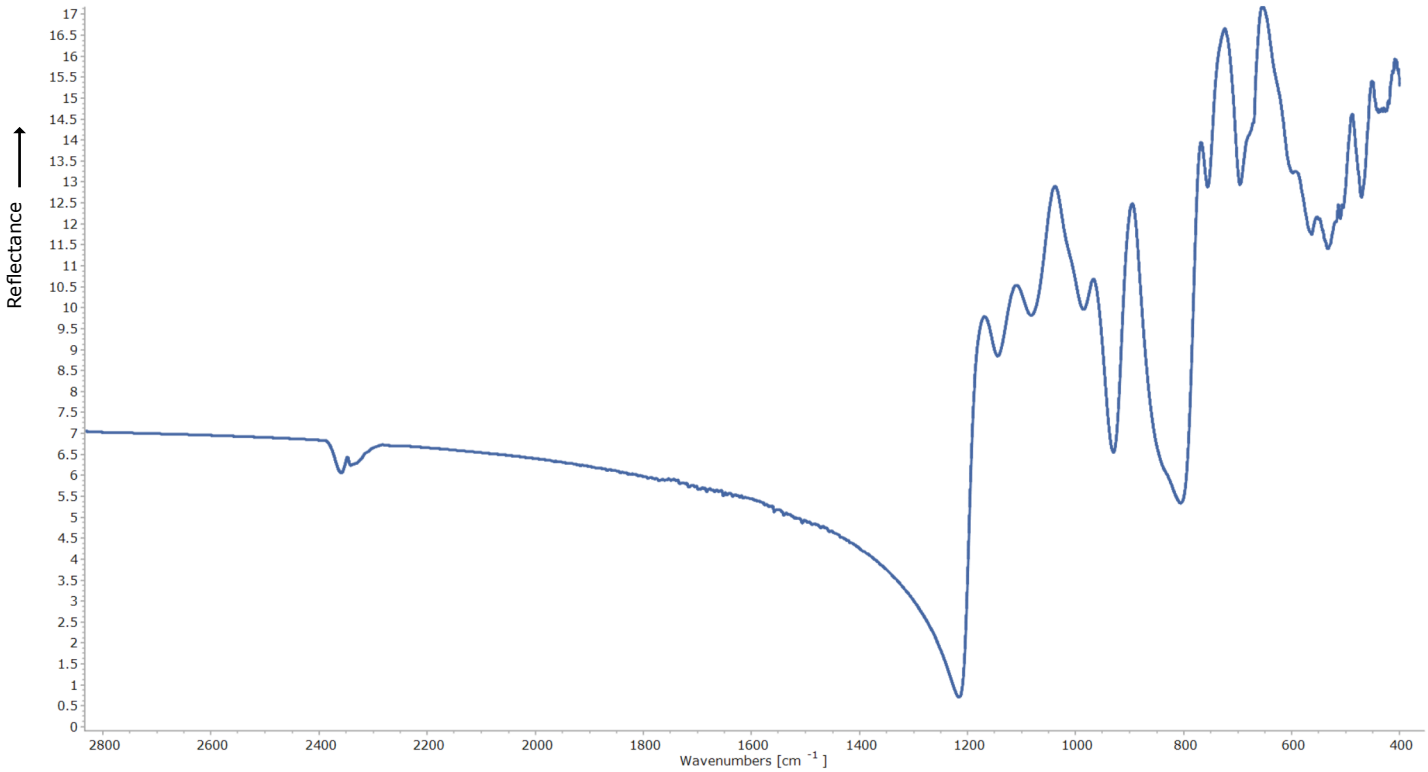

*KUD6*
*8.66 x 7.96 x 5.57 mm*

## EDXRF analysis

| Compound | m/m% | StdErr | El | m/m% | StdErr |
|---|---|---|---|---|---|
| Al2O3 | 46.31 | 0.26 | Al | 24.51 | 0.14 |
| SiO2 | 27.92 | 0.22 | Si | 13.05 | 0.10 |
| MgO | 19.75 | 0.20 | Mg | 11.91 | 0.12 |
| Fe2O3 | 1.38 | 0.13 | Fe | 0.966 | 0.091 |
| TiO2 | 0.150 | 0.015 | Ti | 0.0902 | 0.0088 |
| CaO | 0.101 | 0.005 | Ca | 0.0726 | 0.0036 |
| V2O5 | 0.0152 | 0.0017 | V | 0.0085 | 0.0009 |
| MnO | 0.0149 | 0.0017 | Mn | 0.0115 | 0.0013 |
| Cr2O3 | 0.0125 | 0.0009 | Cr | 0.0086 | 0.0006 |
| Co3O4 | 0.0122 | 0.0033 | Co | 0.0090 | 0.0024 |
| Cl | 0.0104 | 0.0031 | Cl | 0.0104 | 0.0031 |
| K2O | 0.0066 | 0.0016 | K | 0.0055 | 0.0013 |

KnownConc= 3.30 B2O3 REST= 1.00 H2O D/S= 0
Sum Conc's before normalisation to 100% : 76.0 %

## Emission spectra

*KUD6*
*8.66 x 7.96 x 5.57 mm*

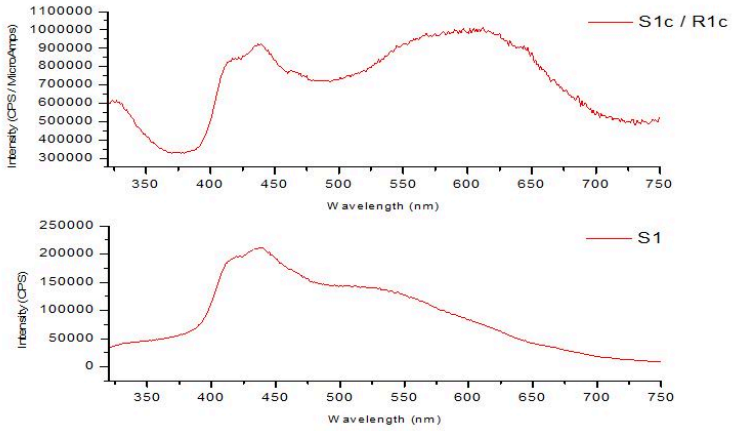


*Emission spectra under λex = 254nm at room temperature*

*S1: measured*
*S1c/R1c: corrected*

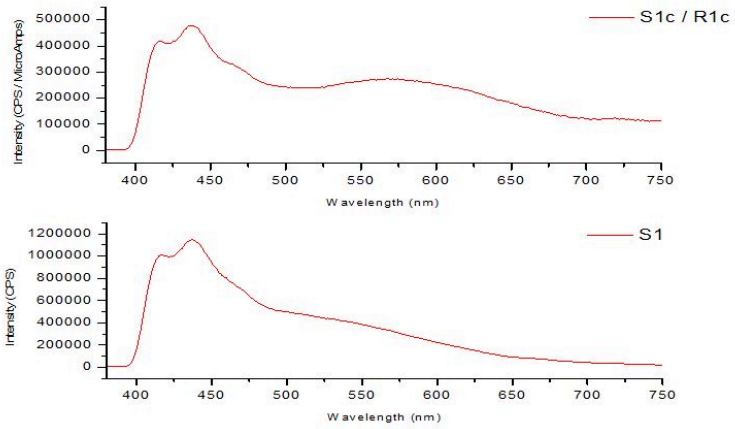


*Emission spectra under λex = 365nm at room temperature*

*S1: measured*
*S1c/R1c: corrected*

## Exitation spectra

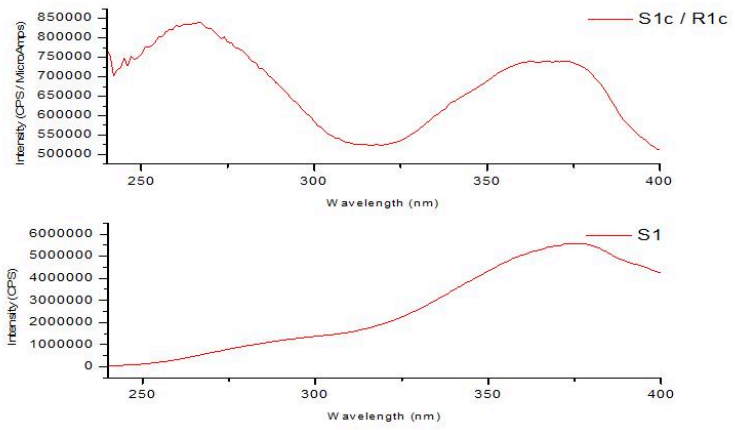


*Excitation spectra under λem = 430nm at room temperature*

*S1: measured*
*S1c/R1c: corrected*

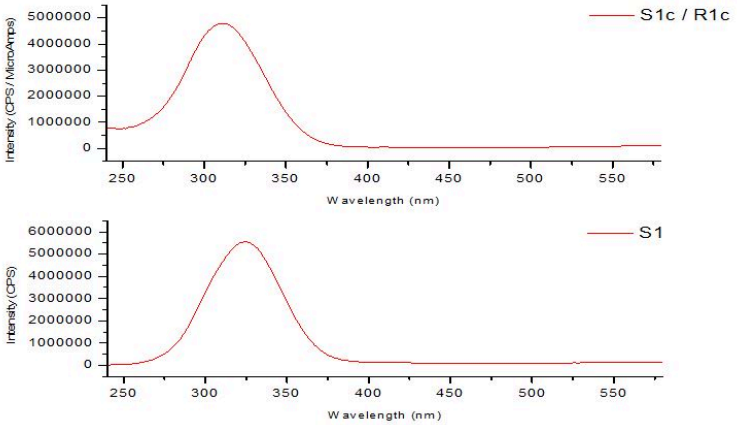


*KUD6*
*8.66 x 7.96 x 5.57 mm*

*Excitation spectra under λem = 610nm at room temperature*

*S1: measured*
*S1c/R1c: corrected*

# Appendix

## *Sample KUD3*

*KUD3*
*10.14 x 9.10 x 5.53 mm*

Raman spectrum

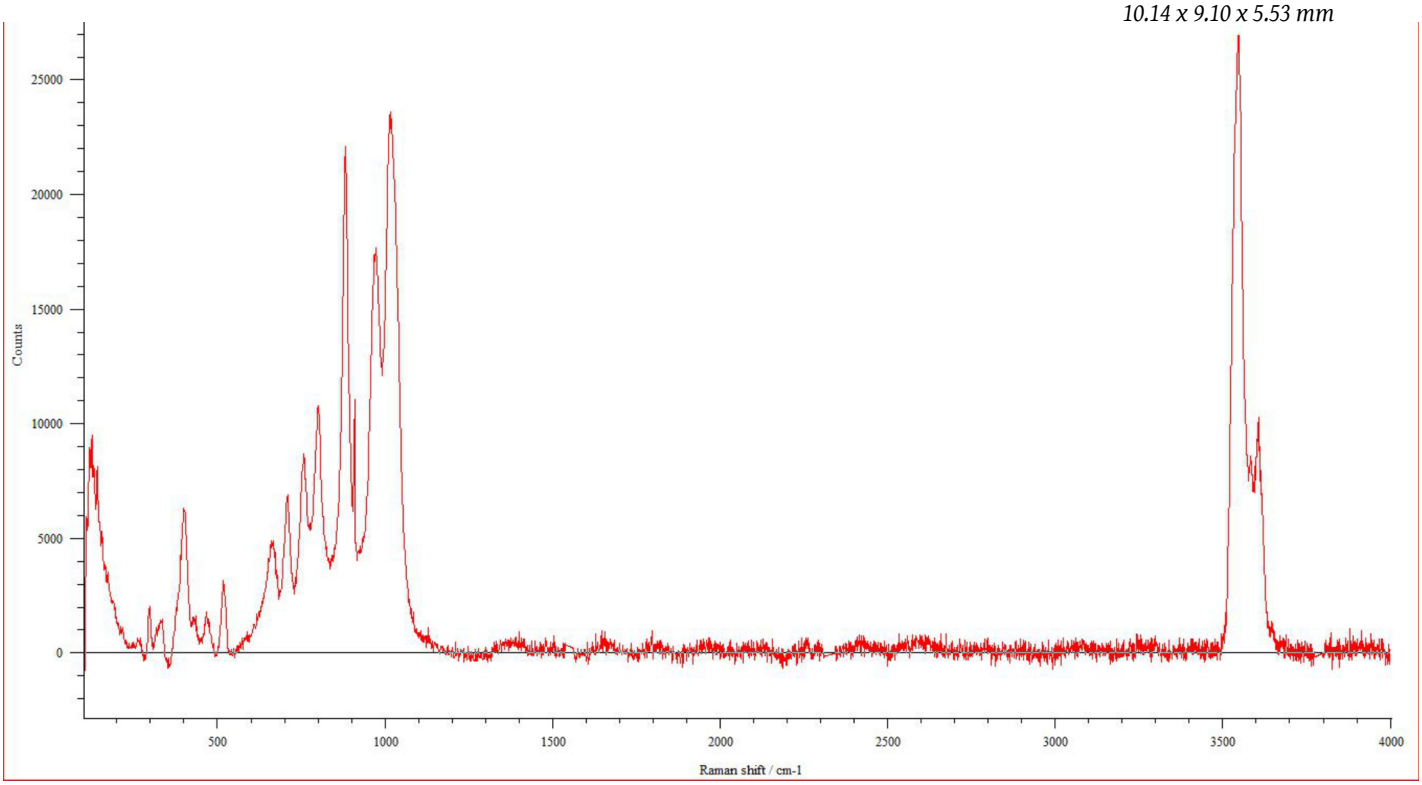


UV-Vis-NIR spectrum

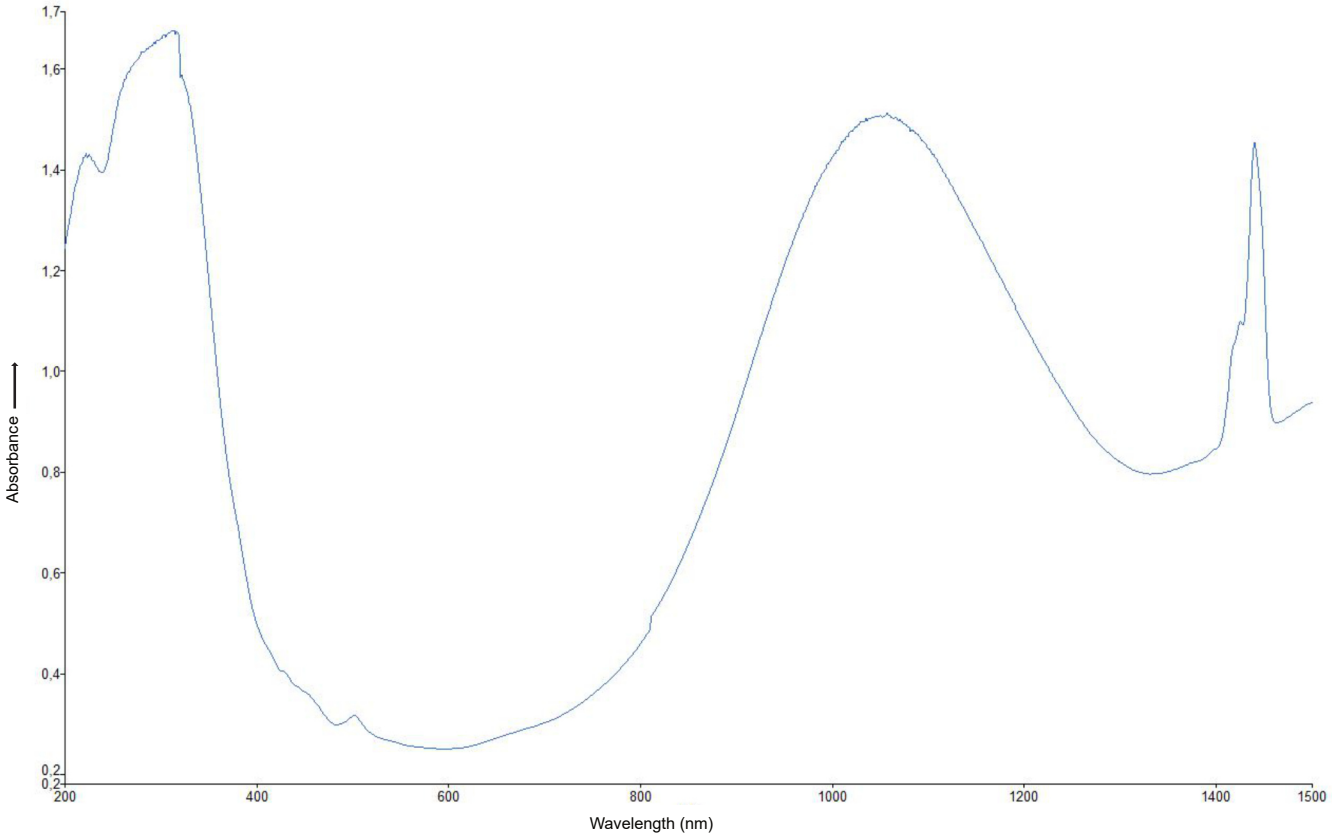

*KUD3*
*10.14 x 9.10 x 5.53 mm*

## FTIR spectrum

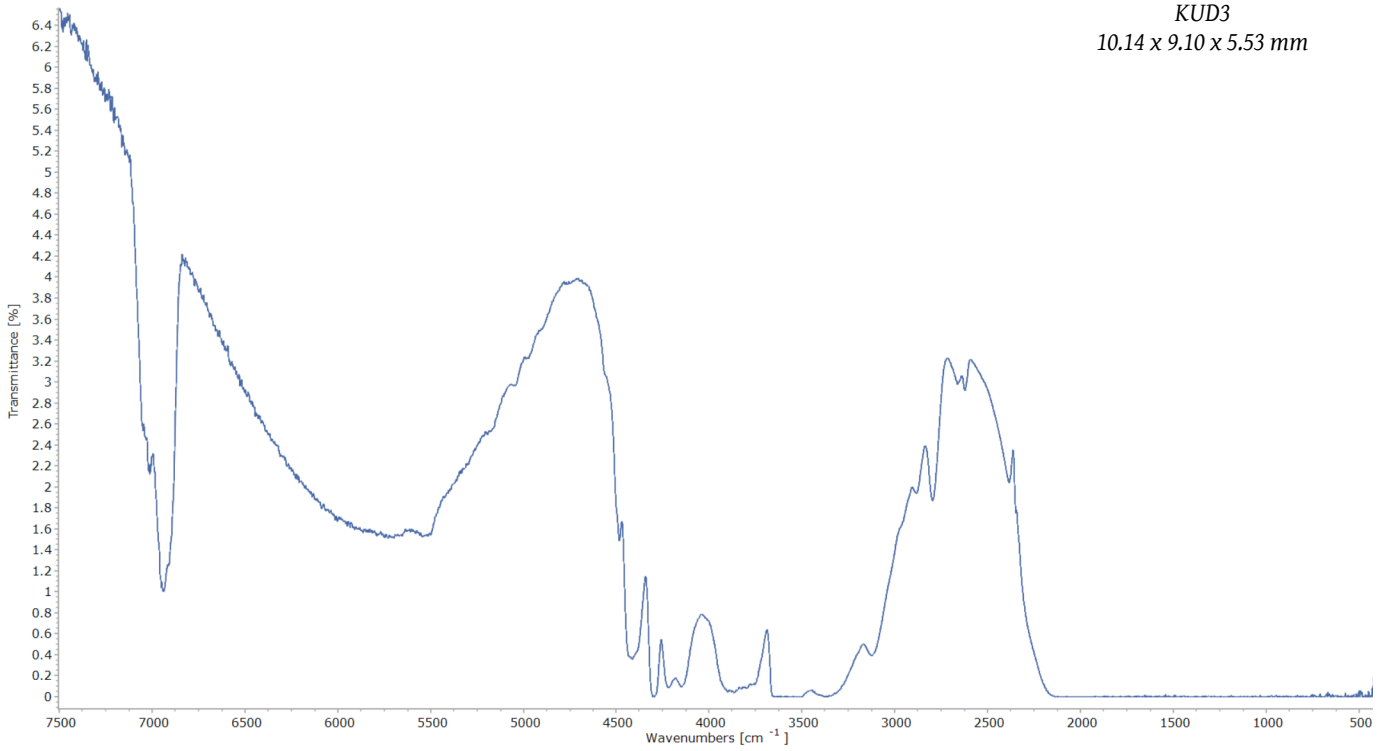


## EDXRF analysis

| Compound | m/m% | StdErr | El | m/m% | StdErr |
|---|---|---|---|---|---|
| Al2O3 | 42.54 | 0.26 | Al | 22.51 | 0.14 |
| SiO2 | 29.92 | 0.22 | Si | 13.99 | 0.10 |
| MgO | 19.91 | 0.20 | Mg | 12.01 | 0.12 |
| Fe2O3 | 3.05 | 0.19 | Fe | 2.13 | 0.13 |
| CaO | 0.147 | 0.007 | Ca | 0.105 | 0.005 |
| Co3O4 | 0.0309 | 0.0073 | Co | 0.0227 | 0.0053 |
| TiO2 | 0.0254 | 0.0025 | Ti | 0.0152 | 0.0015 |
| MnO | 0.0187 | 0.0019 | Mn | 0.0145 | 0.0015 |
| ZnO | 0.0109 | 0.0006 | Zn | 0.0088 | 0.0005 |
| Cl | 0.0101 | 0.0032 | Cl | 0.0101 | 0.0032 |
| V2O5 | 0.0094 | 0.0011 | V | 0.0053 | 0.0006 |
| K2O | 0.0093 | 0.0017 | K | 0.0077 | 0.0014 |
| Ga2O3 | 0.0073 | 0.0006 | Ga | 0.0054 | 0.0005 |

KnownConc= 3.30 B2O3 REST= 1.00 H2O D/S= 0
Sum Conc's before normalisation to 100% : 85.7 %

## Emission spectra

*KUD3*
*10.14 x 9.10 x 5.53 mm*

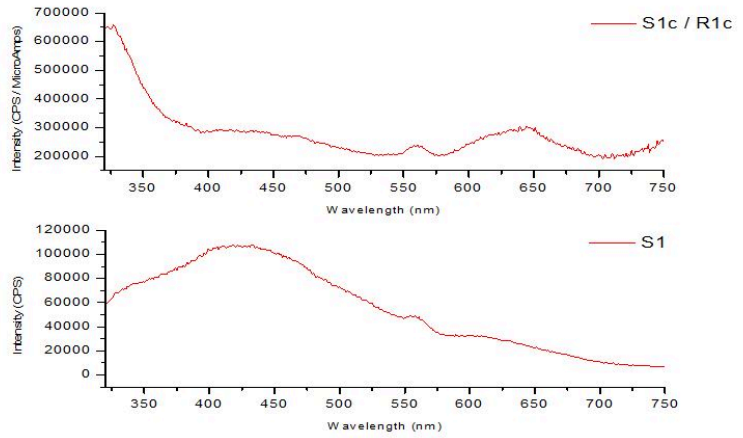


*Emission spectra under λex = 254nm at room temperature*

*S1: measured*
*S1c/R1c: corrected*

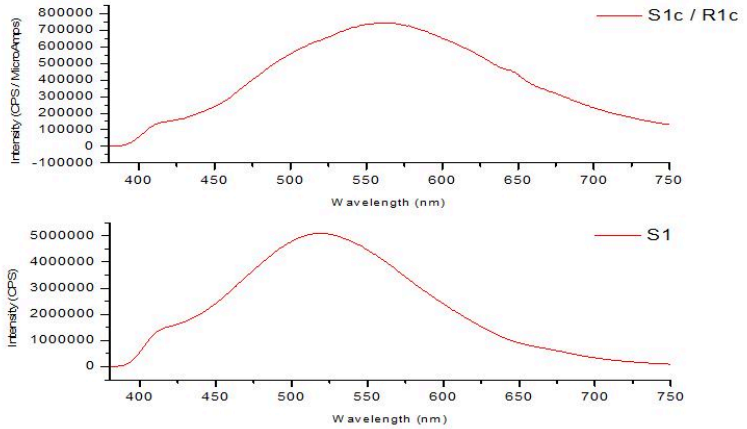


*Emission spectra under λex = 365nm at room temperature*

*S1: measured*
*S1c/R1c: corrected*

## Exitation spectra

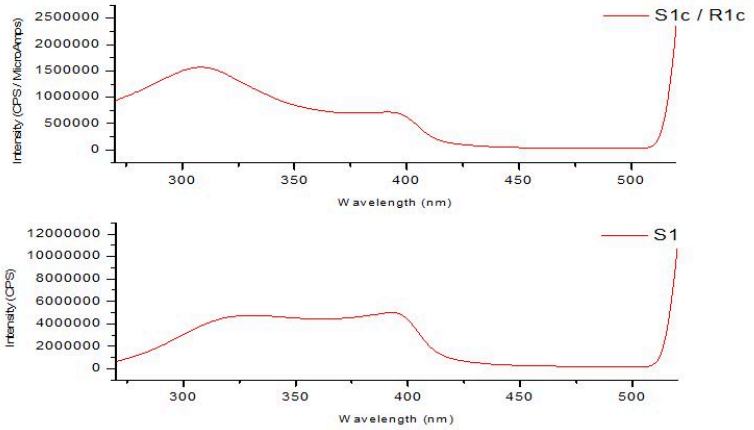


*Excitation spectra under λem = 550nm at room temperature*

*S1: measured*
*S1c/R1c: corrected*

# Appendix

## *Sample KSE4637*

*KSE4637*
*7.66 x 7.47 x 5.28 mm*

Raman spectrum

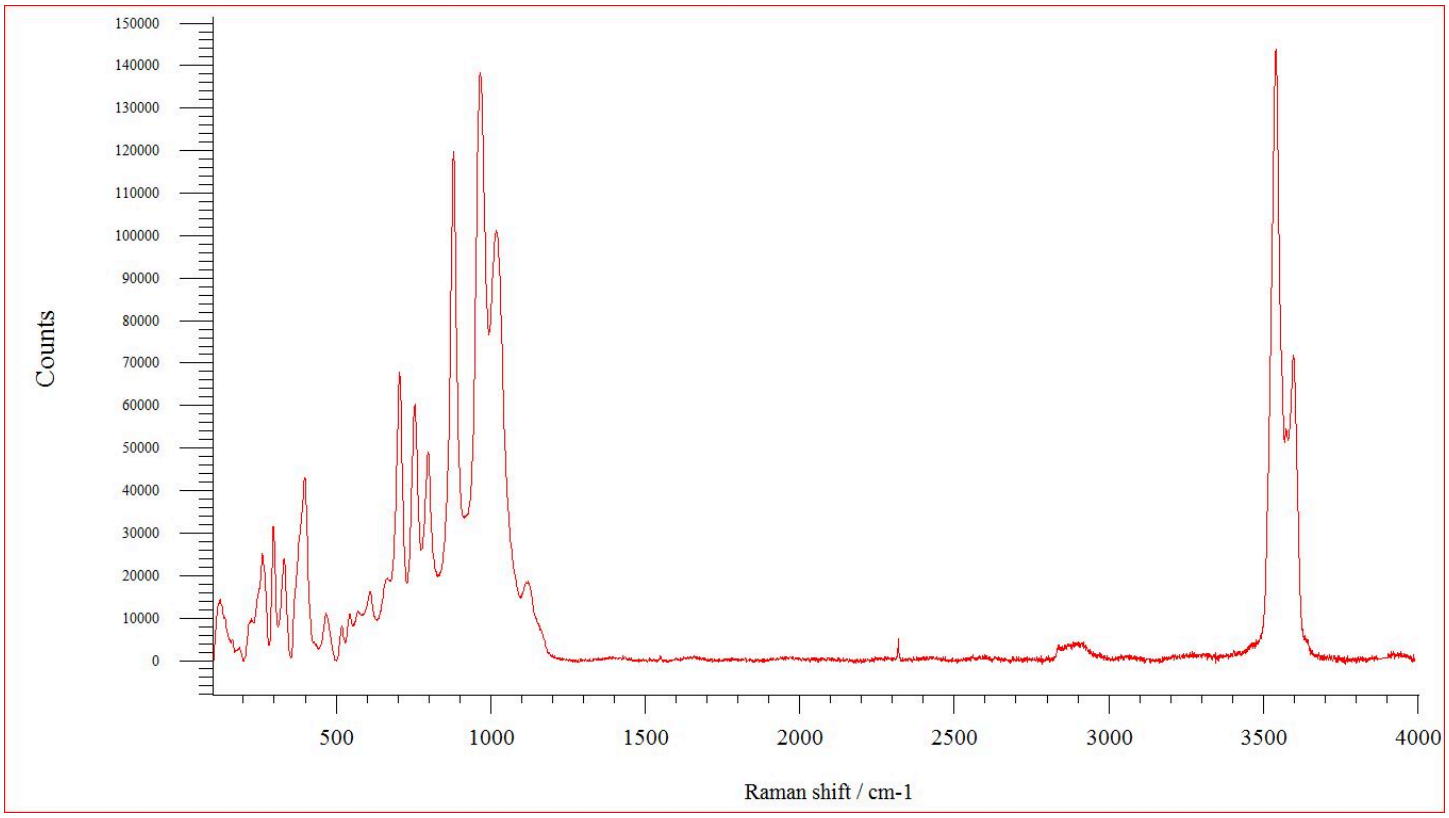


UV-Vis-NIR spectrum

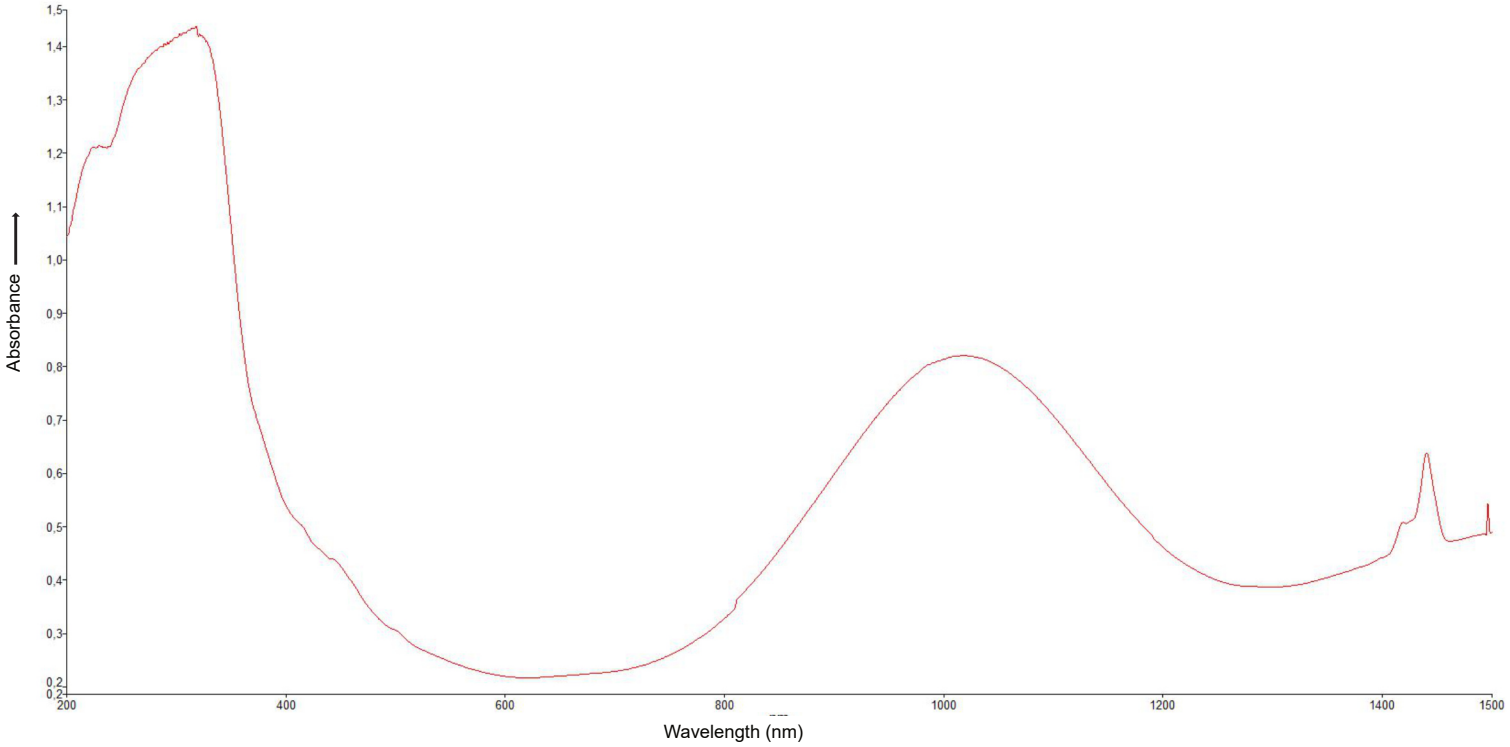

## FTIR spectrum

*KSE4637*
*7.66 x 7.47 x 5.28 mm*

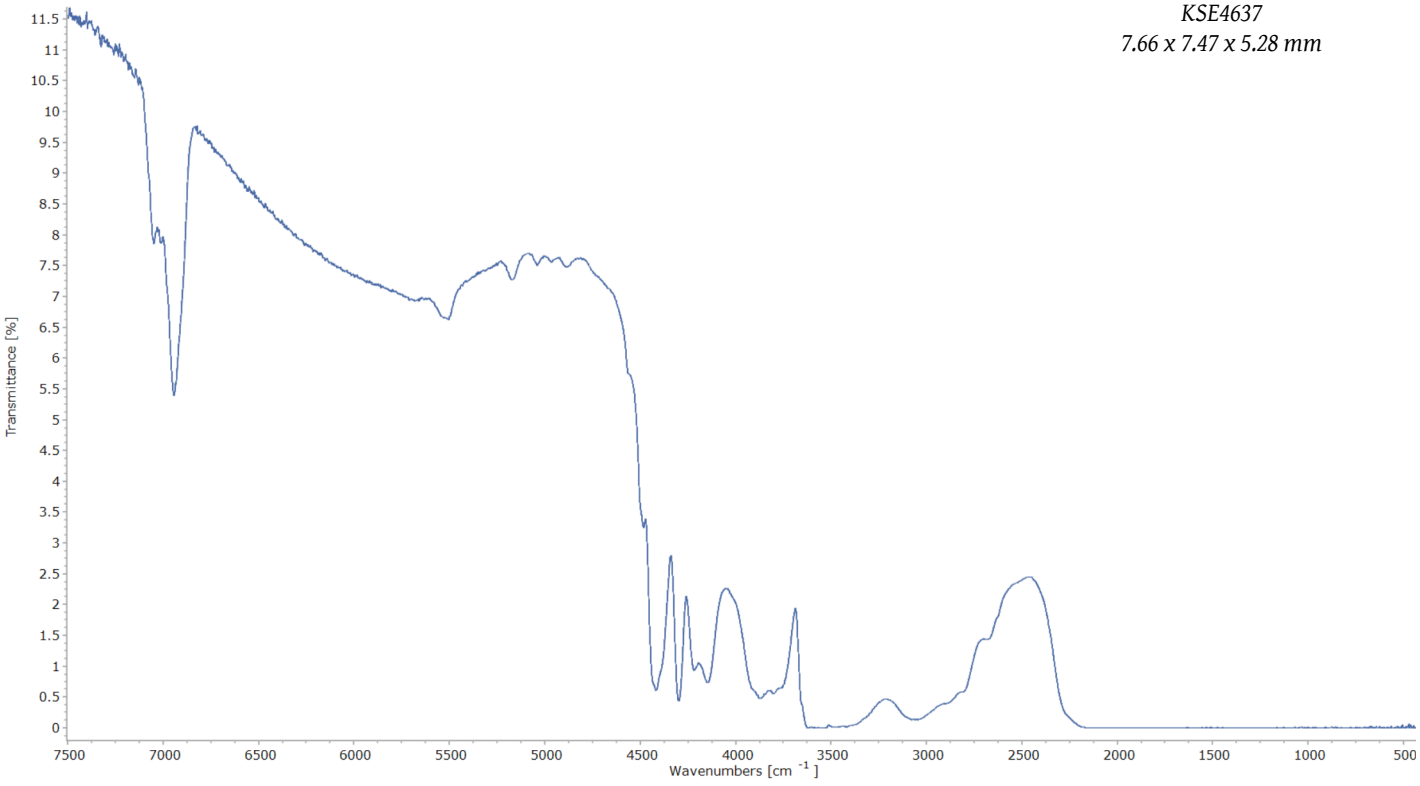


## EDXRF analysis

| Compound | m/m% | StdErr | El | m/m% | StdErr |
|---|---|---|---|---|---|
| Al2O3 | 42.99 | 0.26 | Al | 22.75 | 0.14 |
| SiO2 | 30.13 | 0.22 | Si | 14.08 | 0.11 |
| MgO | 20.33 | 0.20 | Mg | 12.26 | 0.12 |
| Fe2O3 | 2.04 | 0.16 | Fe | 1.43 | 0.11 |
| CaO | 0.0585 | 0.0029 | Ca | 0.0418 | 0.0021 |
| TiO2 | 0.0523 | 0.0051 | Ti | 0.0314 | 0.0031 |
| V2O5 | 0.0263 | 0.0016 | V | 0.0147 | 0.0009 |
| MnO | 0.0245 | 0.0020 | Mn | 0.0190 | 0.0016 |
| Co3O4 | 0.0180 | 0.0049 | Co | 0.0132 | 0.0036 |
| K2O | 0.0143 | 0.0020 | K | 0.0119 | 0.0017 |

KnownConc= 3.30 B2O3 REST= 1.00 H2O D/S= 0
Sum Conc's before normalisation to 100% : 82.0 %

## Emission spectra

*KSE4637*
*7.66 x 7.47 x 5.28 mm*

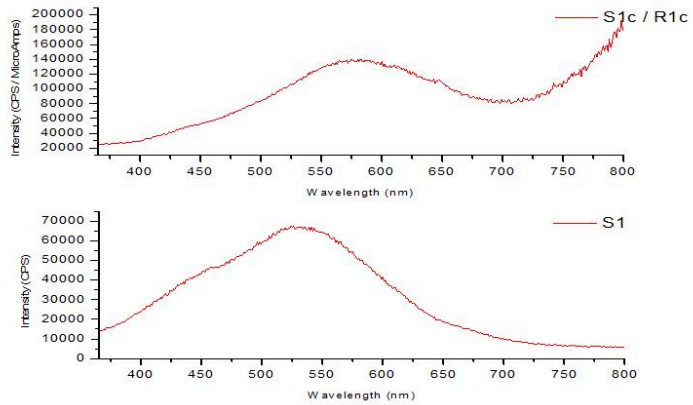


*Emission spectra*
*under λex = 254nm at*
*room temperature*

*S1: measured*
*S1c/R1c: corrected*

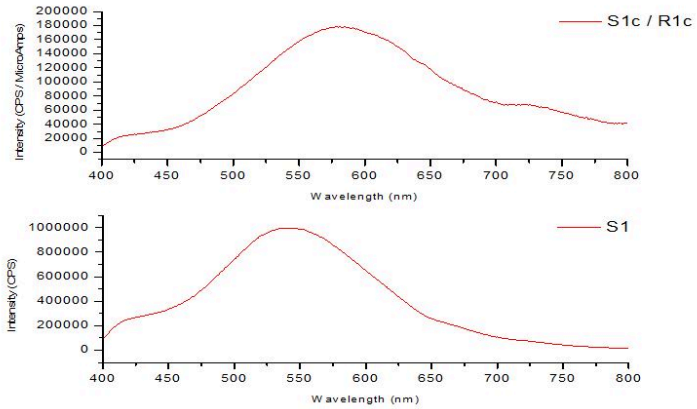


*Emission spectra*
*under λex = 365nm at*
*room temperature*

*S1: measured*
*S1c/R1c: corrected*

## Exitation spectra

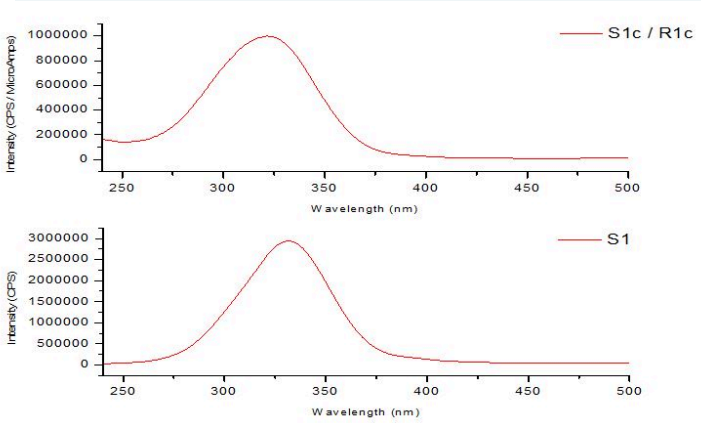


*Excitation spectra*
*under λem = 580nm at*
*room temperature*

*S1: measured*
*S1c/R1c: corrected*

# Appendix

## *Sample KUH*

*KUH*
*6.51 x 5.38 x 3.43 mm*

Raman spectrum

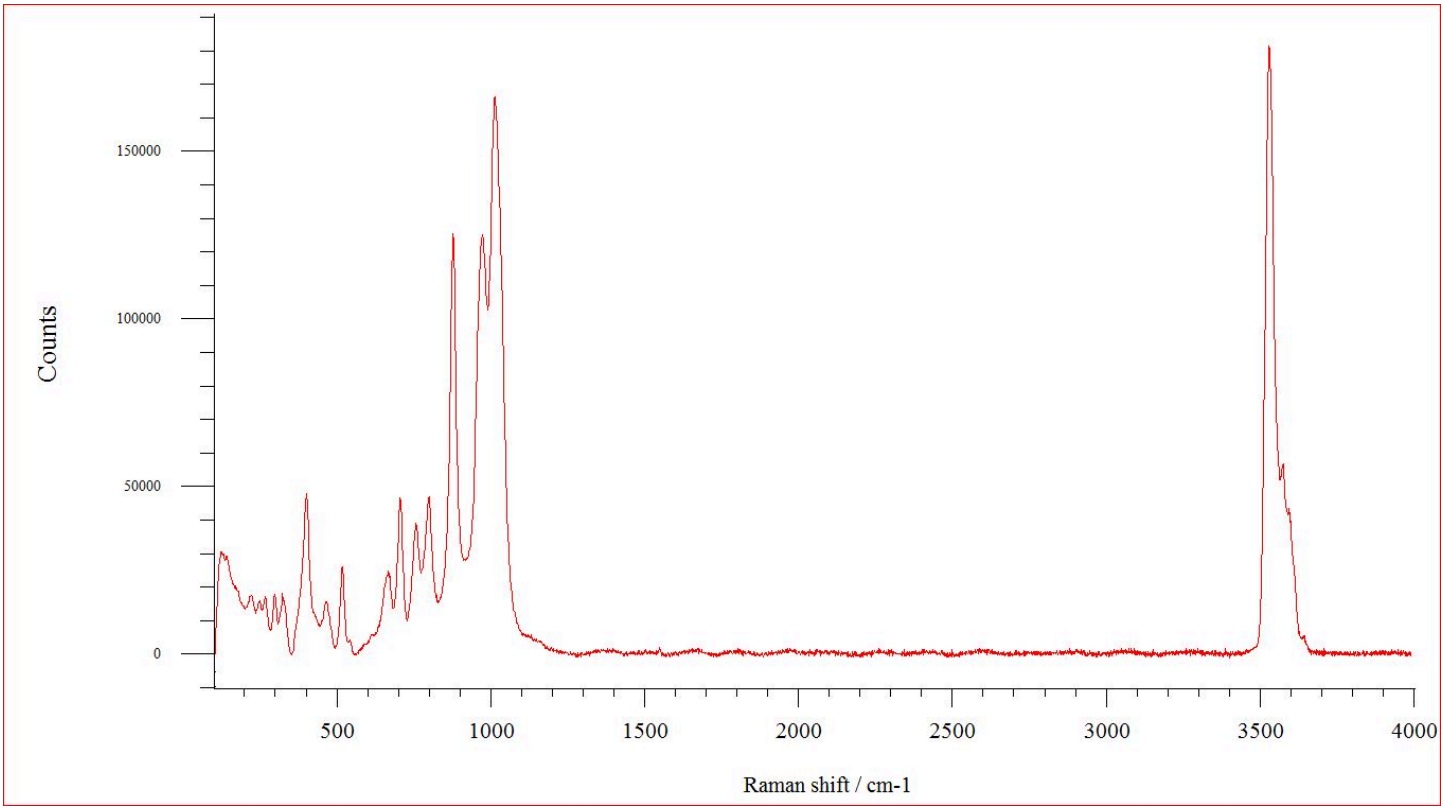


UV-Vis-NIR spectrum

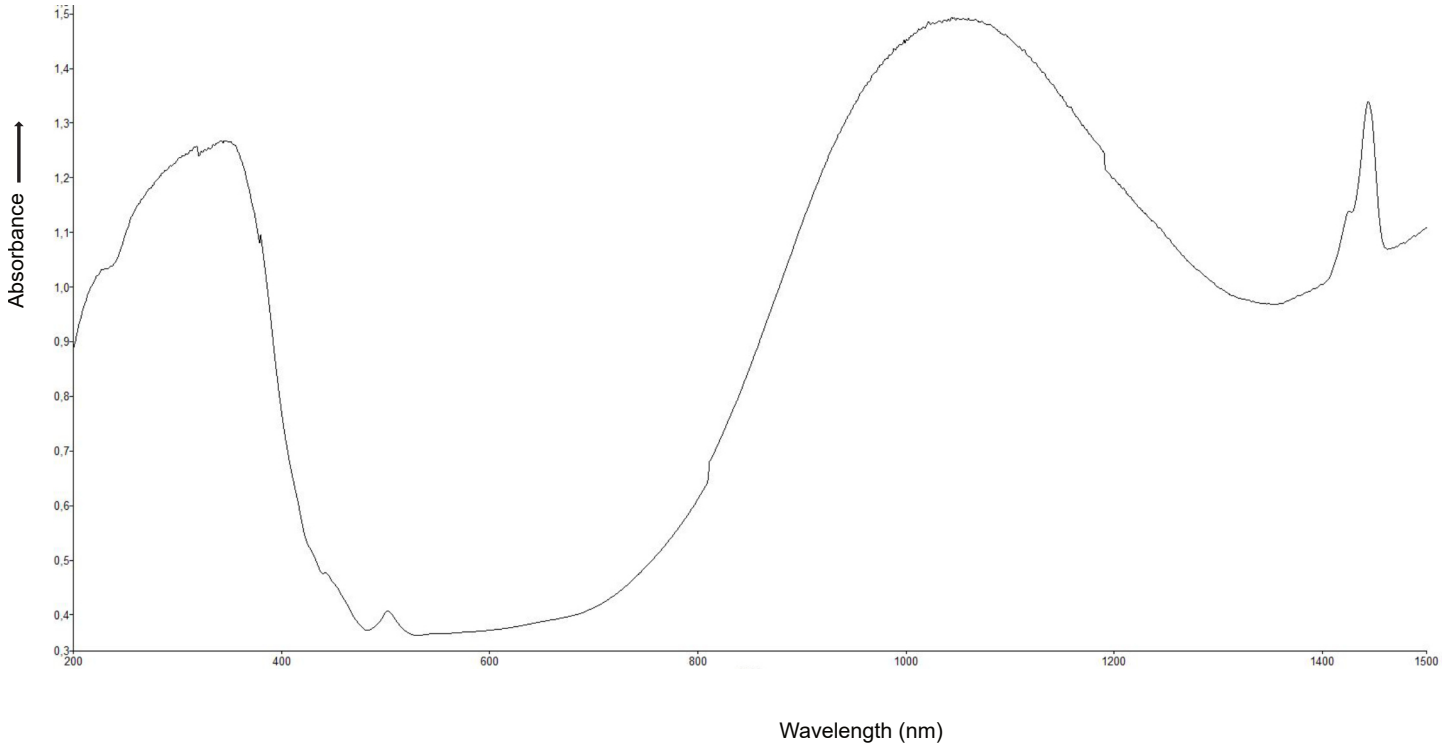

## FTIR spectrum

*KUH*
*6.51 x 5.38 x 3.43 mm*

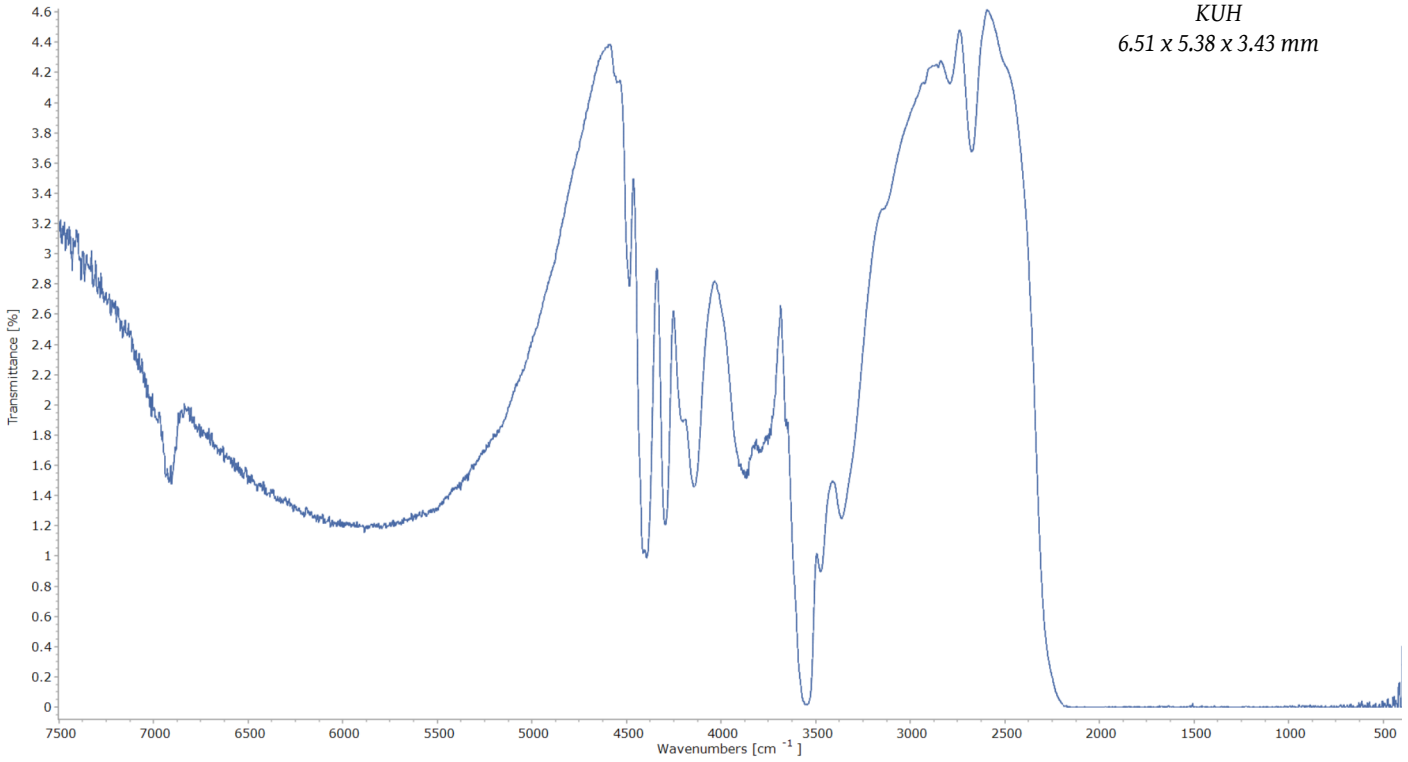


## EDXRF analysis

| Compound | m/m% | StdErr | El | m/m% | StdErr |
|---|---|---|---|---|---|
| Al2O3 | 43.79 | 0.26 | Al | 23.18 | 0.14 |
| SiO2 | 28.46 | 0.22 | Si | 13.31 | 0.10 |
| MgO | 17.63 | 0.19 | Mg | 10.63 | 0.11 |
| Fe2O3 | 5.57 | 0.25 | Fe | 3.90 | 0.18 |
| MnO | 0.111 | 0.008 | Mn | 0.0859 | 0.0065 |
| CaO | 0.0442 | 0.0027 | Ca | 0.0316 | 0.0019 |
| Co3O4 | 0.041 | 0.013 | Co | 0.0298 | 0.0097 |
| ZnO | 0.0180 | 0.0009 | Zn | 0.0145 | 0.0007 |
| Ga2O3 | 0.0123 | 0.0008 | Ga | 0.0091 | 0.0006 |
| Cl | 0.0064 | 0.0031 | Cl | 0.0064 | 0.0031 |

KnownConc= 3.30 B2O3 REST= 1.00 H2O D/S= 0
Sum Conc's before normalisation to 100% : 77.4 %

# Appendix

## *Sample KME3887*

*KME3887*

Raman spectrum of the sample

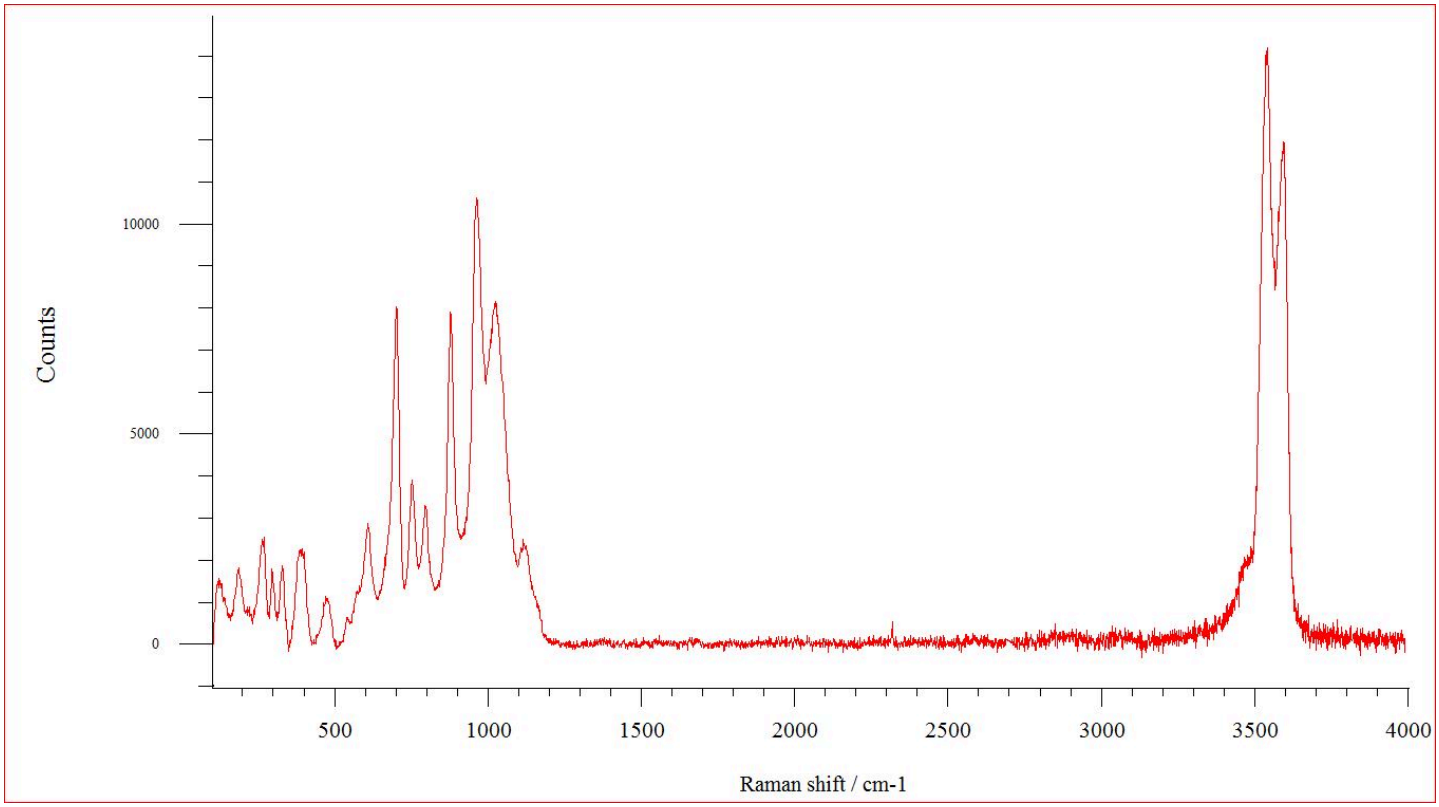


Raman spectrum of the zircon inclusion (black) matching to that of zircon in RRUFF reference data (blue)

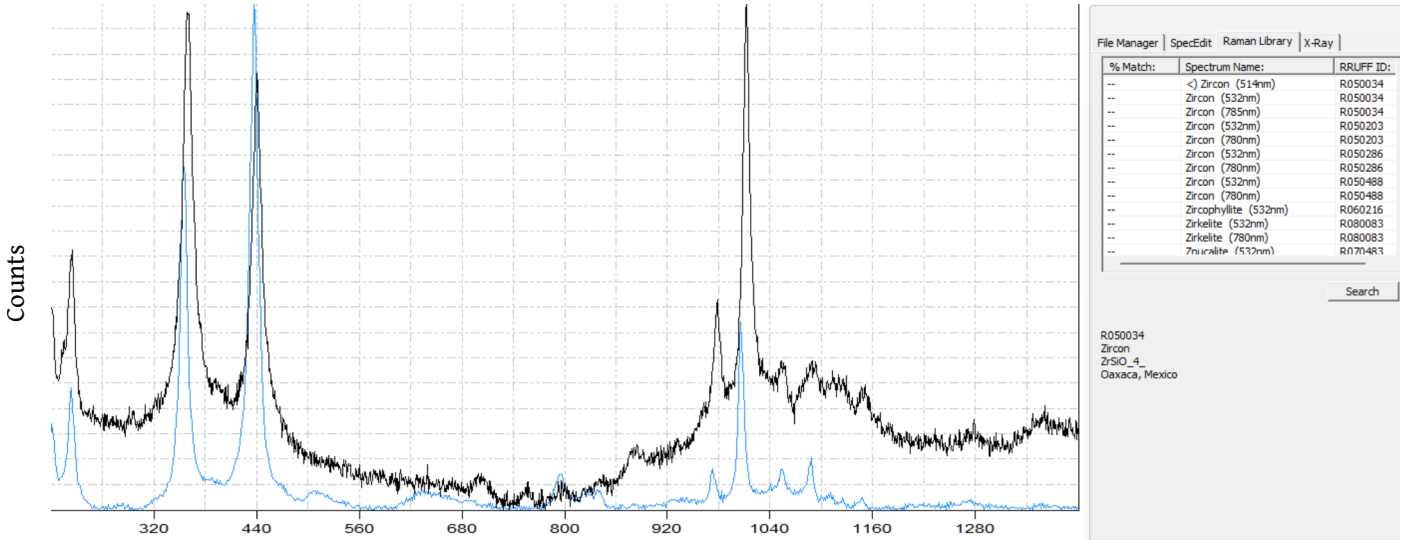

*KME3887*
*8.25 x 6.98 x 3.98 mm*

## UV-Vis-NIR spectra (polarised)

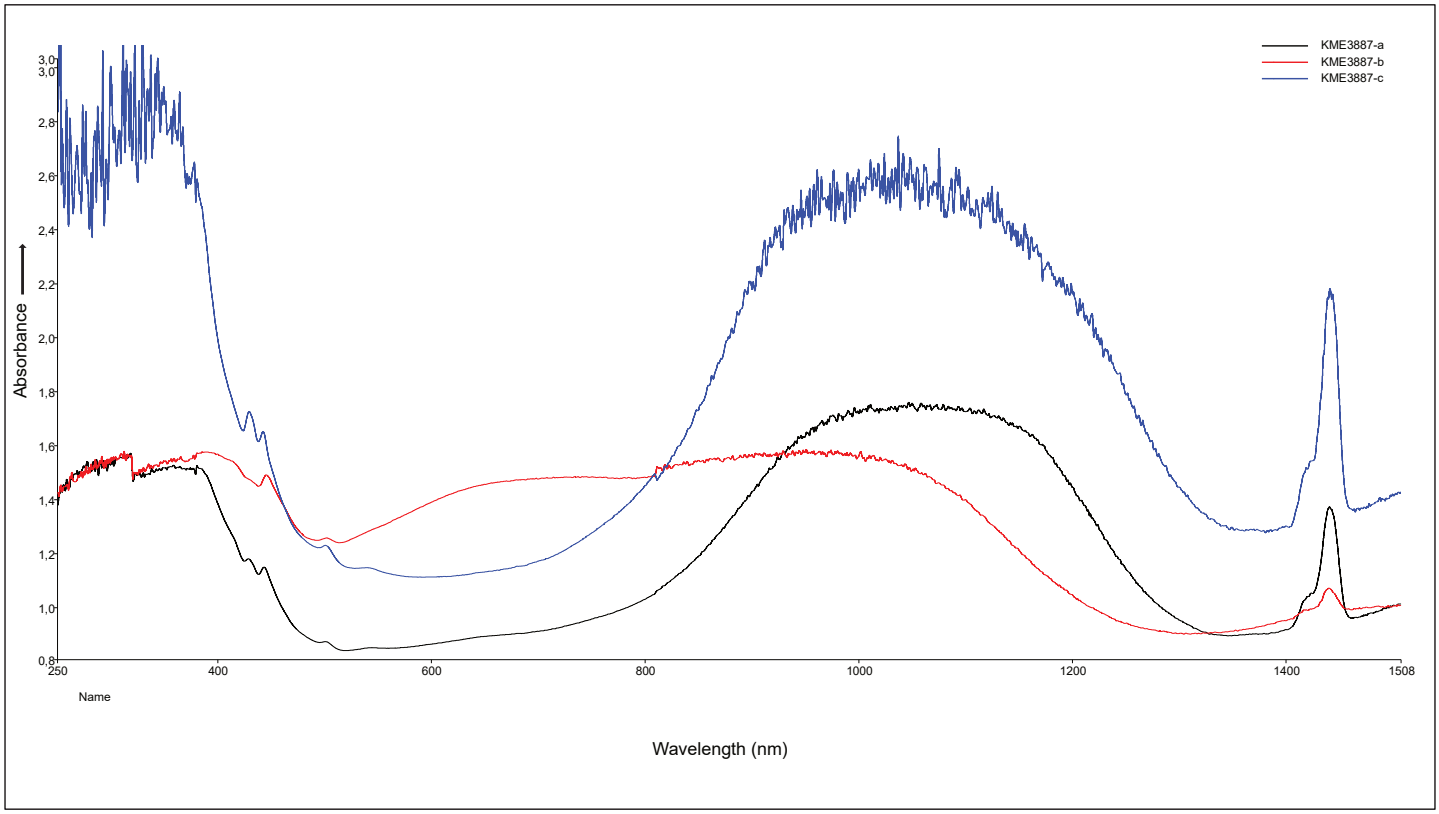


## FTIR-Transmission spectrum

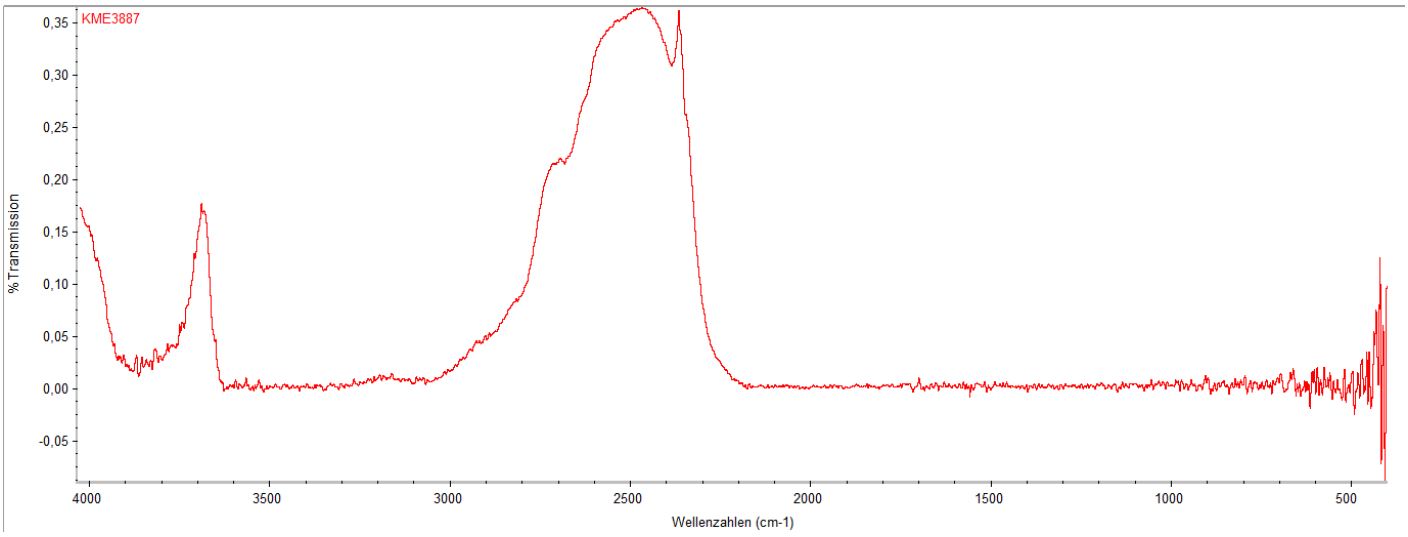

*KME3887*
*8.25 x 6.98 x 3.98 mm*

## FTIR spectrum

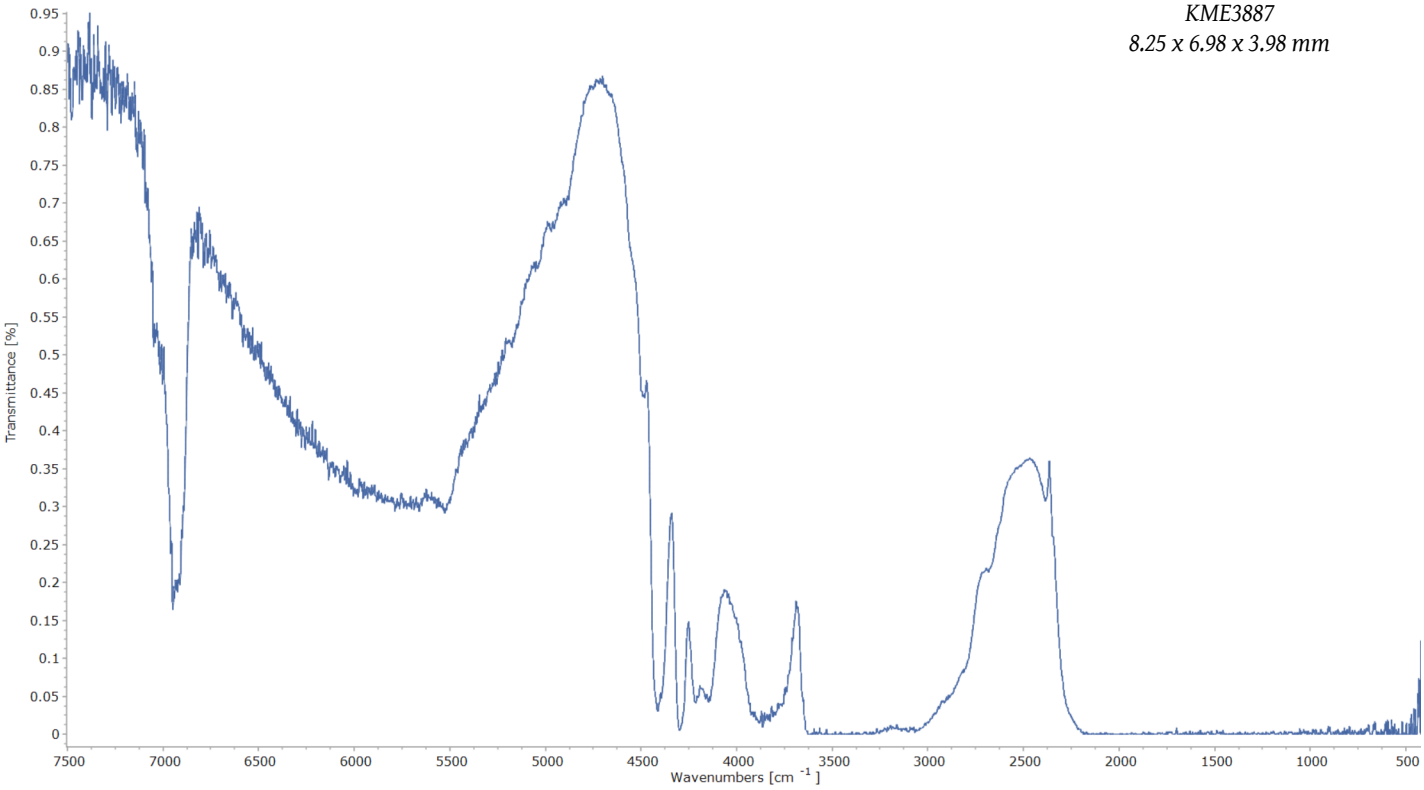


## EDXRF analysis

| Compound | m/m% | StdErr | El | m/m% | StdErr |
|---|---|---|---|---|---|
| Al2O3 | 43.06 | 0.26 | Al | 22.79 | 0.14 |
| SiO2 | 29.07 | 0.22 | Si | 13.59 | 0.10 |
| MgO | 19.22 | 0.20 | Mg | 11.59 | 0.12 |
| Fe2O3 | 4.04 | 0.22 | Fe | 2.83 | 0.15 |
| MnO | 0.147 | 0.011 | Mn | 0.114 | 0.009 |
| CaO | 0.0360 | 0.0023 | Ca | 0.0257 | 0.0016 |
| Co3O4 | 0.0350 | 0.0096 | Co | 0.0257 | 0.0070 |
| TiO2 | 0.0308 | 0.0030 | Ti | 0.0185 | 0.0018 |
| ZnO | 0.0119 | 0.0007 | Zn | 0.0096 | 0.0006 |
| Sc2O3 | 0.0108 | 0.0014 | Sc | 0.0070 | 0.0009 |
| ZrO2 | 0.0104 | 0.0005 | Zr | 0.0077 | 0.0004 |
| Cl | 0.0095 | 0.0028 | Cl | 0.0095 | 0.0028 |
| K2O | 0.0057 | 0.0013 | K | 0.0047 | 0.0011 |
| Y2O3 | 0.0052 | 0.0003 | Y | 0.0041 | 0.0002 |

KnownConc= 3.30 B2O3 REST= 1.00 H2O D/S= 0
Sum Conc's before normalisation to 100% : 84.3 %

# Appendix

## *Sample KUD8*

*KUD8*
*7.30 – 7.39 x 3.26 mm*

Raman spectrum

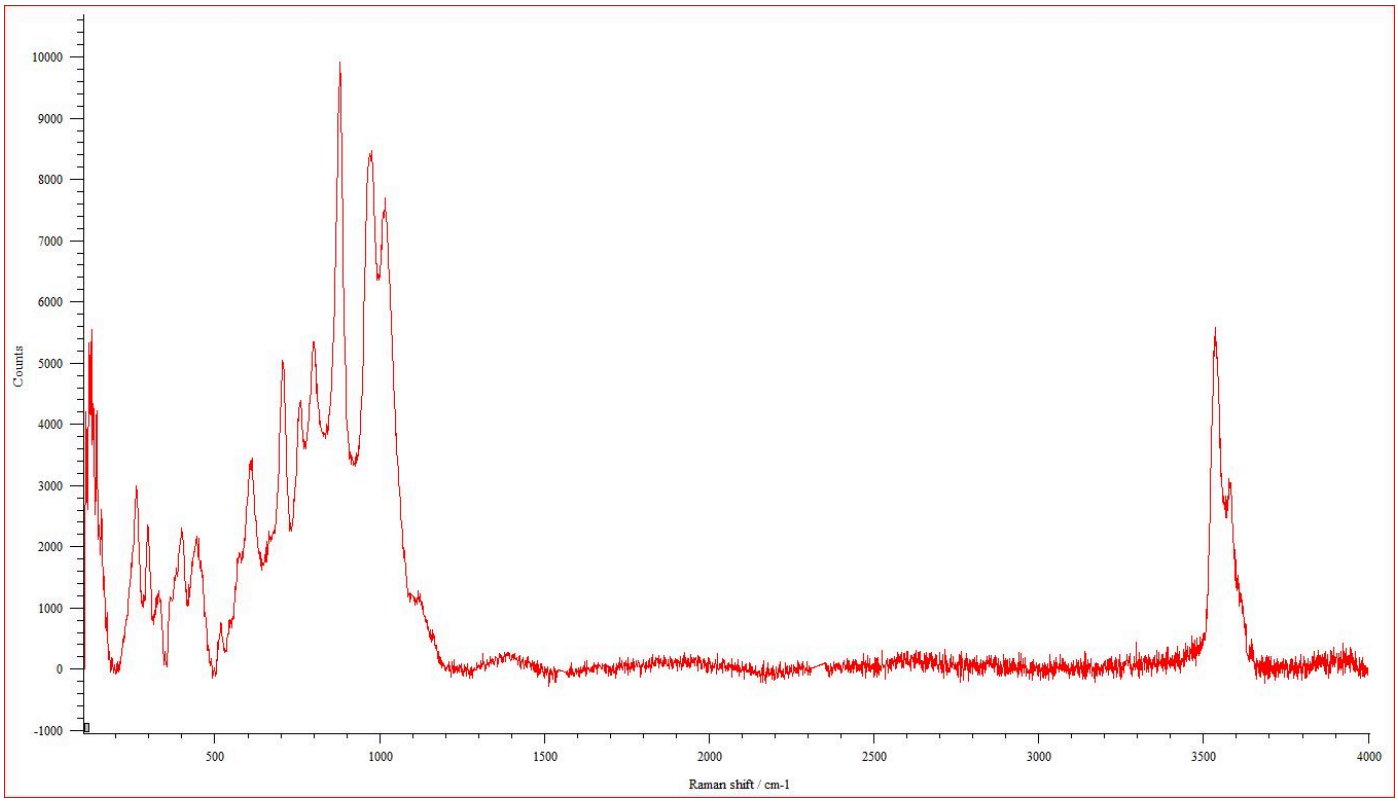


UV-Vis-NIR spectrum

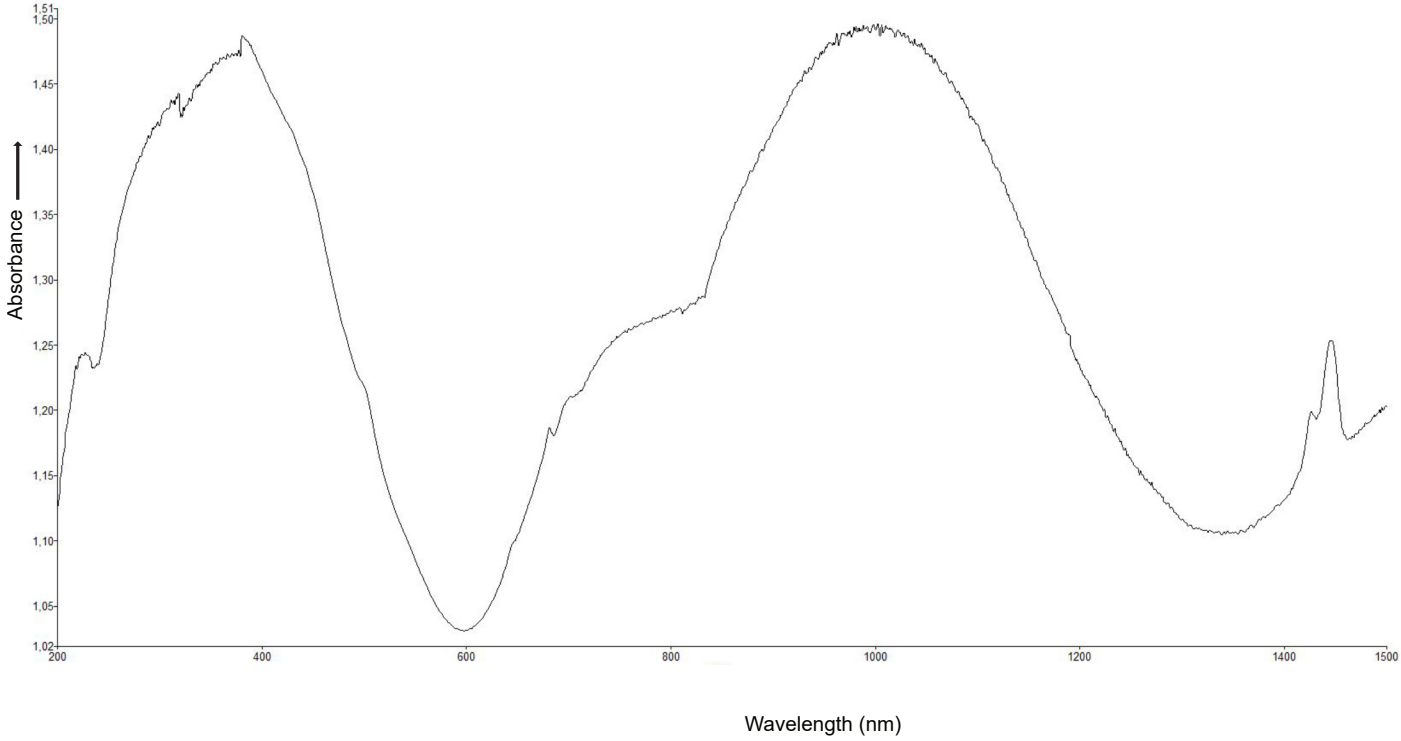

## FTIR spectrum

*KUD8*
*7.30 – 7.39 x 3.26 mm*

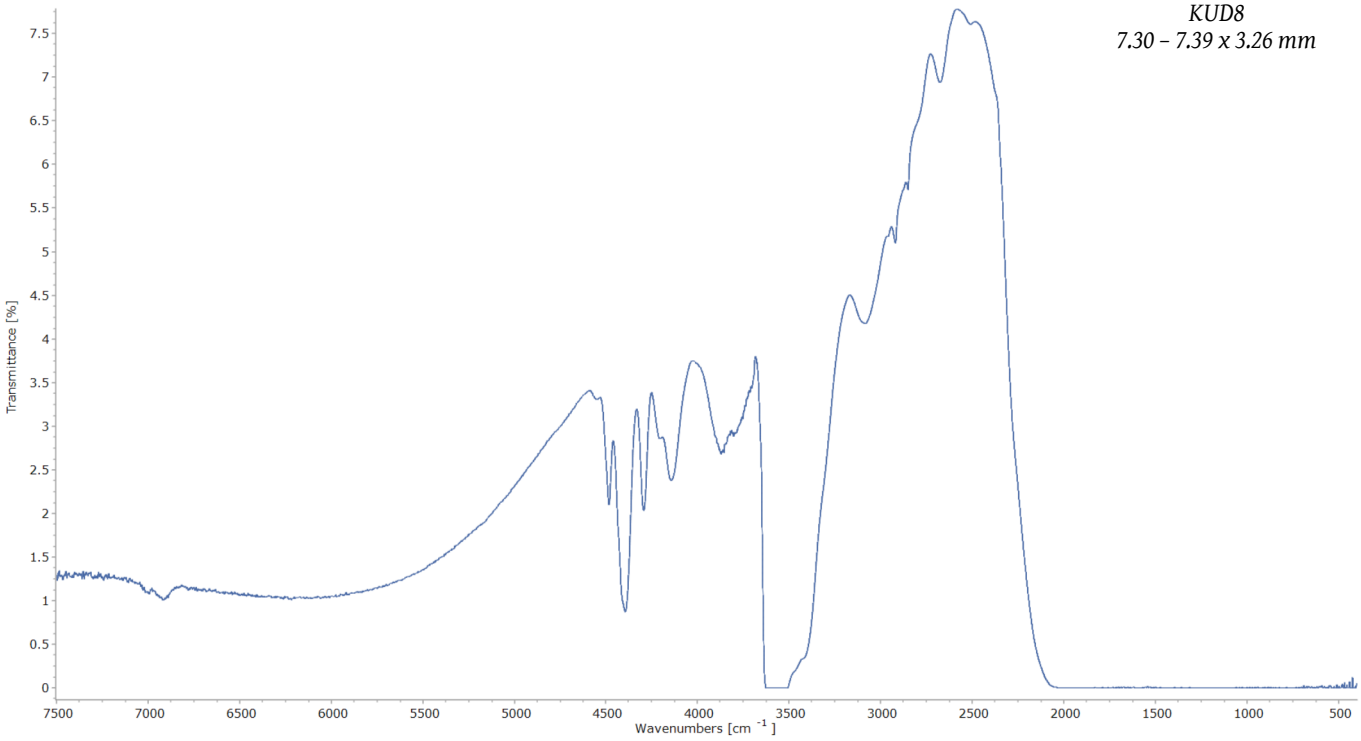


## EDXRF analysis

| Compound | m/m% | StdErr | El | m/m% | StdErr |
|---|---|---|---|---|---|
| Al2O3 | 40.54 | 0.38 | Al | 21.45 | 0.20 |
| SiO2 | 29.01 | 0.22 | Si | 13.56 | 0.10 |
| MgO | 15.14 | 0.18 | Mg | 9.13 | 0.11 |
| Fe2O3 | 8.05 | 0.30 | Fe | 5.63 | 0.21 |
| CaO | 1.87 | 0.07 | Ca | 1.34 | 0.05 |
| TiO2 | 0.301 | 0.029 | Ti | 0.180 | 0.018 |
| SO3 | 0.221 | 0.034 | Sx | 0.088 | 0.014 |
| MnO | 0.188 | 0.014 | Mn | 0.146 | 0.011 |
| Cr2O3 | 0.0995 | 0.0066 | Cr | 0.0681 | 0.0045 |
| Co3O4 | 0.066 | 0.019 | Co | 0.049 | 0.014 |
| ZnO | 0.0631 | 0.0027 | Zn | 0.0507 | 0.0022 |
| V2O5 | 0.0550 | 0.0034 | V | 0.0308 | 0.0019 |
| Cl | 0.0418 | 0.0070 | Cl | 0.0418 | 0.0070 |
| K2O | 0.0382 | 0.0037 | K | 0.0317 | 0.0031 |
| Ga2O3 | 0.0108 | 0.0010 | Ga | 0.0080 | 0.0007 |
| ZrO2 | 0.0052 | 0.0007 | Zr | 0.0038 | 0.0005 |

KnownConc= 3.30 B2O3 REST= 1.00 H2O D/S= 0
Sum Conc's before normalisation to 100% : 66.4 %

# Appendix

## *Sample AUE4100*

*AUE4100*
*8.08 x 6.64 x 3.67 mm mm*

### Emission spectra

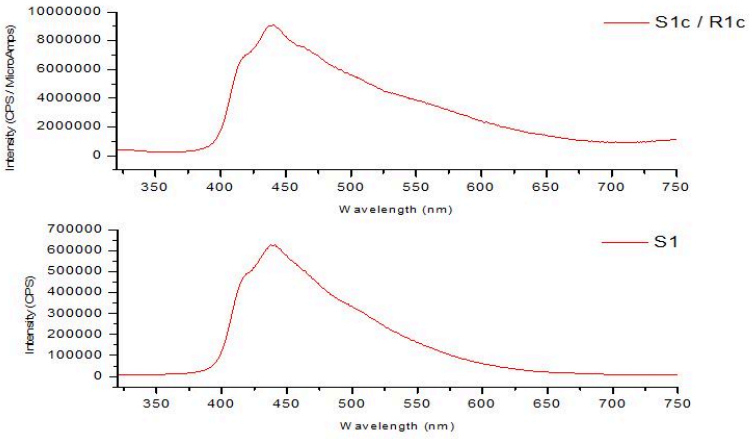


*Emission spectra under λex = 254nm at room temperature*

*S1: measured*
*S1c/R1c: corrected*

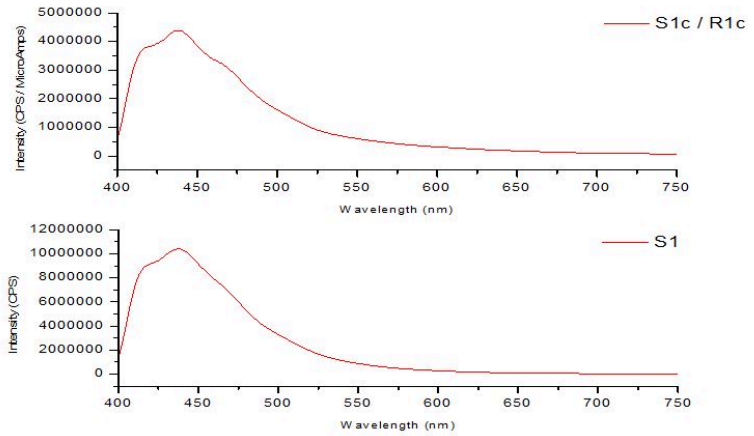


*Emission spectra under λex = 365nm at room temperature*

*S1: measured*
*S1c/R1c: corrected*

### Exitation spectra

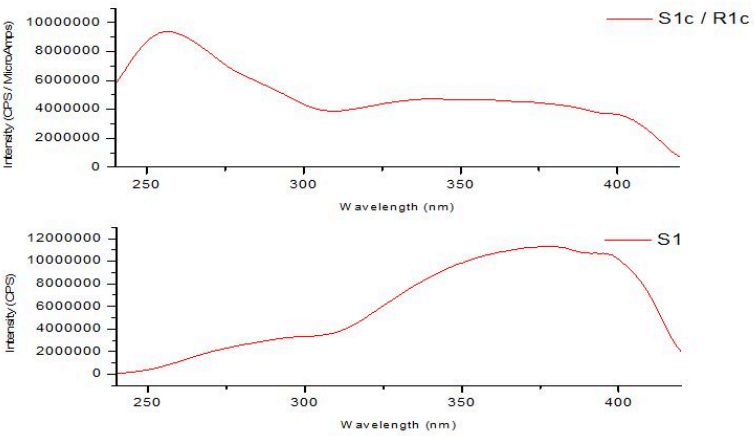


*Excitation spectra under λem = 435nm at room temperature*

*S1: measured*
*S1c/R1c: corrected*

## Phosphorescence decay time spectra

- *λex = 325nm*
- *λem = 550nm*
- *10nm slit*

*AUE4100*
*8.08 x 6.64 x 3.67 mm mm*

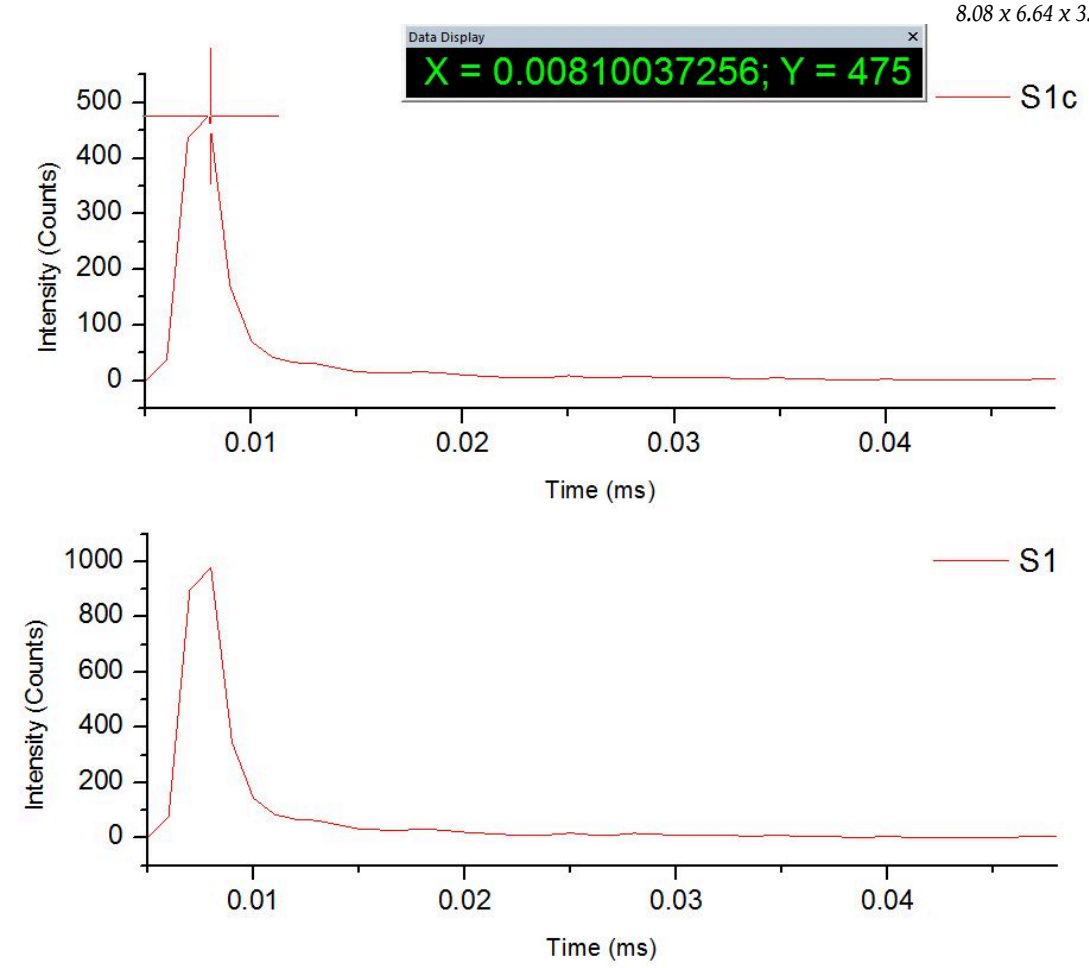


## EDXRF analysis

| Compound | m/m% | StdErr | El | m/m% | StdErr |
|---|---|---|---|---|---|
| Al2O3 | 61.92 | 0.25 | Al | 32.77 | 0.13 |
| SiO2 | 36.80 | 0.24 | Si | 17.20 | 0.11 |
| MgO | 0.928 | 0.053 | Mg | 0.560 | 0.032 |
| Fe2O3 | 0.222 | 0.025 | Fe | 0.155 | 0.017 |
| P2O5 | 0.077 | 0.012 | Px | 0.0335 | 0.0053 |
| K2O | 0.0142 | 0.0020 | K | 0.0118 | 0.0017 |
| TiO2 | 0.0136 | 0.0013 | Ti | 0.0082 | 0.0008 |
| V2O5 | 0.0101 | 0.0011 | V | 0.0057 | 0.0006 |
| Ga2O3 | 0.0076 | 0.0006 | Ga | 0.0057 | 0.0004 |

KnownConc= 0 REST= 0 D/S= 0
Sum Conc's before normalisation to 100% : 74.0 %

# References


Wikipedia page Andreas Nicolaus Kornerup *https://da.wikipedia.org/wiki/Andreas_Nicolaus_Kornerup*

A. Lacroix and A. De Gramont (1921): Sur la recherche spectrale du bore et sur sa présence dans quelques silico-aluminates naturels. *Bulletin de la Société française de minéralogie, 44-4-5, pages 67-77.*

A. Lacroix (1939): Observations sur quelques minéraux de Madagascar. *Bulletin de minéralogie, 62-7-12, pages 300-309.*

W. Schreyer and F. Seifert (1969): High-pressure phases in the system $MgO$-$Al_2O_3$-$siO_2$-$H_2O$. *American journal of science, Schairer 267-A, pages 407-443.*

H. Bank and W. Berdesinski (1974): Stark pleochroitischer durchsichtiger schleifwürdiger Kornerupin aus Ostafrika. *Gemmologie, 23/1, pages 49-51.*

K. Schmetzer, O. Medenbach and H. Krupp (1974): Das Mineral Kornerupin unter besonderer Berücksichtigung eines neuen Vorkommens in Kwale Distrikt, Kenya. *Gemmologie, 23/4, pages 258-278.*

H. H. W. Moenke (1974): Silica, the three-dimensional silicates, borosilicates and beryllium silicates. *The infrared spectra of minerals, chapter 16, pages 374-376.* DOI:10.1180/mono-4.16

H. Bank and W. Berdesinski (1975): Kornerupin-Vorkommen in Tansania. *Gemmologie, 24/2, page 95.*

K. Schmetzer, J. Ottemann, H. Bank and H. Krupp (1977): Blaugrüne Kornerupine aus Kenia und Tansania. *Gemmologie, 26/4, pages 202-204.*

R. Webster (1977): Kornerupine. Gems, their sources, description and identification. *Reprinted third edition, pages 293-294.*

G. Amthauer and K. Schmetzer (1977): Mössbauer- und Ligandenfeldspektroskopische Untersuchungen natürlicher Fe-haltiger Kornerupine. Fortschr. *Miner. 55, Beih. 1, pages 6-7.*

K. Schmetzer (1978): Neues zur Kristalloptik von Kornerupin. *N. Jb. Miner. Mh., H. 12, Pages 554-558.*

G. Werding and W. Schreyer (1978): Synthesis and Crystal Chemistry of Kornerupine in the System $MgO$ - $Al_2O_3$ - $SiO_2$ - $B_2O_3$ - $H_2O$. Contrib. Mineral. *Petrol. 67, pages 247-259.*

K. Schmetzer, J. Ottemann, H. Bank and H. Krupp (1979): Transparent bluish-green kornerupine from east Africa (Kenya and Tanzania). *Journal of Gemmology, XVI, 7, pages 455-457.*

K. Schmetzer (1982): Absorptionsspektroskopie und Farbe von $V^{3+}$-haltigen natürlichen Oxiden und Silikaten – ein Beitrag zur Kristallchemie des Vanadiums. *N. Jb. Miner. Abh. 144, pages 73-106.*

U. Henn (1985): Untersuchungen an Kornerupin und Sinhalit von Elahera, Sri Lanka. *Gemmologie, 34,1/2, pages 13-19.*

E. S. Grew, R. K. Herd and N. Marquez (1987): Boron-bearing kornerupine from Fiskenæsset, West Greenland: a re-examination of specimens from the type locality. *Mineralogical Magazine, 51(363), pages 695-708, December.* DOI:10.1180/minmag.1987.051.363.10

E. S. Grew, M. A. Cooper and F. C. Hawthorne (1996): Prismatine: revalidation for boron-rich compositions in the kornerupine groupe. *Mineralogical Magazine, 60(400), pages 483-491, June.* DOI:10.1180/minmag.1996.060.400.09

B. Wopenka, J. J. Freeman and E. S. Grew (1999): Raman spectroscopic identification of B-free and B-rich kornerupine (prismatine). *American Mineralogist, 84, pages 550–554.* DOI:10.2138/am-1999-0408

E. S. Grew, G. J. Redhammer, G. Amthauer, M. A. Cooper, F. C. Hawthorne and K. Schmetzer (1999). Iron in kornerupine; A $^{57}$Fe Mossbauer spectroscopic study and comparison with single-crystal structure refinement. *American Mineralogist, V84, pages 536-549.* DOI:10.2138/am-1999-0407

U. Henn and C. C. Milisenda (2004): Gemmological Tables, *German Gemmological Association, page 19.*

C. C. Milisenda (2005): Kornerupine cat's-eye from Sri Lanka. *Gemmologie, 54/2/3, pages 67-68.*

C. C. Milisenda and K. Wehr (2009): Kornerupin und Diopsid aus Tansania. *Gemmologie, 58/3/4, pages 78-80.*

M. A. Cooper, F. C. Hawthorne and E. S. Grew (2009): The crystal chemistry of the kornerupine-prismatin series - I. Crystal structure and site population. *The Canadian Mineralogist, 47, pages. 233-262.* DOI:10.3749/canmin.47.2.233

M. A. Cooper, F. C. Hawthorne, E. S. Grew and G. R. Rossman (2009): The crystal chemistry of the kornerupine-prismatine series. II. the role of hydrogen. *The Canadian Meneralogist, 47, pages 263-274.* DOI:10.3749/canmin.47.2.263

Datasheet for a kornerupine from Edward J. Gübelin Collection (GIA Collection Number: 34365). GIA Gem Database, 2011.

R. L. Frost, A. Lópes, Y. Xi and R. Scholz (2014): A Vibrational Spectroscopic Study of the Silicate Mineral Kornerupine. *Spectroscopy Letters, 48, pages 487-491.* DOI:10.1080/00387010.2014.909494

M. Gaft, R. Reisfeld and G. Panczer (2015): Modern Luminescence Spectroscopy of Minerals and Materials. *Springer Mineralogy, Second Edition, reprinted.*

U. Henn and B. Huayasan (2019): Blauer Kornerupin aus Tansania. *GemmologieAktuell 1/2019.*

M. Vigier, E. Fritsch , T. Cavignac, C. Latouche and S. Jobic (2023): Short-wave uv blue luminescence of some minerals and gems due to titanate groups. *Minerals, 13, 104.* DOI:10.3390/min13010104